Molecular characterization of the hexose transporter (PfHT1) of *Plasmodium falciparum* in *Xenopus laevis* oocytes

By
Suzanne Kathryn Manning

Submitted in partial fulfillment of the requirements for the degree of
Master of Science (Biochemistry)
in the
Faculty of Natural and Agricultural Sciences

University of Pretoria
Pretoria

November 2001

ACKNOWLEDGEMENTS

I wish to express my gratitude to the following people:

- My parents **Ian and Angela Manning** for their patience and financial support and for their love and belief in me.

- My supervisor **Professor A. I. Louw** (Department of Biochemistry, University of Pretoria, South Africa) for his much-needed wisdom and advice, and his continual patience and support.

- My co-supervisor **Professor S. Krishna** (Department of Infectious Diseases, St. Georges Hospital Medical School, London) for his generosity, enthusiasm, encouragement and insight.

- My close friend **Uwe Dobberstein** for his encouragement, support and love during the course of this degree.

- **Lyn-Mariè Birkholtz**, **Karen Nel** and **Fourie Joubert** for their patience with my questioning and their forever willingness to help.

- Everyone in the **Biochemistry Department** and especially the **malaria team** who helped me with my projects through the years.

- My **colleagues and friends** at the University of Pretoria for their friendship.

- The **MRC**, **NRF** and the **University of Pretoria** for financial support.

TABLE OF CONTENTS

LIST OF FIGURES

LIST OF TABLES

LIST OF ABBREVIATIONS

1-DOG	1-deoxy-D-glucose
2,5-AHM	2,5-anhydro-D-mannitol
2-DOG	2-deoxy-D-glucose
3-OMG	3-*O*-methyl-D-glucose
6-DOG	6-deoxy-D-glucose
A	Adenine
AMA	Apical merozoite antigen
ATB-BMPA	2-*N*-4-(1-azi-2,2,2-trifluoroethyl) benzoyl-1,3-bis(D-mannos-4-yloxy)-2-propylamine
ATP	Adenosine triphosphate
BFA	Brefeldin A
bp	Base pair
C	Cytosine
C5-DMB-ceramide	*N*-[5-(5,7-dimethylBODIPY)-1-pentanoyl]-D-erythro-sphingosine
C6-NBD-cer	*N*-[7-(4-nitrobenzo-2-oxa-1,3-diazole)] amino-caproyl sphingosine
C6-NBD-Sm	C6-NBD-sphingomyelin
CD36	Cluster determinant 36
CHO	Chinese Hamster Ovaries
CO_2	Carbon dioxide
CTP	Cytidine triphosphate
DEPC	Diethyl pyrocarbonate
DHFR-TS	Dihydrofolate reductase-thymidylate synthase
DHODase	Dihydroorotate dehydrogenase

DNA	Deoxyribonucleic acid
DOG	Deoxy D-glucose
DPM	Decay per minute
EDTA	Ethylenediaminetetraacetic acid
EM	Erythrocyte membrane
ER	Endoplasmic reticulum
FT-IR	Fourier transform infrared
G	Guanine
GFP	Green fluorescent protein
GLUT1	Mammalian glucose transporter 1
GPI	Glycosylphosphatidylinositol
Grp	Glucose-regulated protein
GTP	Guanosine triphosphate
HDEL	His-Asp-Glu-Leu
HEPES	N-2-hydroxylethylpiperazine-N'-2-ethanesulfonic acid
HIF-1	Hypoxia-induced factor 1
ICAM-1	Intercellular adhesion molecule-1
IFN-γ	Gamma interferon
IL	Interleukin
INOS	Nitric oxide synthetase
IPTG	Isopropyl-D-galactoside
IRBC	Infected red blood cell
KAHRP	Knob associated histidine rich protein
KDEL	Lys-Asp-Glu-Leu
K_i	Half-maximal inhibition constant for carrier transport
K_m	Affinity or Michaelis constant

LB Broth	Luria-Bertani Broth
LDH	Lactate dehydrogenase
M	Molar
MFS	Major facilitator superfamily
MHC	Major histocompatibility complex
MS-222	3-Aminobenzoic Acid Ethyl Ester or Tricaine
MSA	Merozoite surface antigen
N	Asparagine
NBMPR	6-((4-nitrobenzyl)thio)-9-β-D-ribofuranosylpurine
NO	Nitric oxide
NPP	New permeation pathways
O_2	Oxygen
ORF	Open reading frame
P.	*Plasmodium*
Pb(ec)	*P. berghei* erythrocyte cytoplasm located protein
Pb(em)	*P. berghei* erythrocyte membrane located protein
pCMBS	*p*-chloromercuribenzene sulfonate
PCR	Polymerase Chain Reaction
PfEMP1	*P. falciparum* erythrocyte membrane protein 1
PfENT1	*P. falciparum* encoded nucleoside transporter 1
PfERC	*P. falciparum* ER-located calcium binding protein
PfERD2	*P. falciparum* ERD2
PfHRP	*P. falciparum* histidine rich protein
PfHT1	*P. falciparum* hexose transporter 1
PfNT1	*P. falciparum* encoded nucleoside transporter 1
PM	Plasma membrane
PNK	T4 Polynucleotide Kinase
PPM	Parasite plasma membrane
PPPK-DHPS	Dihydropteroate synthase-2-amino-4-hydroxy-6-hydroxymethyl-dihydropteridine pyrophosphokinase

PV	Parasite vacuole
PVM	Parasite vacuole membrane
Q	Glutamine
RBC	Red blood cell
RBCM	Red blood cell membrane
RESA	Ring-infected erythrocyte surface antigen
RNA	Ribonucleic acid
SDEL	Ser-Asp-Glu-Leu
SDS	Sodium dodecyl sulphate
SDS-PAGE	SDS-polyacrylamide gel electrophoresis
sERA	Secondary ER of Apicomplexa
SERP	Serine rich protein
SOD	Superoxide dismutase
SP	Sulfadoxine-pyrimethamine
T	Thymine
TAE	Tris-acetate-EDTA buffer
TBE	Tris-borate-EDTA buffer
TBS	Tris buffered saline
THT	Trypanosome hexose transporter
Tm	Melting temperature
TNF	Tumour necrosis factor
Tris	2-amino-2-(hydroxymethyl)-1,3-propandiol
TVM	Tubulovesicular membrane
TVN	Tubulovacuolar network
UTP	Uridine triphosphate
UTR	Untranslated region
UV	Ultraviolet

var	Variant
v/v	Volume/ volume
w/v	Weight/ volume
WHO	World Health Organisation
X-gal	5-bromo-4-chloro-indolyl-β-D-galactoside

SUMMARY

Malaria kills up to 3 million people and affects a further 500 million people annually. Parasite multidrug resistance to most antimalarial drugs is a growing concern. There is therefore a need to develop new and effective drugs against existing validated targets, as well as a need to identify new targets. Recently the *P. falciparum* hexose transporter (PfHT1) was isolated and cloned. This protein has potential as a drug target since the malaria parasite depends solely on glucose provided by the host for its energy.

Studies on the transporter have revealed several differences between it and the human glucose transporter, GLUT1, which is significant towards identifying species-specific drug targets. These include PfHT1s ability to transport glucose at a higher affinity (K_m = 1.0 ± 0.2 mM) than GLUT1 (K_m = 2.3 mM, 2.6 mM). Also, PfHT1 can transport fructose at a relatively high affinity (K_m = 11.5 ± 1.6 mM), whereas GLUT1 cannot (K_m > 50 mM). PfHT1 forms interactions with glucose at positions C-3 and C-4, whereas GLUT1 forms interactions with glucose at positions C-1 and C-3 with a lesser contribution from positions C-4 and C-6. It is also known from the literature that PfHT1 helix 5 Q169 is important for fructose transport.

In this study interactions formed between glucose and PfHT1 helices 5 and 7 were investigated using point mutagenesis. Also the importance of PfHT1 helices 7-12 and the C-terminal tail were investigated using PfHT1/ GLUT1 chimaeric proteins. From the results of this study the helix 7 302SGL motif may be important for interactions with glucose at C-1 and C-5, with a lesser contribution from C-3 and C-6. PfHT1 helix 5 may form interactions with glucose at C-2, C-3, C-5 and C-6. Chimaeras investigated in this study were not functional. However, the importance of the presence of at least 7 amino acids directly after and belonging to transmembrane helix 12 could be investigated as a result of these studies.

Further information into important amino acids for PfHT1-substrate interactions is still required. These studies are pioneering towards understanding the differences that exists between the glucose transporters of the malaria parasite and its human host. The information obtained point the way to further studies on the potentially crucial helices 5 and 7 of PfHT1 that could be targeted by future antimalarial drugs.

OPSOMMING

Tot soveel as 3 miljoen mense sterf jaarliks aan malaria en 'n verdere 500 miljoen word geaffekteer. Die weerstand wat die malaria parasiet teen beskikbare medisyne toon is kommerwekkend. Daar bestaan dus 'n behoefte vir die ontwikkeling van nuwe en effektiewe middels teen beproefde teikens vir die vernietiging van die parasiet asook die karakterisering van nuwe teikens. Die *P. falciparum* heksose transporteerder is onlangs geïsoleer en gekloneer. Hierdie proteïen het die potensiaal om gebruik te kan word as medisinale teiken aangesien die malaria parasiet afhanklik is van die gasheer as bron van glukose vir energie.

Vorige studies het aangetoon dat daar heelwat verskille is tussen die parasiet en die menslike glukose transporteerder GLUT1 wat 'n bydrae kan lewer tot die identifisering van moontlike spesies-spesifieke medisinale teikens. PfHT1 het die vermoë om glukose teen 'n hoër affiniteit te transporteer (K_m = 1.0 ± 0.2 mM) as GLUT1 (K_m = 2.3 mM, 2.6 mM). Verder kan PfHT1 fruktose teen 'n relatief hoë affiniteit transporteer (K_m = 11.5 ± 1.6 mM) terwyl GLUT1 dit nie kan doen nie (K_m > 50 mM). PfHT1 reageer met glukose by C-3 en C-4 terwyl GLUT1 reageer met C-1 en C-3, met kleiner bydraes deur C-4 en C-6. Uit die literatuur is dit bekend dat PfHT1 heliks 5 Q169 belangrik is vir fruktose transport.

Die interaksies tussen glukose en PfHT1 heliks 5 en 7 is in hierdie studie ondersoek deur gebruik te maak van puntmutasies. Die noodsaaklikheid van PfHT1 heliks 7-12 en die C-terminaal stert vir heksose transport was ondersoek deur gebruik te maak van PfHT1/ GLUT1 "chimaera" proteïene. Uit die resultate van die studie blyk dit dat die 302SGL motief in heliks 7 belangrik kan wees vir interaksies met glukose by posisies C-1 en C-5 en tot 'n mindere mate met posisies C-3 en C-6. PfHT1 heliks 5 mag moontlik interreageer met glukose by posisies C-2, C-3, C-5 en C-6. Die "chimaeras" wat ondersoek was is nie funksioneel nie. Die moontlike belangrikheid van die teenwoordigheid van ten minste 7 aminosure onmiddellik na en as deel van die transmembraan heliks 12 kon aangetoon word as 'n gevolg van hierdie studie.

Verdere inligting oor die essensiële aminosure vir PfHT1-substraat interaksies word steeds benodig om die verskille wat bestaan tussen die glukose transporteerder van die malaria parasiet en die menslike gasheer uit te wys. Die inligting wat uit hierdie studie verkry is baan die weg vir verdere studies op helikse 5 en 7 van PfHT1 wat potensieël baie belangrik kan wees as teikens vir toekomstige malaria teenmiddels.

1 CHAPTER ONE:

LITERATURE REVIEW

1.1 Definition

Malaria is both an acute and chronic disease caused by protozoa of the genus *Plasmodium*. Four species cause human malaria namely, *P. falciparum, P. vivax, P. ovale* and *P. malariae*. The protozoa are transmitted to humans by female mosquitoes of the *Anopheles* genus. The parasites asexual stage cycles are spent in the human erythrocyte. *P. falciparum* is the most common to infect humans and causes the most fatalities (Virtual Naval Hospital, 1998).

1.2 Historical review

Malaria is a very old disease and prehistoric man is thought to have suffered from it. Malaria probably originated in Africa and accompanied human migration to the Mediterranean shores, India and South East Asia. In the past it used to be common in the marshy areas around Rome and the name is derived from the Italian word "malaria" or "bad air". It was also known as Roman fever. The association with stagnant waters led the Romans to begin drainage programs, the first action against malaria (Malaria: an Online Resource, 2001; Bradley, 1996).

The malaria parasite was first detected in fresh blood drawn from patients in the 1880s and in 1889 Laveran, working in Algeria, deduced the protozoal cause of malaria. It wasn't until 1897 that the *Anopheles* mosquito was discovered as the vector for the disease. The study of the parasite was hindered by the staining method until in 1892 when an improved method of staining blood smears was developed, and the morphology of the parasite could be studied. This led to the identification of different stages such as the ring forms, trophozoites, schizonts and merozoites. Detail was however unobtainable through the use of light microscopy, and only until the

invention of the electron microscope in 1932 was the study of biological material possible. The electron microscope was first applied to the field of malariology in the study of *Plasmodium vivax* in 1942. Only in 1956 was it established that the parasite was within the host erythrocyte. In 1957 the fine structure of the parasite was eventually studied and various organelles were identified, including a nucleus, mitochondrion, a well-developed endoplasmic reticulum, pigment granules, lipid bodies and a plasma membrane surrounding the parasite (Aikawa, 1971).

The earliest treatment of malaria dates back to 1600 in Peru where the native Peruvian Indians used the bitter bark of the cinchona tree (which contained quinine) to treat the disease. By 1649 the bark was available in England and was known as 'Jesuits powder'. The first radical step towards the annihilation of malaria was in 1944 when DDT made its first debut in Italy after its discovery as an insecticide two years earlier (Bradley, 1996). This initial step made the ideal of global eradication of the malaria vector, *Anopheles*, seem possible and widespread systematic control measures such as DDT spraying, coating marshes with paraffin, draining stagnant water and the use of nets and cheap drugs were implemented (Bradley, 1996).

Incredibly this global eradication policy did not include Africa where the majority of malarial disease is manifest as it had insufficient infrastructure to support the policy. The policy was abandoned in 1969 but countries such as Hungary, Bulgaria, Romania, Yugoslavia, Spain, Italy, Netherlands and Portugal had managed to eradicate their epidemic malaria. The disease is currently epidemic in 91 countries. In 1989 the World Health Organisation (WHO) declared malaria control to be a global priority due to the worsening situation, and in 1993 the urge to increase control measures was made. Today some 500 million people in Africa, India, South East Asia and South America are exposed to endemic malaria and it is estimated to cause 2-4 million deaths annually, one million of which are children (Bradley, 1996).

1.3 The asexual blood stages

The malaria parasite enters into the asexual cycle development stage in the human host. The sporozoites are injected from the mosquito salivary glands into the human

host as the mosquito must inject anti-coagulants to ensure an even-flowing meal. Once in the blood stream the sporozoites travel to the liver and penetrate hepatocytes where they remain for 9-16 days and multiply (Figure 1.1; Sharma, 2000). The hepatocytes rupture to release merozoites into the blood stream for invasion of red blood cells. The invading merozoite appears to be attached to the invaded red blood cell by filamentous material leading from apical organelles at one end. These filaments are cleaved upon entry into the host cell (Howard and Schmidt, 1995; Bannister *et al*, 2000). Apical organelles (rhoptries, micromenes and dense granules) discharge their contents during invasion that change the shape and composition of the invaded red blood cell membrane (RBCM) and assist in erythrocyte invasion. These proteins induce the erythrocyte membrane (EM) to form an invasion pit that eventually envelops the merozoite (Bannister *et al*, 2000).

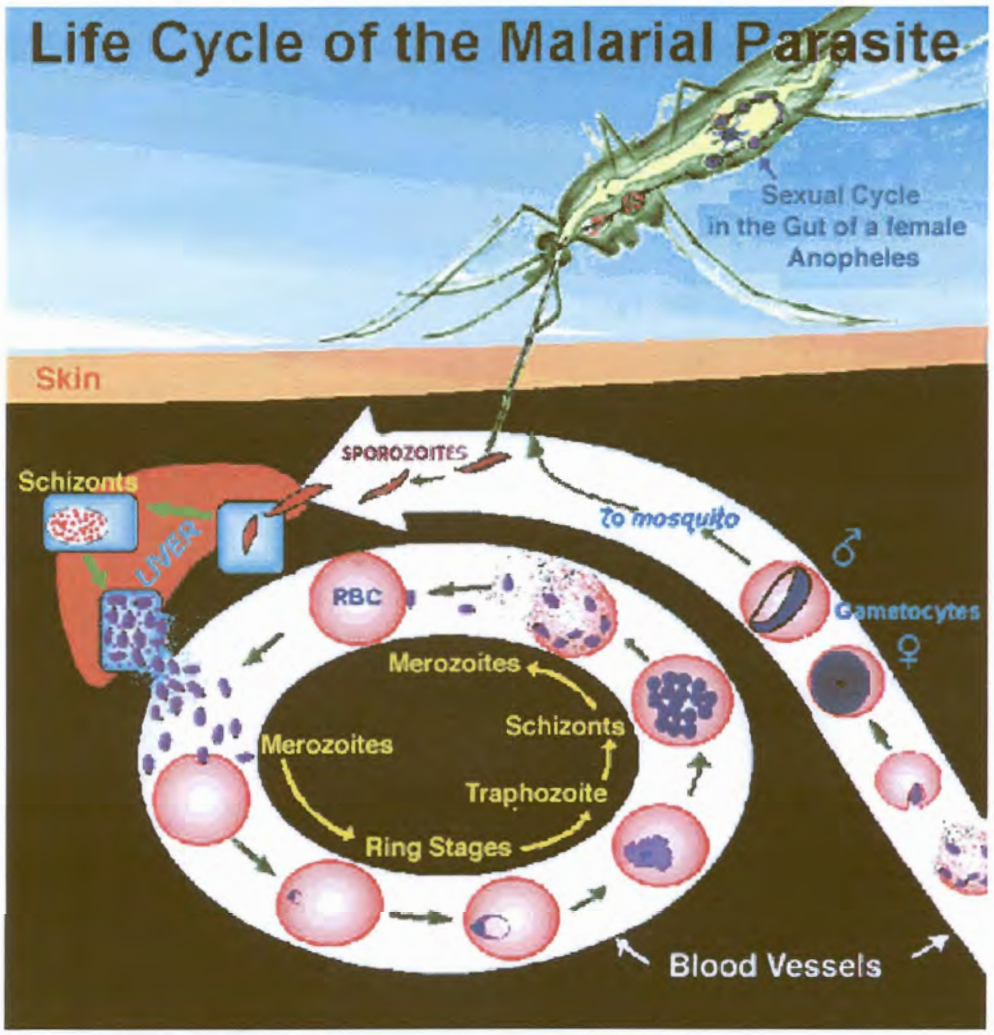

Figure 1.1: Schematic representation of the asexual cycle of *Plasmodium falciparum* in the human host (Sharma, 2000).

The subsequent ring stage parasites are surrounded by a membrane called the parasite vacuole membrane (PVM), which is probably derived from the erythrocyte membrane but is devoid of erythrocyte proteins and cytoskeleton (Howard and Schmidt, 1995; Elford *et al*, 1995). For the next 24 hours the parasite develops organelles such as the tubovesicular membrane (TVM) in the cytoplasm of the infected erythrocyte and a food vacuole within the parasite (Langreth *et al*, 1978).

The surface morphology of the infected erythrocyte is dramatically changed from 10-30 hours post-invasion during the trophozoite stage. From 24-36 hours after invasion the trophozoite matures to a schizont and occupies 80-90% of the volume of the infected erythrocyte. Schizogony (36-48 hours) is the final stage when the parasite engages in mitosis and development in the cytoplasm of secretory structures of the apical complex is prominent. 48 hours after invasion the daughter merozoites are fully developed and are released by rupture of the erythrocyte membrane and parasite vacuole membrane (Langreth *et al*, 1978).

1.4 Pathogenesis of malaria

Clinical symptoms and signs of malaria occur shortly before or at the time of red blood cell lysis. Symptoms include fever caused by the release of merozoites, malaria pigments, parasite proteins and cellular debris (Virtual Naval Hospital, 1998). This results in the host's release of pro-inflammatory cytokines, such as tumour necrosis factor (TNF), which triggers the onset of pathology (Clark and Scholfield, 2000). Patients infected with one of the three less severe human malarias, *P. ovale*; *P. malariae* or *P. vivax* show symptoms of chills followed by high fever that re-occur in a continuous cycle. This is not symptomatic of *P. falciparum*, which produces continual fever with irregular temperature spikes (Virtual Naval Hospital, 1998).

Nearly all of the deaths from malaria in African children are due to *P. falciparum* (Brown *et al*, 2000). It is the only type that causes microvascular disease and tissue damage. Morbidity is usually associated with cerebral malaria, which is symptomatic of seizures and impaired consciousness. Cerebral malaria is caused by microvascular obstruction (cytoadherence and sequestration) that prevents the exchange of glucose

and oxygen at the capillary level and causes hypoglycaemia, lactic acidosis, and fever. This results in impaired brain function but does not cause tissue damage since patients who are given prompt treatment can recover fully (Virtual Naval Hospital, 1998).

Cytoadherence is mediated by a family of antigenic variant (*var*) proteins collectively known as *var*/ PfEMP1 (*P. falciparum* erythrocyte membrane protein; Deitsch and Wellems, 1996). These proteins are associated with knob protrusions that have been implicated in cytoadherence (Cooke *et al*, 2000). Other proteins included in knobs are the knob associated histidine rich protein (KAHRP) and PfEMP3 (Cooke *et al*, 2000; Deitsch and Wellems, 1996). These knobs adhere to endothelial cells or placental syncytiotrophoblasts of the host. Two receptors on the host cell, namely CD36 and ICAM-1 (cluster determinant 36 and intercellular adhesion molecule-1, respectively), have been implicated in cytoadhesion, but recent studies with polymorphisms in ICAM-1 (Fernandez-Reyes *et al*, 1997) and mutations in CD36 (Aitman *et al*, 2000) have challenged the involvement of these receptors in infected red blood cells (IRBC) cytoadherence.

A prognosis of cerebral malaria is a very high plasma concentration of the pro-inflammatory cytokines TNF. A key role has been suggested for the *P. falciparum* toxin glycosylphosphatidylinositol (GPI) released upon rupture of mature schizonts, which appears to be a necessary and sufficient trigger for TNF release in tissues. GPI has now been implicated as the key toxin involved in malaria pathogenesis (Brown *et al*, 2000; Cooke and Cowman, 2000). Side effects similar to those of malaria pathogenesis are observed in tumour patients administered TNF-α. A correlation has been made between TNF-α and interleukin-10 (IL-10) by *in vitro* studies. IL-10 may be produced soon after the production of TNF-α to regulate the inflammatory activities of TNF-α. TNF-α induces fever and elevates body temperature, which can initially help to suppress parasitemia. But prolonged exposure to TNF-α promotes severe disease (Othoro *et al*, 1999). Studies have also shown that TNF-α suppresses erythropoiesis (production of red blood cells) contributing to anaemia development (Clark and Chaudhri, 1988). Therefore persons that produce IL-10 in balanced levels to regulate TNF-α may not develop severe or moderate malaria anaemia (Othoro *et al*, 1999).

T cell subsets and their products are essential in regulating both antibody formation and antibody independent protection. The $CD4^+$ T cell subset is thought to help with blood stage immunity, whilst $CD8^+$ T cells are known for their activity against liver stage parasite infection (Winkler *et al*, 1999). Immunisation of mice (Nussenzweig *et al*, 1967), monkeys (Bianco *et al*, 1970) and humans (Clyde *et al*, 1973) with irradiated sporozoites protected against challenge with live sporozoites, but *in vivo* depletion of $CD8^+$ T cells reduced protection (Weiss *et al*, 1988). Treatment of irradiated sporozoite immunised mice with monoclonal antibodies against gamma interferon (IFN-γ) or with an inhibitor of inducible nitric oxide synthetase also eliminated protection (Schofield *et al*, 1987; Seguin *et al*, 1994). Vaccine development has focused on inducing antibodies against the sporozoite surface to elicit a $CD8^+$ T cells response. Now new data indicates the involvement of $CD4^+$ T cells in irradiated sporozoite immunised mice. Protection against sporozoite challenge was eliminated with treatment of these immunised mice with both anti-$CD4^+$ and anti-$CD8^+$ antibodies (Renia *et al*, 1991; reviewed in Oliveira-Ferreira and Daniel-Ribeiro, 2001).

Another factor induced by the release of cytokines during *P. falciparum* infection is the generation of an inducible nitric oxide synthase (iNOS), which in turn produces a continual supply of nitric oxide (NO; Clark and Schofield, 2000). This short-lived molecule permeates freely through membranes and is responsible for a diverse array of unrelated but essential physiological functions in organs (Clark and Cowden, 1999). NO released in high concentrations under the influence of TNF may produce "nonsense signals" to the brain, which is thought to be a contributing factor towards cerebral malaria pathology (Clark *et al*, 1991). The iNOS is also induced by hypoxia (low oxygen levels in the blood), which is a consequence of infected erythrocyte sequestration (Clark and Cowden, 1999). Hypoxia also acts through the transcription factor hypoxia-inducible factor-1 (HIF-1) to increases other glycolytic enzymes and transport factors including the human glucose transporter GLUT1 required to accelerate glycolysis, which could indicate a common role for NO (Clark and Cowden, 1999). The role of NO production has been debated and its mode of action is not yet known (Brown *et al*, 2000)

Other symptoms of *P. falciparum* infection include renal failure resulting from renal tubules becoming clogged with haemoglobin and released malaria pigment, which causes glucose deprivation at the renal capillaries or tissue level. Pulmonary edema (abnormal accumulation of fluid in the lungs) can also result and causes laboured respiration, shortness of breath and coughing. Parasitised red blood cells can also adhere to microvesicles of the gastrointestinal tract resulting in symptoms of nausea, vomiting and loss of appetite. This has often lead to the misdiagnosis of viral gastroenteritis or hepatitis. One of the most commonly seen symptoms of *P. falciparum* malaria infection is anaemia. This can result from destruction of red blood cells from merozoite release or inhibition of hematopoiesis (production of red blood cells in the bone marrow) by TNF. Unlike the other three *Plasmodiums*, *P. falciparum* infects red blood cells of all ages, which allows infection of all circulating red blood cells (Virtual Naval Hospital, 1998).

1.5 Control of malaria

1.5.1 Chemotherapeutic targets and antimalarial drug discovery

The basic elements of any malaria control program require early diagnosis and correct treatment. The emergence of resistance to widely used antimalarial drugs, such as chloroquine, has elevated the need to discover and validate new targets to generate new drug candidates (Hastings and D'Alessandro, 2000). However, even despite the large collective effort of scientists around the world, the number of compounds tested against malaria remains very small. Of these compounds tested very few prove active in inhibiting parasite growth (Olliaro and Yuthavong, 1999).

The characteristics required of a putative drug target limit the field of targets available for study. The putative target needs to be an essential feature of the parasites life cycle and must differ significantly from any analogous process in the host. There must be no alternative pathways that could circumvent the target and the target must be accessible to the target-specific drug. The whole exercise of putative target evaluation and drug design is long, risky and expensive (Olliaro and Yuthavong, 1999).

Most targets that have been selected for antimalarial chemotherapy are in the parasites blood stages. This is only because blood-stage parasites can be cultured and tested with drugs, and is not by some planned strategy (Olliaro and Yuthavong, 1999). Validated chemotherapeutic targets have been summarised in Table 1.1.

Table 1.1: Summary of principal chemotherapeutic targets in *Plasmodium* (Olliaro and Yuthavong, 1999).

Pathway	Enzyme/process
Haemoglobin metabolism	Plasmepsin I, II (aspartic proteinases; cathepsin D-like) Falcipain (cysteine proteinase; cathepsin L-like) Haem polymerization, depolymerization Haem synthesis
Folate metabolism	Dihydrofolate reductase-thymidylate synthase (DHFR-TS) Dihydropteroate synthase-2-amino-4-hydroxy-6-hydroxy methyl-dihydropteridine pyrophosphokinase (PPPK-DHPS)
Pyrimidine synthesis, electron transport	Carbamoyl-phosphate synthase II Dihydroorotate dehydrogenase (DHODase) Cytochrome oxidase
Purine salvage	Hypoxanthine-guanine phosphoribosyltransferase
RNA/DNA	RNA polymerase Ribonucleotide reductase Topoisomerase I and II
Glucose transport, Glycolysis	**PfHT1** Lactate dehydrogenase (LDH)
Phospholipid metabolism	Phosphatidylcholine/phosphatidylserine synthesis
Artemisinin receptors	Iron haem as activator of protein alkylation
Oxidant damage	Potentiation of oxidant drugs
Oxidant defense	Glutathione reductase Superoxide dismutase (SOD)

These chemotherapeutic targets include processes occurring in the parasites digestive vacuole such as haemoglobin digestion, haem detoxification and antioxidant defence mechanisms. Other targets include enzymes involved in nucleic acid metabolism, phospholipid metabolism, glycolysis and tubulin assembly. Trafficking and signalling processes can also be targeted for antimalarial drugs. Such systems can be used to facilitate selective entry of antimalarial drugs, or to prevent key nutrients from being internalised (Olliaro and Yuthavong, 1999). A good candidate for this type of

antimalarial drug design, but still requiring further elucidation, would be the *P. falciparum* hexose transporter (PfHT1), isolated and sequenced by Woodrow *et al* (Highlighted in bold in Table 1.1; Woodrow *et al*, 1999).

A proposed strategy in treating malaria is to use antimalaria drugs in combination (Hastings and Alessandro, 2000). These combinations give old drugs new uses, which is beneficial for the limited amount of drugs in use (Winstanley, 2000). Drugs used for the treatment of *P. falciparum* malaria are listed below.

Chloroquine is the main drug used against the fight of malaria. It is safe and cheap and is used extensively for treating outpatients (not hospitalised). However, resistance is now extensive, yet it remains the most commonly used first-line drug despite failure rates of over 70% in some areas in Africa (Winstanley, 2000).

Quinine is a naturally occurring compound with relatively low potency. Malaria parasites satisfy most of their amino acid needs by consuming haemoglobin. Haem is the by-product of this digestion and is detoxified through polymerisation. Quinine is thought to act by binding to haem, preventing its polymerisation that would otherwise have reduced its toxicity to the parasite (Olliaro and Yuthavong, 1999). Resistance to the drug has developed, yet clinical failure is low outside Southeast Asia. Intravenous infusion is the preferred administered route, but it can be taken orally if it is taken at least twice daily. This makes it a difficult drug to use in outpatients (Winstanley, 2000).

Artemisinin and its derivatives were first discovered in an herbal remedy, and since then semisynthetic derivatives have been developed. This allows for greater antimalarial potency, but they are more expensive than the naturally occurring compound (Winstanley, 2000). It was hoped that these drugs would help reduce the mortality of severe malaria, but trials have shown that the drug has no clinical advantage over quinine. However it can be used where quinine resistance is evident (Van Hensbroek, 1996).

Pyrimethamine is more commonly used in combinations with other drugs. Sulfadoxine-pyrimethamine (SP) is cheap and is the most widely used combination (Winstanley, 2000). It eliminates slowly and therefore only one dose is needed. SP is however prone to rapid emergence of resistance and is used only for uncomplicated cases of *P. falciparum* malaria because of its slow effect (Winstanley, 2000).

Mefloquine is used for uncomplicated malaria. It is expensive and therefore is not in general use throughout Africa. Resistance has been noted in parts of Southeast Asia (Winstanley, 2000).

Halofantrine is an expensive drug and has been associated with ventricular arrhythmias (disturbances in ventricle rhythm), which has led to its reappraisal. However with resistance emerging to other available drugs, this drug remains in use as an alternative (Winstanley, 2000).

1.5.2 Vaccine development

Pre-erythrocytic vaccines; sporozoites and the intrahepatocytis stages. Rational design of malarial vaccines, like any other vaccine, requires characterisation of the protective immune response and identification of the antigens that elicit the response. Vaccines developed with the help of this information will elicit an immune response identical to that of the parasite antigen (Heal *et al*, 2001). During the past decade major efforts have been made to develop vaccines against the pre-erythrocytic malaria stages. Pre-erythrocytic vaccines may prevent sporozoites entering hepatocytes, or may inhibit parasite development within the hepatocyte (Kwiatkowski and Marsh, 1997). When the malaria parasite invades hepatocytes in the liver, these hepatocytes express antigens via the endogenous pathway and present it to $CD8^+$ T cells in association with major histocompatibility complex (MHC) class I molecules. However most vaccines deliver exogenous antigens via the MHC class II pathway to the host's immune system, inducing a $CD4^+$ T cell response (Heal *et al*, 2001). Evidence also suggests the possible involvement of $CD4^+$ T cells in sporozoite immunity (Tsuji *et al*, 1990). The challenge for the future is to develop a pre-erythrocytic vaccine capable of inducing protective antibodies against sporozoites, as well as inducing $CD8^+$ and $CD4^+$ T cell responses against the hepatocyte stage (Oliveira-Ferreira and Daniel-Ribeiro, 2001).

Vaccines target sporozoites and the intrahepatocyte stages mentioned above, as well as selective antigens of asexual blood stages. There is also the transmission blocking vaccines against gametocytes, gametes, or later stages in mosquitoes (Abath *et al*, 1998). Since one sporozoite is capable of developing into severe blood stage

infection, antisporozoite vaccines must be 100% effective. Vaccines developed from irradiated sporozoites resulted in complete resistance to sporozoite challenge in immunized mice (Jones and Hoffman, 1994).

Merozoite target antigens for vaccine development. Plasmodium species belong to the phylum Apicomplexa, so called for their apical secretory organelles named rhoptries and micronemes. During erythrocyte invasion merozoites transfer rhoptry proteins from these organelles to the erythrocyte surface to facilitate entry into the erythrocyte (Holder *et al*, 1994). Merozoites have been found to possess a number of surface antigens that could assist in erythrocyte adhesion and immune evasion. These surface proteins have been the focus of vaccine development since they represent a group of antigens that the host primarily is exposed to (Howard and Pasloske, 1993). These include the 195 kDa merozoite surface antigen 1 (MSA-1), which is thought to facilitate host immunity evasion and erythrocyte adhesion (Howard and Pasloske, 1993), and merozoite surface antigen-2 (MSA-2; 45kDa). Monkeys immunised against *P. falciparum* MSA-1 were protected against asexual parasite challenge (Etlinger *et al*, 1991), and mice immunised with *P. falciparum* MSA-2 produced antibodies against MSA-2 and protected the mice from challenge by murine malaria *P. chabaudi* (Saul *et al*, 1992).

Other merozoite proteins targeted for vaccine development, which are not found on the merozoites surface, include the apical merozoite antigen (AMA-1, 83kDa), which was first isolated from *P. knowlesi*. AMA-1 induces antibodies in monkeys that protect against further merozoites invasion (Deans *et al*, 1984), and homologues to AMA-1 have since been identified in *P. falciparum* (Preiser *et al*, 2000). Others include RAP-1/2 (80/42kDa) located in the rhoptries, ring-infected erythrocyte surface antigen (RESA, 155kDa) located in the dense granules, EBA-175 (175kDa) in the micronemes or apical end and SPf66, which is a synthetically constructed peptide polymer containing sequences from three merozoite proteins including MSA-1 (Howard and Pasloske, 1993; Hommel, 1990).

Infected erythrocyte membrane surface target antigens. Infected red blood cells express parasite produced antigens on the cell surface that elicits specific

IgG antibodies. PfEMP-1 (250-400 kDa) is one of these antigens and it accounts for sequestration of the IRBC to host endothelial cells in the blood vessels. This is the main cause of blood clots resulting in cerebral malaria that is experienced by patients infected with *P. falciparum* if left untreated. Sequestration of IRBC prevents circulation of these cells through the spleen where cells containing inclusions are systematically destroyed. Vaccine-elicited antibodies against PfEMP-1 may block IRBC sequestration and reduces the pathology of cerebral malaria, and will also allow for the IRBC to be destroyed by the spleen (Howard and Pasloske, 1993). Another similar protein is rosettin (22-28kDa) that mediates rosetting whereby IRBC adhere to each other at the rosettin sites and cause blockage of blood vessels. This gene has not yet been cloned, but like antibodies against PfEMP-1, antibodies against rosettin may reduce pathology of cerebral malaria. Other surface antigens include *P. falciparum* histidine rich protein-2 (PfHRP-2; 65-75kDa) and the high molecular weight protein Ag332 (2500kDa; Howard and Pasloske, 1993).

Infected erythrocyte soluble target antigens. The protein PfHRP-2 is not only expressed on the IRBC surface, but is also secreted into the surrounding plasma from the IRBC. This protein has been considered as a possible target for malarial vaccines, along with others including the serine rich protein (SERP), Ag2 and Ag7. The latter three proteins are released from the IRBC during rupture and release of merozoites. These proteins are released in large doses in relatively short periods of time and elicit host responses such as pro-inflammatory cytokine release mentioned in paragraph 1.4. It has been proposed that removal of these proteins by vaccine-induced antibodies specific for these compounds would stop the cascade of undesirable host responses (Howard and Pasloske, 1993).

1.5.3 Vector control

Female species of the *Anopheles* mosquito are the carriers of the malaria parasite and transmit the disease to humans during feeding. The vector biting behaviour and its longevity as well as its susceptibility to the *Plasmodium* parasite are all important for understanding the development of the parasite in the mosquito, and its transmission to

humans. The vectors biting and resting behaviour is an important factor in determining the use of insecticides (Toure', 1999).

The tools that exist for malaria vector control include chemicals such as DDT and other insecticides. Environmental management techniques such as eliminating standing water to reduce vector breeding; implementing the use of larvivorous fish and other mosquito larva eating predators as well as applying bacterial pathogens to malaria breeding sites can help implement vector control. Humans in endemic areas or experiencing epidemics of malaria can implement control by using repellents and bed nets, or simply by swatting vectors (Mwenesi, 1999).

Bed nets have been used for approximately 2000 years for personal protection against malaria (Lindsay and Gibson, 1988). The concept of treating bed nets with insecticides was first implemented in the Second World War by soldiers stationed in malaria areas (Harper *et al*, 1947). Insecticides used for the treatment of bed nets include DDT (Mwenesi, 1999); alpha-cypermethrin; cyfluthrin, deltamethrin; etofenprox and permethrin (Lines and Zaim, 2000).

1.5.4 Resurgence of malaria

Malaria is currently responsible for 2-4 million deaths annually resulting from the 300-500 million people who contract the disease, 10 000-30 000 of these cases are as a result of people travelling to endemic areas (Doolan and Hoffman, 2001). Spraying with DDT insecticide in the 1960s and 1970s was very successful in reducing the prevalence of malaria. However, because of the bad publicity created against the use of DDT and the high cost involved in using alternatives, resurgence occurred (Curtis and Lines, 2000). A severe case of resurgence of malaria was reported in Madagascar after the halt of DDT use in the 1960s, which resulted in a recovery of the vector causing an epidemic in 1988-1991 that killed thousands (Curtis and Lines, 2000).

Other causes of resurgence originate from the increase in antimalarial drug resistance. The emergence of drug resistant parasites to the drugs that were useful in the past means that new drugs are developed which often have side effects such as fatal heart

rhythms, fatal skin disease, neurological disturbances or gastrointestinal distress (Doolan and Hoffman, 2001). There is an overall lack in chemical diversity in the antimalarial drugs in use, which has led to cross-resistance between drugs (Olliaro and Yuthavong, 1999). By understanding the parasites metabolic processes, and its pathology, more rational drug and vaccine targets may be revealed and researchers may be able to provide solutions to this growing epidemic.

1.6 Parasite nutrient requirements and uptake

During its asexual cycle the malaria parasite invades the erythrocyte, a cell devoid of all intracellular organelles and incapable of *de novo* protein synthesis (Liem *et al*, 1994). Erythrocytes are specialists in carrying molecular oxygen (O_2) from the lungs to the tissues of the body and for carrying carbon dioxide (CO_2) in the opposite direction. Haemoglobin, which is responsible for the red colour of blood, is the oxygen-carrying protein in erythrocytes. The mature mammalian erythrocyte is further adapted by lacking a nucleus. The amount of oxygen required by the cell for its own metabolism is thus very low, and most oxygen carried can be freed into the tissues. Although they use glucose to produce energy necessary for their survival, they cannot synthesize protein; therefore reparative processes are not possible (Lodish *et al*, 1995). Hence the interior of the host erythrocyte represents a highly unusual extracellular environment for the parasite inside (Kirk, 2001).

The interior of the erythrocyte has high concentrations of K^+ and proteins, low levels of Na^+ and only trace levels of Ca^+. Therefore the invading parasite must provide its own means of regulating its chemical composition and obtaining nutrients from the host erythrocyte cytosol. The parasite must also contend with the hosts own metabolism and also take measures to avoid the hosts immune system and systematic destruction of red blood cells via the spleen (Kirk, 2001). Such measures require alterations of the host erythrocyte membrane such as knobs for sequestration discussed previously, and permeation pathways to allow the entry of nutrients, which will be discussed below.

1.6.1 Proposed parasite solute transport pathways

For solutes to gain entry into the intracellular parasite they first have to gain entry into the erythrocyte cytosol across the EM. From there the solutes move into the parasite by crossing the parasite vacuole membrane and the parasite plasma membrane (PPM; Foley and Tilley, 1998). Three possible models have been proposed for this molecular trafficking, namely the conventional model and two direct access models: the 'metabolic window' and the 'duct' (Kirk, 2001).

1.6.1.1 The conventional model

For the conventional model, solutes enter and leave the cell via the erythrocyte cytoplasm and have to cross the three separate membranes in passing from the blood plasma to the parasite cytoplasm. Solutes pass through the erythrocyte membrane via two different means (Kirk, 2001).

Firstly, a number of endogenous host cell transporters have been shown to have an increased activity in parasite-infected erythrocytes. Such transporters include the Na^+-K^+ pump, which has a two-fold increased activity compared to uninfected cells (Kirk *et al*, 1991). Another example is putrescine uptake in *P. knowlesi* infected cells. There is an increase in putrescine uptake in *P. knowlesi* infected monkey red blood cells, with a similar K_m to that of uninfected erythrocytes but a three-fold higher V_{max} (Singh *et al*, 1997).

Secondly, solutes gain access to the erythrocyte cytoplasm through new permeation pathways (NPP). These pathways are induced by the parasite and have very different properties to endogenous transporters and bestow on the host cell an increased permeability to a wide range of solutes (Kirk, 2001). These pathways are induced in the erythrocyte membrane 10-20 hours post-invasion. They have a broad specificity and are permeable to both organic and inorganic cations and anions, zwitterions and non-electrolytes (Kirk, 2001). NPP make a small contribution to the net uptake of glucose (Krishna *et al*, 2000), but have a low to negligible permeability to sucrose (M_r = 342; Ginsburg *et al*, 1985). It is therefore unclear whether NPP have a fixed size cut

off but they have been shown to accommodate compounds with a molecular weight as large as 613 dalton (Kirk, 2001).

Once in the erythrocyte cytoplasm the solutes diffuse to the parasite vacuole membrane and cross it via a nutrient channel. Once in the space between the parasite vacuole membrane and the parasite plasma membrane they are taken up into the parasite by either endocytosis or by transport pathways of varying specificity (Gero and Kirk, 1994; Desai *et al*, 1993).

1.6.1.2 The direct access model

In the direct access model, solutes gain access to the parasite cytoplasm by more direct means. Firstly, solutes may enter and leave the erythrocyte cytosol in the same ways as in the conventional model. From the cytosol, the solutes may gain access to the parasite by either endocytosis or by diffusing through channels that span both the parasite vacuole membrane and the parasite plasma membrane thereby connecting the two and creating a direct passage. The 'metabolic window' involves all three membranes in close opposition allowing substrate to be taken up in one step possibly through a channel connecting all three membranes. An alternative suggestion is that solutes may reach the parasite plasma membrane directly through a 'duct' and then be taken up into the parasite by endocytosis or by a nutrient channel in the parasite plasma membrane (Kirk, 2001).

1.6.2 Nutrient requirements

1.6.2.1 Glucose

The asexual stage malaria parasite and the erythrocyte it invades have no carbohydrate reserves and are completely dependent on monosaccharides supplied from the host's blood plasma. The rate of glucose consumption by *P. falciparum* is up to two orders of magnitude higher than that in normal uninfected-erythrocytes (Krishna *et al*, 2000). Glucose is the key carbon source for both the host erythrocyte and the parasite, and both depend on glycolysis for ATP production (Tanabe, 1990).

The earliest *in vitro* studies demonstrated that externally added glucose disappeared more rapidly from the medium surrounding infected erythrocytes than it did from the medium surrounding uninfected erythrocytes (Sherman, 1988). Non-metabolised analogues of D-glucose such as 2-deoxy-D-glucose, 3-*O*-methyl-D-glucose and 6-deoxy-D-glucose (2-DOG; 3-OMG and 6-DOG, respectively) can be used to study glucose transport thereby distinguishing transport from catabolic processes (Tanabe, 1990). The glucose analogue 3-OMG was used by Sherman and Tanigoshi (1974) to study the transport of glucose in *P. lophurae* (bird) -infected erythrocytes. They determined that the increased rate of entry of 3-OMG was related to parasite growth and they hypothesised that entry was mediated by simple diffusion as well as facilitated diffusion. This facilitated diffusion was hypothesised to be from the endogenous glucose transporter since the V_{max} increased 8-fold whilst K_m was the same as the endogenous transporter. Other studies involving mice parasite-infected erythrocytes revealed that whilst the uninfected erythrocyte was impermeable to L-glucose, permeability to L-glucose increased in parasite-infected erythrocytes, indicating transport via an alternative route and not via the endogenous glucose transporter GLUT1 (Tripatara and Yuthavong, 1986).

With the successful cultivation of *P. falciparum in vitro* (Trager and Jensen, 1976), permeability studies could be extended to human parasite-infected erythrocytes. Studies by Ginsburg *et al* (1986) using solute-induced haemolysis of *P. falciparum*-infected erythrocytes revealed that permeability to carbohydrates was selective. Based on the entry characteristics of a variety of substrates they postulated the involvement of a positively charged pore. Transport was later postulated to be via simple diffusion (Ginsburg and Stein, 1987), which would account for the stereo-specific indiscrimination observed in infected erythrocytes with L- and D-glucose.

Tanabe (1990) postulated that L- and D-glucose gained entry into the infected erythrocyte cytoplasm by parasite induced NPP, and then crossed the parasite plasma membrane via an H^+:D-glucose cotransporter. An ATPase coupled proton pump would then replenish the protons, generating an electrochemical proton gradient across the parasite plasma membrane (Tanabe, 1990). Kirk *et al* (1996) set out to determine whether transport across the IRBC membrane was via an active transport

process or rather a passive (equilibrative) transport process. By using non-metabolised glucose analogues 2-DOG and 3-OMG they noted that the analogues failed to accumulate in the infected erythrocytes to levels above those of the external medium. They therefore determined that transport of glucose into the infected erythrocyte was via a passive glucose transport system, and not an active one (Kirk *et al*, 1996). This was later confirmed with the glucose analogue 6-DOG (Goodyer *et al*, 1997). By using cytochalasin B, a potent inhibitor of GLUT1, Goodyer *et al* postulated that most of the glucose transported into parasite-infected cells was via this endogenous transporter, and that a small amount was transported via NPP. This additional transport via NPP would account for the small levels of L-glucose transported into the parasite-infected erythrocyte (Goodyer *et al*, 1997).

A *P. falciparum* hexose transporter was recently isolated and sequenced by Woodrow *et al* (1999). By using an immunolocalization technique with antibodies raised against the N-terminal (residues 6-21) of PfHT1 and immunofluorescence they determined the transporter to be on the PPM. The stage specific expression of PfHT1 mRNA was monitored in synchronous *P. falciparum* cultures relative to that of a housekeeping gene β-tubulin. An early peak of mRNA expression was detected at the ring stage, which represents a time point of parasite development 8-16 hours after invasion. After 16 hours PfHT1 mRNA levels drop and increase again to intermediate levels during trophozoite and merozoites development (Woodrow *et al*, 1999).

Unlike the mammalian glucose transporter GLUT1, PfHT1 is capable of transporting fructose as well as glucose. Human erythrocytes also have a separate fructose transporter GLUT5 (Concha *et al*, 1997). It is therefore postulated that monosaccharides, glucose and fructose gain entry into the parasite by first crossing the IRBC via GLUT1 and GLUT5. Small amounts of monnosaccharides also cross the IRBC via NPP, accounting for stereo-isoforms (L-glucose) not usually permitted into uninfected erythrocytes. Substrates then cross the parasite vacuole membrane via high-capacity, non-selective channels. Both glucose and fructose are then transported across the parasite plasma membrane by PfHT1 (Figure 1.2; Krishna *et al*, 2000).

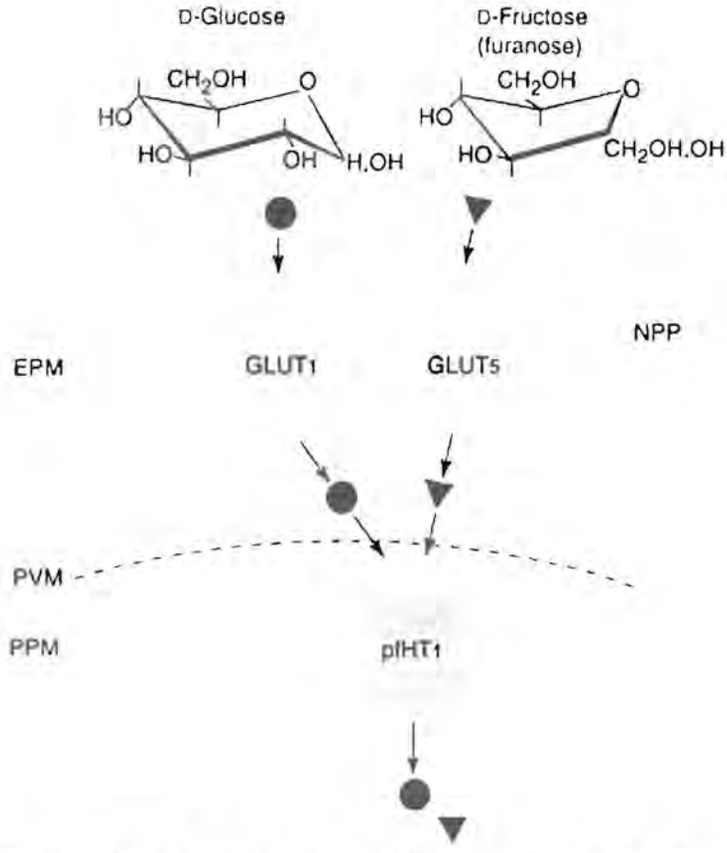

Figure 1.2: A model for hexose transport in the *Plasmodium falciparum* infected erythrocyte (Krishna *et al*, 2000). Glucose is represented by circles and fructose is represented by triangles. EPM, erythrocyte plasma membrane; PPM, Parasite plasma membrane; PVM, Parasite vacuole membrane; EPM, Erythrocyte plasma membrane; GLUT1, Mammalian glucose transporter 1; GLUT5, Mammalian glucose transporter 5; pfHT1, *P. falciparum* hexose transporter 1; NPP, New permeation pathway.

Since it is postulated that the majority of glucose and fructose gain entry into the IRBC by being transported via the endogenous GLUT1 and GLUT5 transporters, it is relevant to consider the transport properties of the uninfected erythrocyte membrane. The most active transporter in human erythrocytes is GLUT1, which comprises 3-5% of the total erythrocyte membrane proteins (Gould and Holman, 1993). GLUT1 was first isolated in the early 1980s by Baldwin *et al* (1982). To date 5 plasma membrane facilitated sugar transporters have been isolated and cloned (GLUT1-5; Walmsley *et al*, 1998) and a further 3 have been identified, namely the pseudogene GLUT6 (Kayano *et al*, 1990), the microsomal glucose transporter GLUT7 (Waddell *et al*, 1992) and the blastocyst glucose transporter GLUT8 (Carayannopoulos *et al*, 2000). These transporters fall into the major facilitator superfamily (MFS) also called the uniporter-symporter-antiporter family. Most of these families consist of proteins

predicted to have 12 transmembrane segments. The remainder have 14 predicted transmembrane segments (Pao *et al*, 1998).

The 12-transmembrane structure was first predicted for GLUT1 by Mueckler *et al* (1985) from analysis of a hydropathy plot, which was predicted from the transporter amino acid sequence (Figure 1.3). One *N*-linked oligosaccharide was predicted to be localised to either the C- or N-terminal third of the molecule at Asn^{45} or Asn^{411}. From the hydropathy plot Asn^{411} was predicted to lie within the membrane-spanning domain, therefore they predicted Asn^{45} to be the glycosylated site (Mueckler *et al*, 1985). By using *N*-glycasane treated human glucose transporter reconstituted in liposomes, this *N*-linked oligosaccharide was determined to be essential for glucose transport activity (Feugeas *et al*, 1990). From the hydropathy plot GLUT1 was predicted to have a small N-terminal hydrophilic domain assigned to the cytoplasmic face, and a larger hydrophilic C-terminal also on the cytoplasmic side (Mueckler *et al*, 1985). These findings were confirmed by proteolytic digestion with trypsin (Cairns *et al*, 1987).

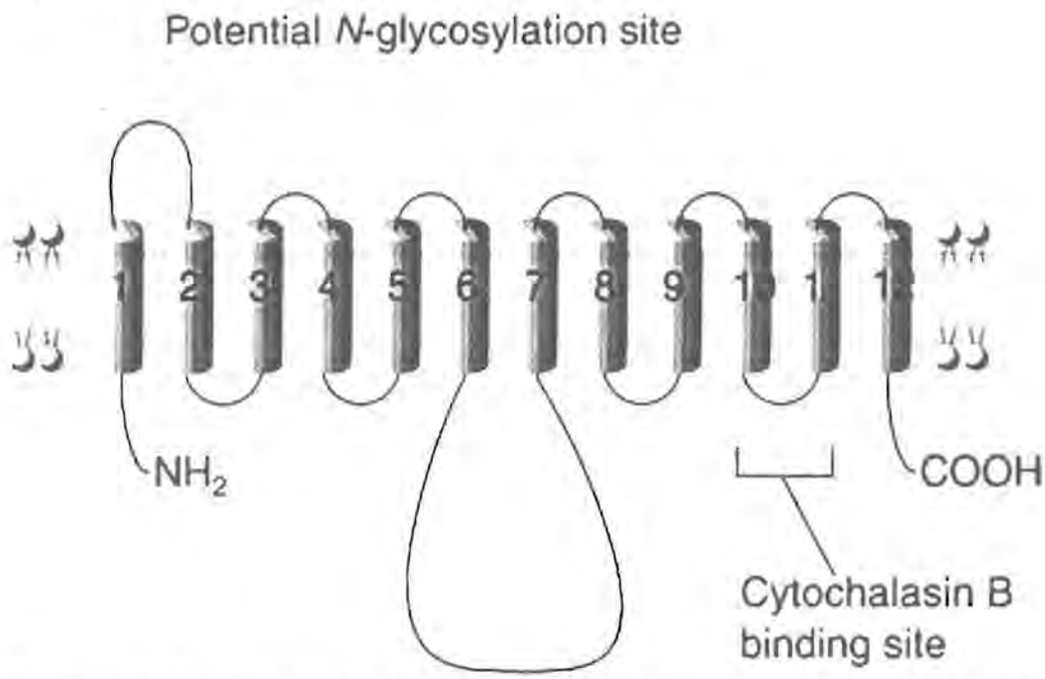

Figure 1.3: Schematic model of GLUT1 based on Mueckler's original proposal (Mueckler *et al*, 1985). Both the N- and C-terminal ends face inward. The *N*-glycosylation site lies between helices 1 and 2. A large endofacial loop lies between helices 6 and 7.

The transporter has both inward and outward facing sugar-binding sights predicted from binding of ethylidene glucose and cytochalasin B that fix the transporter in its

exofacial (outward facing) and endofacial (inward facing) conformations respectively (Walmsley, 1988). The kinetic mechanism of sugar transport is thought to be by sugar binding to the endofacial site causing a conformational change, which translocates the sugar across the membrane to be released from the exofacial conformation. Therefore sugar translocation occurs as the transporter oscillates between these conformations (Walmsley *et al*, 1998).

1.6.2.2 Amino acids and peptides

It was already established more than 40 years ago that the malaria-infected erythrocytes had an increased permeability towards amino acids (Sherman, 1988). As with uptake of exogenously supplied glucose, uptake of amino acids was dependent on the parasite species, size and its environmental condition (Sherman, 1988). The malaria parasite is thought to have limited ability to synthesise amino acids and most of its required amino acids are therefore derived from alternative sources (Kirk, 2001). The parasite is able to obtain amino acids in three ways: biosynthesis from other carbon sources, uptake from external media and catabolism of host haemoglobin (Kolakovich *et al*, 1997).

The parasite utilises haemoglobin as its primary source of amino acids. This hypothesis is supported by a 25-75% decrease in haemoglobin content of infected erythrocytes (Rosenthal and Meshnick, 1996). An acidic organelle called the digestive organelle is the site of haemoglobin proteolysis. The ingestion of the haemoglobin occurs through a structure called a cytosome. This is a mouth-like apparatus, which opens through the double membrane separating the parasite and erythrocyte cytoplasms. The cytosome buds off in the parasite forming a transport vesicle that then joins with the digestive vacuole where the haemoglobin is degraded (Rosenthal and Meshnick, 1996).

Inside the digestive vacuole two aspartic proteases, plasmepsins I and II, and one cysteine protease, falcipain, cleave haemoglobin into peptides. It was previously thought that peptides were degraded into single amino acids inside the digestive vacuole, but recent work by Goldberg's group contradicts this idea (Kolakovich *et al*,

1997). According to this work peptides are transported out of the vacuole and into the cytoplasm where exopeptidase convert the peptides into individual amino acids.

The short-term survival of *P. falciparum in vitro* requires exogenously supplied isoleucine and methionine, and growth over longer periods requires the supply of glutamine, glutamate, cysteine, proline and tyrosine to the growth medium (Divo *et al*, 1985). However, even amino acids that are not essential to the parasite are taken up from the extracellular medium (Kirk, 2001). The erythrocyte plasma membrane has a variety of different amino acid transport systems, and the majority of required amino acids seem to be transported via these endogenous transporters (Kirk, 2001). Glutamate does not gain entry via the endogenous transporters (Kirk, 2001) and may gain entry into the erythrocyte via NPP (Ginsburg *et al*, 1985). Whether amino acids gain entry into the infected erythrocyte via endogenous transporters or parasite-induced pathways still remains to be elucidated.

1.6.2.3 Nucleosides

Unlike mammalian cells, the malaria parasite is incapable of *de novo* synthesis of the purine ring. The parasite is therefore dependent on transporters and salvage pathways for purine nucleotide synthesis from host precursors (Parker *et al*, 2000). A number of purine salvage enzymes have been identified in the parasite, for example hypoxanthine-guanine-xanthine phosphoribosyltransferase (Keough *et al*, 1999). The parasite is however able to synthesise pyrimidines, and salvage pathways have not been identified for pyrimidine rings. Several antimalarial drugs target *de novo* pyrimidine metabolism, for example sulfadoxine is an inhibitor of parasite dihydropterate synthase and pyrimethamine and cycloguanil inhibit dihydrofolate reductase (Parker *et al*, 2000).

The host erythrocyte has endogenous nucleoside transporters, which are enantiomerically selective (Upston and Gero, 1995). The endogenous nucleoside transporters in infected erythrocytes are responsible for 50% of the total nucleoside transport into the cell and are potently inhibited by a structural analogue of adenosine 6-((4-nitrobenzyl)thio)-9-β-D-ribofuranosylpurine (NBMPR). The parasite derived nucleoside transporters are distinct from the endogenous transporters in their inability

to be inhibited by NBMPR and were found to be a combination of nonsaturable and carrier-mediated transporters (Upston and Gero, 1995).

Recently the *Xenopus* oocyte expression system has been used to express and characterise a *P. falciparum* encoded nucleoside transporter. This transporter was identified by two independent research groups and was designated two different names, PfENT1 (Parker *et al*, 2000) and PfNT1 (Carter *et al*, 2000). The nucleoside transporter in each paper has an identical protein sequence, but there are discrepancies regarding its substrate affinities between the two studies. In the study by Carter *et al* the K_m for D-adenosine was reported to be 13,2 μM, and in the study by Parker *et al* the K_m was determined to be 320 μM. Other discrepancies included the transport of nucleobases such as hypoxanthine. Where PfNT transport of D-adenosine was not inhibited to any significant degree by hypoxanthine, PfENT1 was with a K_m for hypoxanthine of 0.41 mM. It was also reported that PfNT1 was 85% inhibited by dipyridamole, whereas PfENT1 was not inhibited at all by dipyridamole (Carter *et al*, 2000; Parker *et al*, 2000). Further elucidation of this transporter is required.

1.7 Trafficking and secretion in *Plasmodium*

Understanding the malaria parasites trafficking mechanisms can give scientists a better understanding of this pathogen, as well as help to identify potential antimalarial targets. Since *P. falciparum* is a eukaryotic organism, it can be assumed that the organism will have similar trafficking mechanisms to other eukaryotes for the synthesis and export of proteins.

1.7.1 General eukaryotic secretion

Secretory activities are conserved in higher eukaryotes that have been studied to date, which include yeasts and mammals. The largest membrane in an eukaryotic cell is the endoplasmic reticulum (ER). The smooth ER is the site of synthesis and metabolism of fatty acids and phospholipids. The rough ER synthesizes certain membrane and organelle proteins as well as all proteins to be secreted from the cell. A signal sequence on all newly synthesized secretory proteins targets them to the ER. This sequence is 16-30 amino acids long and directs the ribosome to the ER membrane and

initiates the transport of the growing polypeptide across the membrane. The chaperone Bip binds to the growing chain on the ER luminal surface and with the help of hydrolysis of ATP, releases the newly synthesized chain into the lumen of the ER. Bip also facilitates the eventual folding of many secretory proteins. Cytosolic proteins are released into the ER lumen or the ribosome is released from the ER membrane and continues to synthesise the membrane protein in the cytosol. Enzymes on the luminal side of the ER add carbohydrates to the chain (Lodish *et al*, 1995).

Several minutes after their synthesis, most proteins leave the rough ER within membrane-bounded transport vesicles that bud off from the ER. The vesicles carry the proteins to the Golgi complex, which has three defined sections: the *cis*, *medial* and the *trans*. The transfer vesicles fuse with the *cis* region of the Golgi where they deposit their proteins. The proteins then progress from the *cis* to the *medial* to the *trans* regions where different enzymes modify secretory and membrane proteins differently. After modification the proteins are transported out of the complex by a second set of transport vesicles that bud off from the *trans* domain. The transport vesicles fuse with the plasma membrane resulting in the release of its secretory proteins, or the fusion of its membrane bound protein with the plasma membrane (Lodish *et al*, 1995).

1.7.2 Trafficking of proteins within the malaria parasite

In order to get to the IRBC membrane cytosolic, surface and parasite derived proteins have to transverse the PPM, parasite vacuole membrane and through the IRBC cytosol (Foley and Tilley, 1998). Classical secretory mechanisms such as those mentioned in Paragraph 1.7.1 may be involved to take the protein as far as the PPM, but thereafter secretory mechanisms involved in taking the protein to its final destination are speculations.

1.7.2.1 The parasitic endoplasmic reticulum

Since the first application of the electron microscopy to malariology in 1957, evidence has existed for the presence of an ER that was observed in the parasitized

cell (Aikawa, 1971). Further evidence for a parasitic ER can be gained from proteins which transverse through the ER on their way to their final destination. These proteins can be detected by immunoelectron microscopy close to the cytoplasmic side of the parasite nuclear membrane where an ER would be located. One such protein is PFGCN20, which is located in the lumen of the parasite vacuole (PV) or in PV protrusions. PFGCN20 is an ATP-binding cassette protein and is closely related to the yeast translation regulator Gcn20p. It has been detected in membranous structures at the side of the nuclear membrane before transport to the PV (Bozdech *et al*, 1998).

Homologues of trafficking components such as the 78 kDa glucose-regulated protein (grp78) identical in sequence to the globulin-binding protein Bip, whose function is summarized in Paragraph 1.7.1, has also been identified (Kumar *et al*, 1988). This homologue in *P. falciparum* is called Pfgrp and has a carboxylic terminus Ser-Asp-Glu-Leu (SDEL; Kumar *et al*, 1991). This is similar to mammalian grp78 proteins that have a C-terminus, Lys-Asp-Glu-Leu (KDEL) and in yeast cells that have a C-terminus His-Asp-Glu-Leu (HDEL; Kumar and Zeng, 1992). This C-terminus sequence is essential for the proteins retention in the lumen of the ER (Munro and Pelham, 1987). Synthesis of grp78 is induced by the presence of misfolded protein and forms tight bonds with misfolded proteins and assists in their proper assembly and folding (Kassenbrock *et al*, 1988). Using a highly specific antiserum in an investigation by immuno-gold electron microscopy, Pfgrp was localized in the cytoplasm of the parasite in ER-like membranous structures (Kumar *et al*, 1991).

1.7.2.2 An alternative ER-like organelle

Studies have shown that many *Plasmodium* proteins that are destined for export are not processed by the ER and Golgi, but are exported via an alternative pathway (Wiser *et al*, 1997). This is based on blockage experiments with Brefeldin A (BFA). BFA is a unique fungal antibacterial agent that has a 13-membered macrocyclic lactone ring (Misumi *et al*, 1986). BFA is known to inhibit protein secretion in higher eukaryotes by disrupting the integrity of the Golgi apparatus (Benting *et al*, 1994). In a study conducted by Misumi *et al* (1986) they attempted to determine the effect of BFA on the transport of secreted proteins. They found that BFA had little effect on

protein synthesis but had a dose-dependent inhibitory effect on protein secretion from the classical secretory pathway. Treatment with BFA caused a marked alteration in the ER. The ER with or without ribosomes was markedly dilated and contained unstructured material in the ER lumen, which they postulated to be secretory proteins (Misumi *et al*, 1986).

Lippincott-Schwartz *et al* (1989) established that in BFA treated murine cells *cis/medial* Golgi compartments redistributed to and became part of the ER. This resulted in glycoproteins being processed by *cis/medial* Golgi enzymes within the ER lumen. The effect of BFA was reversed upon removal of the drug. Golgi proteins were then transported from the ER into a newly formed Golgi whilst ER-resident proteins, with which they had been mixed, remained in the ER (Lippincott-Schwartz *et al*, 1989).

Treatment of *Plasmodium* infected rodent cells with BFA caused the formation of a single BFA-induced compartment in which secreted proteins such as Pb(em)65, a *P. berghei* erythrocyte membrane located protein, accumulated (Wiser *et al*, 1997). After BFA treatment, Pb(em)65 was associated with the parasite in a single BFA-induced structure that was observed at the parasite periphery. A similar pattern was observed for Pb(ec)13 and Pb(ec)31, which are normally localized to non-membrane bound inclusions in the erythrocyte cytoplasm. A parasite protein that resides in the lumen of the ER, Pfgrp, was used as a control and was found to accumulate in membrane vesicles at the cytosolic side of the nucleus after treatment with BFA. This suggests that Pfgrp remains in the ER and is not affected by BFA treatment, and that the inclusion at the parasite periphery was not the ER. Therefore Pb(em)65 was not transversing through the ER but accumulated in a previously undetected compartment. This ER-like organelle located at the parasite periphery may specialize in export of proteins to the erythrocyte cytoplasm and EM. Wiser *et al* proposed to call this ER-like compartment sERA: secondary ER of apicomplexa (Wiser *et al*, 1997).

1.7.2.3 Golgi vesicles

The Golgi is the major site for sorting of proteins and lipids in eukaryotic cells. *N*-glycosylation is one of the major markers used for Golgi detection, since *N*-glycosylation occurs in the ER and the *N*-glycosylated protein can then be monitored as it transverses through the Golgi vesicles. PfHT1 is predicted to have *N*-linked oligosaccharides. Potential glycosylation sites (NXT or S, where X is any amino acid) are at asparagines 69 and 72 (Woodrow *et al*, 1999) located similarly to GLUT1 asparagine 45 (Meuckler *et al*, 1985). *N*-linked oligosaccharides in *P. falciparum* are predicted to occur at low concentrations and therefore have not been used as a Golgi marker (Gowda and Davidson, 1999).

An enzyme that is normally associated with the Golgi, sphingomyelin synthase, is one Golgi marker that has been detected in the malaria parasite (Haldar *et al*, 1991). Uninfected erythrocytes are incapable of sphingomyelin synthesis. Studies with both fluorescent and radiolabelled ceramides have shown that ceramides are converted to sphingomyelin in infected but not in uninfected erythrocytes. The levels of sphingomyelin in the host cell membrane are decreased upon infection with *P. falciparum*, which suggests that the host's sphingomyelin is internalised and degraded to ceramide by the parasite and presumably re-converted to sphingolipids in the Golgi apparatus (Haldar *et al*, 1991).

The binding and metabolism of a fluorescent ceramide analogue *N*-[7-(4-nitrobenzo-2-oxa-1,3-diazole)] amino-caproyl sphingosine (C6-NBD-cer) was investigated in *P. falciparum* infected cells. Earlier studies on live mammalian cells showed that C6-NBD-cer was metabolised to C6-NBD-cerebrosides and C6-NBD-sphingomyelin (C6-NBD-Sm), providing *trans* Golgi markers (Pagano *et al*, 1989). In *P. falciparum*-infected erythrocytes these markers were found to accumulate in the parasite vacuole membrane and flattened cisternae in the infected-erythrocyte cytosol (Haldar *et al*, 1991; Elmendorf and Haldar, 1994). This was the first report on the distribution of Golgi markers and also raised speculation on Golgi-like elements beyond the parasite membrane. This is comparative to other eukaryotic studies such as those done on rat liver cells where 87% of sphingomyelin synthase activity was found in the Golgi and

the remaining 13% in the plasma membrane, suggesting a second site of sphingomyelin activity in cells (Elmendorf and Haldar, 1994).

A *P. falciparum*-derived protein homologous to ERD2, a Golgi marker in higher eukaryotes, was discovered. For soluble proteins in the ER the signal for retention is a tetrapeptide sequence at the C-terminus mentioned in paragraph 1.7.2.1. ERD2 is found in the *cis*-Golgi and recognises this signal on polypeptides that stray from the ER and returns them. The *P. falciparum* ERD2 (PfERD2) has 42% identity to the higher eukaryotic ERD2. Immunofluoresent studies of PfERD2 conducted on parasitized cells localized it to a tightly defined perinuclear spot (Elmendorf and Haldar, 1993).

Additional Golgi markers have been identified that are members of a GTP-binding protein family namely rab1, rab6 and rab11. Like PfERD2, rab6 has been localised to tubulovesicular membranes in the parasite, with multiple dispersed sites in the ring stage and the trophozoite stage, and in closer proximity to the plasma membrane than that seen for PfERD2. This suggests that Golgi membranes lack cisternal structure and are rather tubulovesicular, and since they are also dispersed suggests that the Golgi elements in the parasite are not stacked as in mammalian Golgi (Van Wye *et al*, 1996).

1.7.3 Trafficking of proteins beyond the parasite periphery

As in any eukaryote, secreted proteins of *Plasmodium* can be transported within the parasite cell via conventional modes of transport such as the ER and Golgi apparatus, which will take them as far as the PPM. Some proteins need to transverse further than the parasite plasma membrane such as erythrocyte cytosolic parasite antigens and antigens presented on the infected erythrocyte membrane.

1.7.3.1 Proposed models of trafficking beyond the parasite plasma membrane and PVM

There is an added complexity to the protein trafficking in malaria infected erythrocyte in that the parasite needs to transport proteins beyond the confine of its own plasma membrane. To date two models have been proposed for the translocation of the secreted proteins across the parasite plasma membrane and parasite vacuole membrane (Lingelbach, 1997; Foley and Tilley, 1998).

1.7.3.1.1 The two-step model

In this model proteins may enter the ER and are secreted into the PV via a classical vesicle-mediated pathway (Figure 1.4, steps 1 and 2). All secreted proteins are targeted to the PV and are sorted there. Once in the PV, proteins destined for the IRBC cytosol and the IRBC membrane will need to be translocated across the parasite vacuole membrane possibly via membrane pores (Figure 1.4, step 3; Foley and Tilley, 1998).

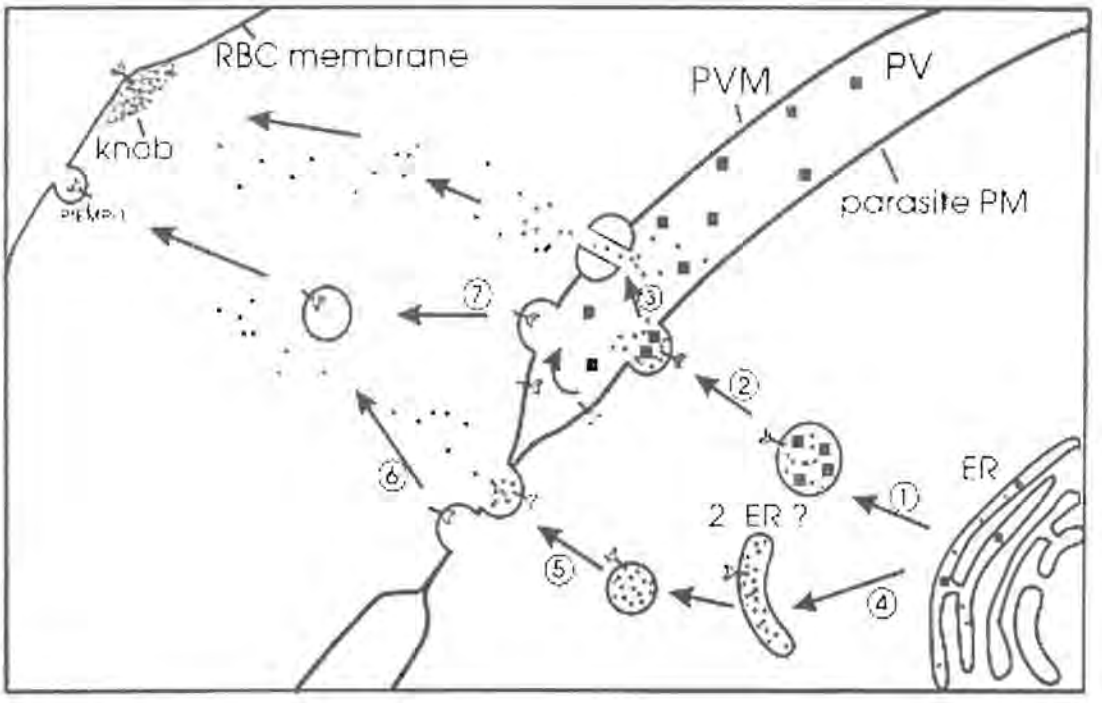

Figure 1.4: Models for sorting of proteins destined for different compartments in malaria-infected erythrocytes (Foley and Tilley, 1998). Proteins (squares) destined for the parasite vacuole (PV) remain trapped in the PV (Steps 1 and 2). Proteins (circles) that are destined for the erythrocyte cytoplasm or the red blood cell

membrane (RBC membrane) may be secreted into the PV and then translocated across the parasite vacuole membrane (PVM; Step 3). Alternatively, they may be sorted into a specialised secretory organelle (Step 4) and secreted directly into the erythrocyte cytoplams at a fused site in the parasite plasma membrane (parasite PM) and parasite vacuole membrane (Step 5). Transport to the red blood cell (RBC) membrane may occur by budding vesicles or by protein aggregate diffusion (Steps 6 and 7).

1.7.3.1.2 The single-step model

In this model malaria proteins located beyond the parasite plasma membrane are targeted to sites where the parasite plasma membrane and parasite vacuole membrane have fused. Therefore the proteins are translocated across two membranes in a single step. The proteins are contained in transport vesicles. Since some proteins would be transported to the PV or parasite vacuole membrane and some to the RBC cytosol and RBCM, two different types of transport vesicles would be required. One type of vesicle would target proteins to a PPM-PVM fusion site for transport to the IRBC membrane and IRBC cytosol (Figure 1.4, steps 4-5). The other type of vesicle would fuse to the parasite plasma membrane to release proteins into the PV (Figure 1.4, steps 1-2). This would require a detailed secretory mechanism apart from the ER, where the sERA possibly play a part (Figure 1.4, step 4; Lingelbach, 1997; Foley and Tilley, 1998).

1.7.3.2 Intra-erythrocytic membranes for transport beyond the PVM

The malaria parasite produces a complex membrane structure within red blood cells that it infects. The most prominent structure is the tubulovacuolar network (TVN), which is also known as the tubulovesicular membrane (TVM) originally coined by Elmendorf and Haldar (1993).

The tubovesicular membrane appears to be continuous with the parasite vacuole membrane and extends into the cytoplasm of the IRBC. Some researchers have claimed that the tubovesicular membrane functions to transport proteins to the IRBC membrane but have so far failed to find any evidence for a direct connection between the cytoplasmic side of the IRBC membrane and the extended arms of the tubovesicular membrane (Fujioka and Aikawa, 1993). The tubovesicular membrane

does however appear to have some function similar to the Golgi, since sphingomyelin synthase activity appears to be partially located within the tubovesicular membrane (Elmendorf and Haldar, 1994). However limitation of tubovesicular membrane growth by treatment with sphingomyelin synthase inhibitor does not prevent protein transport. The tubovesicular membrane also appears much later (33h post invasion) than parasite antigen presentation on the IRBC membrane. The necessity of the tubovesicular membrane for protein export is therefore debatable (Lauer *et al*, 1997).

1.8 Conclusion

The malaria parasite species most responsible for malaria related devastation, *P. falciparum*, is slowly building up resistance to the armoury of drugs used against it. Its vector, the *Anopheles* mosquito, is itself building up resistance to current insecticides and remaining options such as a vaccine remains elusive. The great hope for eradication of malaria held during the 1960s has not been realised and more people are exposed to malaria today than were during the last century.

Hope now exists in new drug target identifications that may lead to more affordable and effective drugs. To achieve this, researchers must focus on validated targets for drug design and identify targets by studying basic and metabolic processes essential for the parasites survival. One valid and obvious target would be to focus on the parasites main source of energy: glucose. The parasite has no glycogen reserves and is dependent on its host for its glucose supply. *P. falciparum* parasites are able to sustain life in fructose-substituted glucose-free medium and therefore if one parasite derived transporter exists for the transport of both monosaccharides to the parasite, this could be a valid drug target. Recently one such transporter was discovered: PfHT1 (Woodrow *et al*, 1999).

The research on the *P. falciparum* glucose transporter has only just begun, and compared to research on the mammalian glucose transporter GLUT1, much work is needed to elucidate the mechanism of this transporter to identify parasite specific properties. Already a discrepancy has emerged in that the PfHT1 transports both glucose and fructose, whereas GLUT1 does not. It has been hypothesised by Krishna

et al that glucose and fructose gain entry into the IRBC via GLUT1 and GLUT5, and a small amount via NPP (Krishna *et al*, 2000).

As yet no parasite derived hexose transporters have been identified except for PfHT1. Identification of the regions of PfHT1 responsible for glucose and fructose transport that distinguishes it from GLUT1 would be important information for drug design. Inhibiting PfHT1 is anticipated to have two advantages, that (1) diversion of essential glucose away from the parasite will prevent problems symptomatic of malaria such as hypoglycaemia, and (2) killing parasites may be more effective if inhibitors of PfHT1 are combined with common antimalarials than by using antimalarials alone (Woodrow *et al*, 1999).

1.9 Aims and strategy of the study

With the isolation, cloning and sequence analysis of the *P. falciparum* hexose transporter already accomplished, its characterisation is underway. So far little is known as to what distinguishes this transporter from all the other well described mammalian transporters (GLUT1-5). The main question is: what allows this transporter the ability to transport both glucose and fructose, whereas no such transporter exists for higher eukaryotes? This question has been addressed in a recent study conducted by Woodrow *et al* (2000) and is extended by research described in the current study.

Until a crystal structure becomes available of the facilitated glucose transporters, indirect methods have to be applied to elucidate their mechanisms. Indirect mechanisms methods include mutational studies applied to GLUT1 to identify helices within the transporter that are thought to arrange in an aqueous core and interact directly with the substrate. Glucose analogue studies can also aid the identification of carbon atoms on the glucose ring involved in protein-substrate interactions. Mutational studies also help identify amino acids essential for protein-substrate interactions to discover the properties needed for putative chemotherapeutic drugs to be affective inhibitors of glucose transport.

A mutational strategy based on PCR to produce point mutations will be outlined in Chapter 2. Kinetic studies on these point-mutated hexose transporters are described in Chapter 3 using a *Xenopus* oocyte expression system. Then finally studies with mammalian/ PfHT1 chimeras, along with Western blotting are described in Chapter 4. These results contribute towards a better understanding of the PfHT1 transporter of the malaria parasite.

t=0hrs, frozen samples from 3 Feb 02

	0	20	40	60	80	100	120	140	160	180
	0.23	0.213	0.208	0.197	0.184	0.17	0.156	0.139	0.119	0.104
	0.234	0.204	0.22	0.196	0.187	0.168	0.155	0.14	0.127	0.111
	0.228	0.207	0.21	0.199	0.186	0.173	0.156	0.144	0.119	0.111
AVE	######	0.208	0.2127	0.1973	0.1857	0.1703	0.1557	0.141	0.1217	0.1087
AVE-0.0	######	######	######	######	######	######	######	######	######	######
%ABS	100	87.792	90.305	82.047	75.763	67.504	59.605	51.706	41.293	34.291

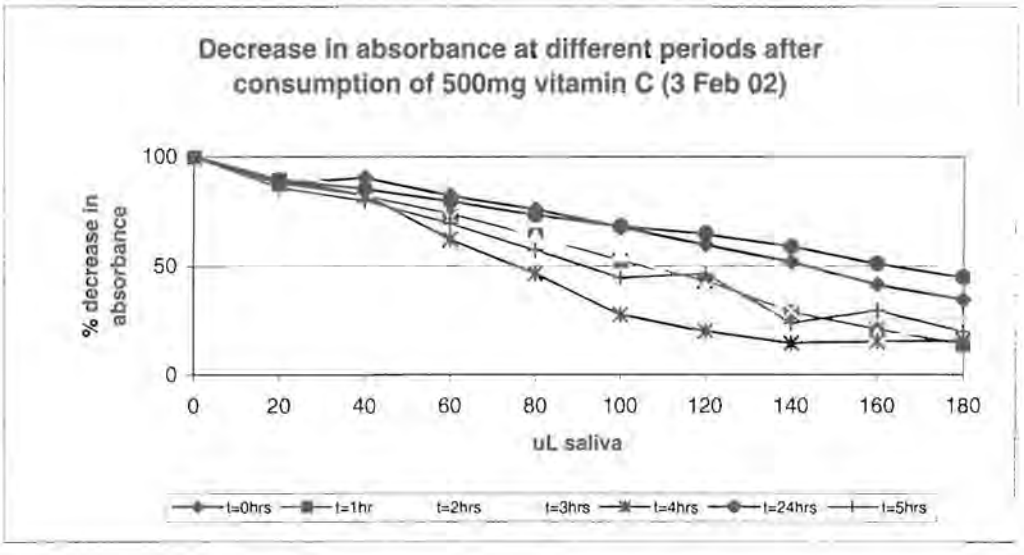

2 CHAPTER TWO:

CLONING, NUCLEOTIDE SEQUENCES AND RNA SYNTHESIS OF MUTATED *P. FALCIPARUM* HEXOSE TRANSPORTERS

2.1 Introduction

For glucose transport, mammalian cells employ Na^+-dependent co-transporters and the simple facilitative uniporters. The facilitative glucose transporters (GLUT1-5) are the most thoroughly studied of all facilitated diffusion transport systems. They are energy-independent systems that only transport down a concentration gradient, and are therefore most effective in environments where continual exposure to high concentrations of substrate is experienced (Mueckler, 1994).

Indirect approaches such as glycosylation-scanning mutagenesis (Hresko *et al*, 1994), cysteine-scanning mutagenesis (Olsowski *et al*, 2000) and site-directed mutagenesis (Seatter *et al*, 1998) have been applied extensively to GLUT1 and have provided insight into its secondary and tertiary structure. Mueckler *et al* (1985) proposed a 12 transmembrane helical model for the glucose transporter from human HepG2 hepatoma cells. Two alternative topographic assignments of GLUT1 have since been proposed. One favours a secondary structure with 16 β-strands resembling the bacterial porin protein (Fischbarg *et al*, 1993). The other favours an α-helix-β-strand transmembrane structure with 14 membrane spanning segments (Ducarme *et al*, 1996). Studies conducted by Alvarez *et al* (1987) using Fourier transform infrared (FT-IR) spectroscopy revealed that more than 80% of the polypeptide backbone of GLUT1 is accessible to solvent which is consistent of a pore like structure. Circular dichroism measurements have indicated that the protein is made largely of α-helices (70%) with 20% β-turns and 10% random coil (Chin *et al*, 1986). These findings support the 12 α-helical model. The results obtained from a glycosylation scanning mutagenesis study conducted by Hresko *et al* (1994) also strongly supported this

model. A potential site of *N*-linked glycosylation (Asn-X-Ser or Thr, where X is any amino acid) was identified at Asn^{45} for the 12 helical model (Muekler *et al*, 1985).

There are 10 invariant amino acid residues in all members of the sugar transporter family (Kayano *et al*, 1990). Humans, rats, mice, pigs and rabbits all have GLUT1s that have 492 residues and are more than 97% identical in sequence (Mueckler, 1994). For the proposed 12 helical model, 5 of the 12 transmembrane helices (helices 3, 5, 7, 8 and 11) are capable of forming amphipathic α-helices and are predicted to form an aqueous pore (Mueckler and Makepeace, 1999). Most structure/ function studies concerning facilitated glucose transporters have been conducted on GLUT1 mainly on the 5 proposed amphipathic helices and conserved amino acids. As a result a few interesting details have appeared in the literature in accordance with the proposed 12 helical model.

Tryptophan is a rare amino acid in proteins and usually plays a role in structure and catalytic activity. GLUT1 has 6 Tryptophan residues, three of which are conserved in GLUT1-5. In a study conducted by Garcia *et al* (1992) the tryptophan residues in GLUT1 were changed to either glycine or leucine residues. Transport was decreased in the Trp-388 (helix 10) and Trp-412 (helix 11) mutants but was unaltered in all the other mutants. Proline 385 in helix 10 when mutated to isoleucine resulted in the transporter being fixed in the inward facing conformation (Tamori *et al*, 1994). Cysteine 429 within the 6^{th} external loop, and cysteine 207 at the beginning of the large intracellular loop connecting helix 6 and 7 was predicted to contribute towards the transport of glucose (Wellner *et al*, 1994). Glutamine 161 (helix 5) was predicted to form part of the exofacial ligand binding site of GLUT1 and when mutated to leucine or asparagine the transport activity is reduced by 50% and 10%, respectively (Mueckler *et al*, 1994). Proline residues in helix 6 and 10 were investigated with point mutations. Proline residues in GLUT1, conserved in all human glucose transporter isoforms, were mutated to either alanine or the corresponding amino acid in GLUT2. The results revealed that no single proline residue was essential for transport activity. However proline substitutions in helix 10 to neutral residues completely abolished transport of 2-deoxy-D-glucose. Therefore the proline residues cis-trans shift is not

important for transporter activity but rather the chemical compositions of the amino acid side chains (Wellner *et al*, 1995).

Interest has been centred on the differences in transportation of glucose and fructose, and on amino acids responsible for the selectivity of substrate. For instance, the mammalian transporters GLUT1, 3 and 4 transport glucose only and all contain a conserved QLS motif in helix 7, whereas GLUT2 and 5 are capable of fructose transport and do not have this conserved motif (Table 2.1; Seatter *et al*, 1998). Arbuckle *et al* (1996) used chimaeric GLUT2/GLUT3 constructs to establish the site responsible for fructose transport. GLUT3 constructs containing the GLUT2 helix 7 segment were able to transport fructose to some degree (Arbuckle *et al*, 1996). Seatter *et al* (1998) took this idea one step further and prepared two mutants in which QLS of GLUT3 was substituted with the corresponding HVA from GLUT2 and *vice versa*. Their results suggested that the QLS motif in helix 7 is in some way responsible for the ability of GLUT 1, 3 and 4 to transport D-glucose and their inability to transport fructose.

Table 2.1: Sequence alignments of different hexose/ glucose transporter putative transmembrane helix 7 segments. The ability of each transporter to transport fructose and/ or glucose is indicated. Human glucose transporters have a common QLS motif (highlighted in bold) whereas human fructose transporters do not, and neither do the hexose transporters from the other organisms mentioned (Kayano *et al*, 1990; Barret *et al*, 1998). GLUT1-5, mammalian glucose transporters 1-5; PfHT1, *Plasmodium falciparum* hexose transporter; THT1, *Trypanosome brucei* hexose transporter one.

Transporter	Sequence	Transport of:
GLUT1	279 **QLS**QQLSGINA	Glucose
GLUT2	311 HVAQQFSGING	Glucose (low affinity) and Fructose
GLUT3	277 **QLS**QQLSGINA	Glucose
GLUT4	295 **QLS**QQLSGINA	Glucose
GLUT5	285 MGGQQLSGVNA	Fructose
PfHT1	302 SGLQQFTGINV	Glucose and Fructose
THT1	311 AGTLQLTGINA	Glucose and Fructose

Interest has also been placed on the 5 helices that are capable of forming amphipathic structures and therefore predicted to lie close to one another to form an aqueous core. Work involving GLUT1 helix 7 has established its role in exofacial ligand binding. Mutations in this helix, more specifically glutamine 282, resulted in reduced affinity for outside site-specific ligands 2-*N*-4-(1-azi-2,2,2-trifluoroethyl) benzoyl-1,3-bis(D-mannos-4-yloxy)-2-propylamine (ATB-BMPA) and 4,6-*O*-ethylidene-D-glucose indicating its possible role in substrate binding (Seatter *et al*, 1998; Hashiramoto *et al*, 1992). A cysteine-scanning mutagenesis study conducted by Hruz and Mueckler (1999) on helix 7 showed that cysteine replacement at positions near the exofacial side of the cell membrane, namely Gln^{282}, Gln^{283}, Ile^{287}, Ala^{289}, Val^{290} and Phe^{291} produced transporters that were inhibited by *p*-chloromercuribenzene sulfonate (pCMBS), which binds extracellularly. This provided evidence to support the hypothesised accessibility of this helix to the external solvent. The authors also proposed a possible model for GLUT1 helix packaging (Figure 2.1B; Hruz and Mueckler, 1999).

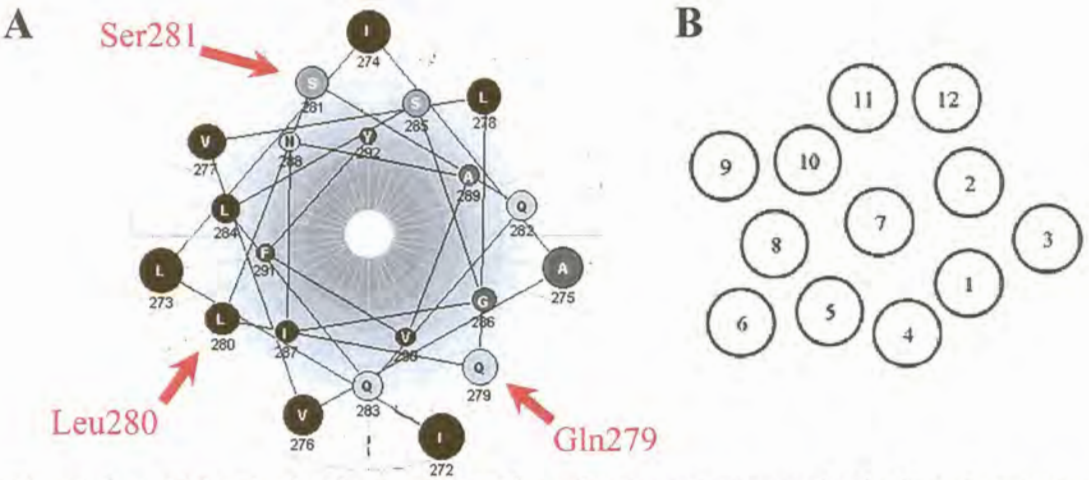

Figure 2.1: Helical wheel representation of transmembrane helix 7 and proposed model for GLUT1 helix packaging (Hruz and Mueckler, 1999). Figure A: Helix 7 wheel. The amino acids indicated by arrows, Gln279; Leu280 and Ser281, correspond to the amino acids Ser 302; Gly303 and Leu304 in PfHT1 focused on in this study. The schematical representation enables one to note the proximity of these amino acids to the exterior medium. **Figure B:** Proposed model for helical packaging in GLUT1. This view allows one to notice the proximity of each helix to its neighbours.

The recent discovery of the *P. falciparum* hexose transporter PfHT1, which is expressed in the asexual stage of the parasite, has opened up a whole new pathway for drug target development (Woodrow *et al*, 1999). This discovery is useful since the

intra-erythrocytic malaria parasite depends on glucose from its host for energy, which is metabolised via glycolysis (Kirk *et al*, 1996). Parasite-infected erythrocytes exhibit an increase in glucose uptake when compared to uninfected erythrocytes and it is believed that PfHT1 is the major hexose transporter for the intraerythrocytic parasites (Krishna *et al*, 2000). Work done by Woodrow *et al* (1999) revealed that *PfHT1* is a single copy gene with no close homologues within the translated region when compared to other related and non-related species. Expression of *PfHT1* peaks 8h after invasion, which is consistent with an increase in glucose consumption as ring forms mature to trophozoites. PfHT1 has a relatively high affinity for hexoses with a ten-fold higher affinity for D-glucose compared to the mammalian erythrocyte and endothelial located glucose transporter GLUT1 (Woodrow *et al*, 1999).

Analyses of substrate specificity of PfHT1 expressed in *Xenopus laevis* oocytes have shown that fructose binds in a furanose conformation and glucose in a pyranose conformation. Helix 5 appears to be involved in fructose transport, since this is ablated by mutation of Q169 to asparagine, which lies within helix 5 (Woodrow *et al*, 2000). The most important sites on the glucose molecule for interaction with PfHT1 appear to be C-3 and C-4 (Woodrow *et al*, 1999), and for GLUT1 the most important appear to be the ring oxygen and hydroxyls at C-1 and C-3, with a lesser contribution from C-4 and C-6 (Baldwin, 1992).

Although phylogenically unrelated to both mammals and *Plasmodium* species, kinetoplastid organisms (*Trypanosoma* and *Leishmania* species) also require glucose at certain stages of their life cycles. Protozoa of the order kinetoplastida habitat many areas and several species are important parasites of humans. Many glucose transporters from kinetoplastids have been cloned and they all belong to the major facilitator superfamily. Kinetoplastida include African trypanosomes, which cause sleeping sickness in humans (*Trypanosoma brucei*) and South American trypanosomes such as *Trypanosoma cruzi*, which causes Chagas' disease (Tetaud *et al*, 1997).

African *Trypanosoma* are transmitted by tsetse flies or other biting insects and live free in the blood, central nervous system and other tissue fluids. *T. cruzi* by contrast

live intracellularly in their mammalian hosts (Barrett *et al*, 1998). Two separate isoforms of the trypanosome hexose transporter (THT1 and THT2) were isolated from *T. brucei* by Bringaud and Baltz (1993). THT1 is the most abundantly expressed isoform in the bloodstream form parasite. The trypanosome glucose transporters have features that distinguish them from the mammalian glucose transporters. These include insensitivity to cytochalasin B and the ability to transport D-fructose. Also the long intracellular loop between helix 6 and 7 in GLUT1 is not present in trypanosomal glucose transporters (Barrett *et al*, 1998). The most important hydrogen bonding sites on THT1 appear to be C-3 and C-4. The K_m for D-glucose of the *T. brucei* blood stream form is 0.49-1.18 mM (Barrett *et al*, 1998; Tetaud *et al*, 1997) and the K_i for D-fructose is approximately 2.56 mM (Tetaud *et al*, 1997). Kinetoplastid organisms share many common challenges during their mammalian parasitic stages with the malaria parasite. Therefore sugar transporters of the kinetoplastids offer an exceptional model to study the ways in which the sugar transporters have evolved to meet different environmental challenges (Tetaud *et al*, 1997). A correlation can be made between THT1 and PfHT1 in how they differ from GLUT1, which could lead to an understanding of the significance of their differences. PfHT1 was mutated to contain a motif from THT1 that could contribute towards the ability of the two parasitic glucose transporters to transport fructose. This motif corresponds to the QLS motif in GLUT1 (Table 2.1, Figure 2.1A) that is conserved in the mammalian GLUT glucose transporters and is thought to play a part in glucose/ fructose recognition.

2.2 Materials and methods

2.2.1 Primer design

Primers were designed to incorporate point mutations within helix 7 (302SGL motif). This motif was mutated to the *T. brucei* hexose transporter THT1 helix 7 motif (311AGT) since THT1 also transports glucose and fructose. Four sets of primers were designed: three complementary sets for incorporation of the point mutations and one set for the extension of the full-length gene (Table 2.2). Primers HTKB1&2 lie at opposite ends of the full-length gene and include the start and stop codons

respectively. The primers also contain *Bgl*II restriction sites at their 5' ends for cloning into the *X. laevis* expression vector pSP64T. Upon delivery, primers were diluted in double distilled water to stocks of 80 µM concentrations.

Table 2.2: Sequences of primers used for PCR 1 and 2. Primers are in the 5' to 3' direction. Numbering (1 and 2) refers to forward and reverse primers respectively. Mutated bases are indicated in bold italics. Start and stop codons are in bold. The Kozak sequence in the HTKB1 primer is in italics. Restriction sites are underlined.

Primer name	Primer sequence (5'→3')	Restriction sites
AGT1	GGATGTTTG***C***TA***G***CTGGT***AC***ACAACAATTTACAGG	*NheI*
AGT2	CCTGTAAATTGTTGT***GT***ACCAG***C***TA***G***CAAACATCC	
AGL1	GGATGTTTG***C***TA***G***CTGGT***C***T***G***CA***G***CAATTTACAG	*NheI*, *PstI*
AGL2	CTGTAAATTG***C***TG***C***A***G***ACCAG***C***TA***G***CAAACATCC	
SGT1	GGATGTTTG***C***TATCTGGT***ACC***CAACAATTTACAG	*KpnI*
SGT2	CTGTAAATTGTTG***GGT***ACCAGATA***G***CAAACATCC	
HTKB1	ACGTACAGATCT*CACC***ATG**ACGAAAAGTTCGAAAG	*BglII*
HTKB2	ACGTACAGATCT**TCA**TACAACCGACTTGGTC	

Table 2.3: Characteristics of the primers used to synthesise mutant S302A and L304T constructs.

Primer	AGL1/AGL2	SGT1/SGL2	HTKB1	HTKB2
Length	34	34	35	31
%A/T	56	58	57	55
Tm Genosys[1]	76.6	72.6	75.6	71.4
Calculated Tm[2]	68.2	67.0	68.4	66.8

[1] Melting temperature (Tm) supplied with the primers and calculated by Sigma-Genosys.

[2] Tm is calculated according to the following equation (Rychlik *et al*, 1990):

$69.3 + (0.41 \times \%GC) - 650/length$

The primers that produced the mutations were designed to contain the mutated area in the middle of the primer and a restriction site over or near the mutated area that would be used to confirm the presence of the mutation without sequencing. All primers were

synthesised by Sigma-Genosys Ltd, London, UK. The Tm of each primer was calculated. The characteristics of the primers are summarised in Table 2.3.

2.2.2 Polymerase Chain Reaction (PCR) for the construction of helix 5 and helix 7 mutations

2.2.2.1 PCR 1: construction of mutants

The Polymerase Chain Reaction for the production of the S302A and L304T mutants had to be optimised for each set of primers (mutant 302SGL→AGT was already constructed by Charles Woodrow). Wild-type PfHT1 in the pSP64T *X. laevis* expression vector at a concentration of 200 ng/µl was used as template in a 1:1000 dilution (Woodrow *et al*, 1999). Reaction volumes of 25 µl for each reaction were set up under optimised reaction conditions as summarised in Table 2.4.

Table 2.4: Optimised reaction conditions for the synthesis of the S302A and L304T mutants in 25 µl reaction volumes.

Reaction component	Final in 25 µl
Cloned Pfu reaction buffer 10×	1×
dNTP 2 mM each	0.16 mM each
$MgCl_2$ 25 mM	2 mM
Mutation-inducing primer (AGL1, SGT1, AGL2 or SGT2)	10 pmol
Gene primer (HTKB1 or HTKB2)	10 pmol
Cloned Pfu DNA Polymerase 2500 units/ml	0.625 Units

The DNA polymerase Pfu from the hyperthermophilic archae *Pyrococcus furiosis* (Stratagene, USA) was used. It has 3' to 5' exonuclease proofreading activity that enables the polymerase to correct nucleotide miss-incorporation errors but lacks extendase activity, which results in blunt-end PCR products. The cycling profile consisted of an initial heating step at 94°C for 5 minutes followed by 35 cycles of denaturation at 94°C for 30 seconds, annealing at 55°C for 45 seconds and extension at 72°C for 1 minute. A final extension at 72°C for 5 minutes concluded the PCR

reaction. PCR was conducted in 0.2 ml thin-walled tubes (Quality Scientific Plastics, CA, USA) in a Perkin Elmer GeneAmp PCR system 2400 (PE Applied Biosystems, CA, USA).

2.2.2.2 Agarose gel electrophoresis of PCR products

All PCR products were analysed on a 1% (w/v) agarose gel (Promega Corporation, Madison, USA) made up in TBE (0.098 M Tris base, 0.098 M boric acid, 2 mM EDTA pH 8.0) or TAE (0.04 M Tris-Acetate, 1 mM EDTA, pH 8.0) containing ethidium bromide added to the gels at <50°C before pouring at a final concentration of 0.4 µg/ml. Electrophoresis was carried out at 70-100 Volts in a minicell EC370M electrophoresis system (E-C Apparatus Corporation, USA) in 1×TBE or TAE buffer. DNA samples were loaded with 10 µl Gel Loading Solution (containing 0.25% w/v bromphenol blue, 0.25% w/v xylene cyanole FF, 40% w/v sucrose; Sigma-Aldrich, USA). 1 µg of a 1 Kb Plus DNA Ladder™ (Life Technologies, USA) was loaded in a separate line for size comparison. DNA fragments were visualised on a UV transilluminator (UVP Inc., CA, USA) and photographed with a Polaroid direct screen instant camera (shutter speed of 1 second), or on a TC-312A 312nm UV transilluminator (Spectroline Corporation, NY, USA) and visualised with a CCD camera (Kodak Digital Systems, NY, USA) linked to a computer system.

2.2.2.3 Gel extraction of PCR 1 products

Each half of the mutated PfHT1 construct was excised with a clean scalpel from a 1% (w/v) agarose/ TBE gel stained with ethidium bromide whilst being visualised on a UV transilluminator. Exposure to the UV was kept to a minimum whenever possible to limit damage of the DNA sustained by UV exposure (e.g. formation of thymine-dimers; Adams *et al*, 1992). Each gel slice was weighed in a 1.9 ml microfuge tube. The QIAquick Gel Extraction Kit (Qiagen Ltd, West Sussex, UK) was used according to the manufacturers instructions. Three volumes of Buffer QG (containing guanidine thiocyanate and pH indicator: yellow at pH ≤7.5, violet at pH >7.5) was added to one volume of gel (100 mg ≈ 100 µl) and incubated at 50°C and vortexed every 2-3 minutes until the gel was dissolved. Once the gel slice was dissolved the colour of the

mixture was checked for the correct pH (≤ 7.5) for maximum absorption on the silica-gel membrane. If the mixture indicated a high pH, 3 M sodium acetate at pH 5.0 was added. The mixture was pipetted into a QIAquick spin column with a 2 ml collection tube and centrifuged for 1 minute at 13000 rpm. The DNA bound to the silica-gel membrane was washed with Buffer QG to remove all traces of agarose and then with Buffer PE (containing ethanol) and centrifuged for 1 minute at 13000 rpm at a time. All trace of Buffer PE was removed by an additional centrifugation step for 1 minute at 13000 rpm. DNA was eluted with Buffer EB (10 mM Tris-Cl, pH 8.5) in a clean 1.9 ml microfuge tube.

2.2.2.4 PCR 2: to obtain the full-length mutants

Both halves of each mutated construct isolated from the agarose gel by the QIAquick gel extraction kit were used as template in two subsequent PCR reactions to extend the full-length gene. The optimal reaction conditions were the same as those indicated in Table 2.4 with HTKB1 and HTKB2 as forward and reverse primers respectively. The gel isolated PCR 1 products were used as template with 0.5 µl of each per reaction. Thermocycling consisted of an initial 5 minute denaturation at 94°C followed by 5 cycles of denaturation at 94°C for 30 seconds, an annealing temperature of 55°C for 90 seconds, and extension at 72°C for 4 minutes to allow for full extension of each half at its 3'end. Before the start of the sixth cycle, primers HTKB1 and HTKB2 were added. Annealing temperature was increased to 60 °C to facilitate higher specificity of priming, otherwise the cycling parameters were the same as for PCR 1.

The number of required cycles after addition of primers had to be optimised. To achieve this, aliquots of 12.5 µl were removed from a 50 µl reaction after 15, 20 and 25 cycles of a 30-cycle reaction. Subsequent reactions were carried out for 15 cycles after addition of primers and the extension time of the last cycle was increased to 8 minutes to accommodate the full 1.5 Kb expected product length. PCR 2 products were isolated from 1% (w/v) agarose gels using the QIAquick Gel Extraction kit as described in Paragraph 2.2.2.3 and concentration of each mutant construct was determined by comparison on an ethidium bromide stained gel with a band from the 1

Kb Plus DNA ladder of known concentration. The pmols of each mutant construct were calculated.

2.2.3 Cloning strategies

2.2.3.1 *Phosphorylation of the 5'-ends of the PCR 2 products*

For the insert to be ligated to the vector by T4 DNA Ligase, the 5'-ends of the PCR 2 product had to be phosphorylated. This was achieved by the Ready-To-Go T4 Polynucleotide Kinase (PNK) kit (Amersham Pharmacia Biotech, London, UK), where the gamma-phosphate of ATP was transferred to a 5'-OH of the PCR 2 products. The Ready-To-Go T4 PNK contains in 50 µl 8-10 units of FPLCpure T4 Polynucleotide Kinase, 50 mM Tris-HCL (pH 7.6), 10 mM $MgCl_2$, 5 mM DTT, 0.1 mM spermidine, 0.1 mM EDTA (pH 8.0), 0.2 µM ATP and stabilizers. It is recommended by the product protocol to add 5-10 pmols of 5'ends of oligonucleotide, but due to a low yield of PCR 2 product after gel extraction only <1 pmol of each could be added. This mixture was incubated at 37°C for 30 minutes. The reaction was stopped by the addition of 5 µl of 250 mM EDTA.

Resulting product was cleaned through the QIAquick PCR purification kit (Qiagen, UK) according to the manufacturer's instructions. This involved adding five volumes of Buffer PB to one volume of the final T4 PNK reaction, and pipetted into a QIAquick spin column contained in a 2 ml collection tube. This was spun for 1 minute at 13000 rpm and then washed with Buffer PE and eluted in 30 µl Buffer EB. Assuming a 100% recovery of the DNA from the columns, a rough estimate was made of the pmols of each sample available for ligation into the pUC18 vector.

2.2.3.2 *Cloning into SmaI cut pUC18 vector*

Three vector-to-insert ratios (measured in pmols) were utilised to determine which ligation ratio would produce the most colonies after transformation. The vector to insert ratios decided on were 1:0.5, 1:1 and 1:3 with the pUC18 vector at 0.056 pmols per ligation reaction. The Ready-To-Go pUC18 *SmaI*/ BAP + Ligase kit (Amersham

Phamacia Biotech, London, UK) was utilised for ligation of the phosphorylated PCR 2 products into *Sma*I cut pUC18 vector that was already dephosphorylated. The manufacturer's instructions were followed and involved adding the DNA and reactants to a final volume of 20 µl and incubating for 3-5 minutes at room temperature. In 20 µl the kit contains 100 ng of pUC18 *Sma*I/ BAP and a minimum of 6 Weiss units of FPLCpure T4 DNA Ligase, 66 mM Tris-HCl (pH 7.6), 6.6 mM $MgCl_2$, 0.1 mM ATP, 0.1 mM spermidine, 10 mM DTT and stabilisers (0.01 Weiss units will ligate 1 µg of DNA in 20 minutes). After the initial incubation at room temperature, the mixture was pipetted and centrifuged to create a homogenous solution and then incubated at 16°C for 30-45 minutes. No heat inactivation of the reaction was necessary.

2.2.3.3 *Transformation of competent cells*

The pUC18 vector-containing insert was transformed into *Epicurian Coli* XL2-Blue Ultracompetent Cells (Stratagene, USA) according to the manufacturer's instructions. The ultracompetent cells were thawed on ice and then aliquoted into prechilled 15 ml Falcon 2059 polypropylene tubes (Strategene, USA). To this β-mercaptoethanol was added to a final concentration of 25 mM. The cells were incubated on ice for 10 minutes while being gently stirred. 2 µl of the ligation reaction from paragraph 2.2.3.2 was added and incubated on ice for a further 30 minutes. The pUC18 plasmid (10 pg) was used as a positive control. The tubes were pulse heated at 45°C for 30 seconds and incubated on ice for 2 minutes. 900 µl of preheated (42°C) NZY^+ broth (1% w/v NZ amine, 0.5% w/v yeast extract, 0.5% w/v NaCl, 12.5 mM $MgCl_2$, 12.5 mM $MgSO_4$, 20 mM glucose, NaOH to pH 7.5) was added and the tubes incubated at 37°C for 1 hour while shaking at 225-250 rpm. 100 µl of each reaction was plated on LB broth plates (1% w/v tryptone, 0.5% w/v yeast extract, 1% w/v NaCl, 1.5% w/v agar, 100 µg/ml ampicillin). Since the pUC18 vector contains the LacZ gene there was also the option of blue/ white selection and therefore the plates were first prepared with 40 µl of 2% w/v X-gal (LacZ gene encoded protein substrate) and 4 µl of 1 mM IPTG (LacZ gene activator).

2.2.4 Plasmid isolation

2.2.4.1 *Conventional miniprep plasmid isolation*

White colonies were selected off plates produced from the transformation reaction mentioned in Paragraph 2.2.3.3 and a preliminary screening of these colonies for the presence of an insert was carried out using an alkaline lysis protocol (Sambrook *et al*, 1989). Five white colonies were selected off each plate (S302A and L304T) and grown up in 3ml LB broth containing 50 µg/ml ampicillin. 1 ml of each was aliquoted into a 1.9 ml microfuge tube and centrifuged at 13000 rpm for 1 minute. The pellet was resuspended in 100 µl Solution 1 (50 mM glucose, 25 mM Tris-HCl pH 8.0, 10 mM EDTA pH 8.0). Lysis of the bacteria was induced by addition of 100 µl Solution 2 (1% w/v SDS, 0.2 M NaOH) and incubation at room temperature for no longer than 5 minutes. This lysis was stopped by the addition of 150 µl Solution 3 (3 M potassium acetate, 5 M Acetic acid) followed by incubation for 5 minutes and centrifugation at 13000 rpm for 10 minutes. The plasmid DNA was precipitated with ice-cold 100% ethanol and washed with ice-cold 70% v/v ethanol. The pellet was dissolved in TE buffer (1 mM Tris-HCl pH 8.0, 1 mM EDTA, 2 ug/ml RNase, no incubation required) and resolved on a 1% w/v agarose gel containing 0.4 µg/ml ethidium bromide alongside 1 µg of a 1 Kb Plus DNA Ladder, and visualised over a UV transilluminator.

2.2.4.2 *High pure plasmid isolation*

Of the five colonies selected for each mutant construct, S302A had four positive clones and L304T five positives. All clones that tested positive for correct insert and mutation (Section 2.2.5) were re-grown in LB broth containing ampicillin. The plasmid was isolated using the QIAprep spin miniprep kit (Qiagen Ltd, West Sussex, UK) following the manufacturer's instructions. 3 ml of each culture was pelleted in 1.9 ml microfuge tubes. The pellet was resuspended in Buffer P1 (50 mM Tris-HCl pH 8.0, 10 mM EDTA, 100 µg/ml RNase A). Lysis Buffer P2 (200 mM NaOH, 1% w/v SDS) was added to each sample and incubated at room temperature for no longer than 5 minutes. The Lysis reaction was stopped by addition of chilled Buffer N3 (containing chaotropic salts) with immediate mixing. This was incubated on ice for 5

minutes and then centrifuged for 10 minutes at 13000 rpm. The supernatant was pipetted into a QIAprep spin column with 2 ml collection tube and spun for 1 minute at 13000 rpm. The column was washed with Buffer PE (containing ethanol) and centrifuged twice at 13000 rpm to remove residual buffer. The DNA was eluted off the column with Buffer EB (10 mM Tris-HCl, pH 8.5).

2.2.5 Restriction mapping of recombinant clones

2.2.5.1 Isolation of insert

Plasmids from 5 selected colonies of each mutant were isolated with the conventional method (Paragraph 2.2.4.1) and were digested with *Bgl*II (Life Technologies, London, UK) to release the insert and simultaneously with *Hha*I (Life Technologies, London, UK) to fragment the pUC18 vector. The most suited buffer compatible with both enzymes (REact3, 50 mM Tris-HCl pH 8.0, 10 mM $MgCl_2$, 100 mM NaCl) was added, with 0.3 mg/ml BSA in a 20 µl reaction volume. The reactions were incubated at 37°C overnight. 5 µl of the reaction was run on a 1% w/v agarose gel containing 0.4 µg/ml ethidium bromide alongside a 1 Kb Plus DNA Ladder, and visualised over a UV transilluminator. Inserts required for cloning into the *X. laevis* expression vector pSP64T were extracted with the QIAquick Gel Extraction kit (Paragraph 2.2.2.3).

2.2.5.2 Mapping of mutants

A restriction site had been devised for each mutant over the mutated area during primer design (Paragraph 2.2.1). Mutant S302A was identified by restriction digestion with *Pst*I and mutant L304T by restriction digestion with *Kpn*I (Table 2.2). 4 µl of the digestion mixture described in Paragraph 2.2.5.1 was used in a 10 µl reaction containing each individual enzymes supplied buffer and 0.5 mg/ml BSA. The reactions were incubated at 37°C overnight and were run on a 1% w/v agarose gel containing 0.4 µg/ml ethidium bromide alongside a 1 Kb Plus DNA Ladder, and visualised over a UV transilluminator. Clones that contained the correct mutant insert were frozen in glycerol stocks (15% v/v glycerol) at -70°C.

2.2.6 Expression vector (pSP64T) cloning strategy

2.2.6.1 Cloning into pSP64T

The pSP64T expression vector is described further in Paragraph 3.1. One clone was chosen for each mutant construct S302A and L304T that had been determined to contain the correct mutation by restriction digestion (Paragraph 2.2.5.2). The inserts contained in the pUC18 clone were digested out (Paragraph 2.2.5.1) and isolated from an agarose gel with the QIAquick Gel Extraction kit (Paragraph 2.2.4). Aliquots of the isolated fragments were run on a 1% (w/v) agarose gel and the concentrations were estimated by comparison of a known standard in the 1 Kb DNA Ladder. The final concentration of the *Bgl*II digested, dephosphorylated pSP64T vector was 25 ng/µl. A 2:1 vector to insert molar ratio was used, which by prior ligation reactions was determined to produce the best results. Vector and insert were added to a 1.9 ml microfuge tube together with 1× T4 DNA Ligase buffer and 5 Units of T4 DNA Ligase (Pharmacia Biotech Ltd., UK). The reaction mixture was heated at 45°C for 5 minutes to separate self-attached fragments, followed by incubation at 16°C overnight. The ligation reaction was used directly for transformation into *E. Coli* XL2-Blue Ultracompetent Cells following the strategy described in Paragraph 2.2.3.3.

2.2.6.2 Screening for pSP64T vector containing insert

The transformed cells were plated on LB agar plates (15% w/v agar) containing 100 µg/ml Ampicillin. Clones were picked and grown up in LB broth containing 50 µg/ml Ampicillin. Plasmids were isolated using the conventional plasmid isolation method described in Paragraph 2.2.4.1. All clones that contained insert were linearised with *Xba*I (Life Technologies, London, UK) with incubation at 37°C and visualised on a 1% w/v agarose gel containing ethidium bromide on a UV transilluminator (expected size ≈ 4.7 Kb).

Since there is only one RNA promoter region in the pSP64T expression vector (SP6, Appendix Ia) that can be used for cRNA transcription, the orientation of the insert was checked by digestion with *Hind*III (Life Technologies, London, UK). This was possible because PfHT1 contains only one *Hind*III site within its ORF, which is

200 ng/µl of template was used in each reaction with 3.2 pmols of primer and 2 µl BigDye™ Terminator Cycle Sequencing Ready Reaction Mix (Perkin-Elmer Applied Biosystems, UK) to 5 µl final reaction volume. PCR was performed on a Perkin Elmer GeneAmp PCR system 9700 (PE Applied Biosystems, CA, USA) with 32 cycles of 96°C for 10 seconds, 50°C for 5 seconds and 60°C for 4 minutes. The PCR reaction products were precipitated with 100% ice-cold ethanol at room temperature for 25 minutes, centrifugated at 13000 rpm for 15 minutes and washed with 70% ice cold ethanol. The resulting pellet was dried *in vacuo* and refrigerated at 4°C until use. The sequencing product was analysed on a 36 cm gel in an automated ABI Prism 377 DNA Automatic Sequencer (PE Applied Biosystems, California, USA) and the raw data were analysed with the ABI Prism Sequencing Analysis Version 3.0 software. Sequence alignments were analysed with the ABI Prism Sequencing Navigator Version 1.0.1 software.

2.2.9 Synthesis of cRNA

2.2.9.1 Linearisation and purification of DNA template

Plasmids obtained from the QIAprep spin miniprep kit were linearised with *XbaI* in a 50 µl reaction volume containing appropriate buffer and 0.2 mg/ml BSA with incubation at 37°C overnight. The restriction enzyme was digested by the addition of 7 µg/µl Proteinase K (Macherey-Nagel) in a 1×buffer (10 mM Tris-HCl, 2 mM $CaCl_2$, pH 8.0) and incubation at 50°C for 1 hour. The resulting digest was extracted with an equal volume of phenol/ chloroform and again with an equal volume of chloroform. The organic phase was re-extracted with 50 µl of water. The DNA was precipitated overnight at -20°C with $1/10^{th}$ the volume of 3 M NaAc and 2.5× the volume of 100% ethanol. The precipitate was collected by centrifugation at 13000 rpm for 20 minutes and then washed with 70% ethanol. The dried pellet was dissolved in filtered, DEPC treated water (0.1% diethyl pyrocarbonate in double glass-distilled, deionised H_2O, with removal of DEPC by autoclaving). The resulting DNA was quantified using a fluorometer (Paragraph 2.2.7).

2.2.9.2 *Transcription reaction*

Transcription of cRNA was achieved with the use of two separate kits. The initial kit used was the mMESSAGE mMACHINE™ (Ambion, UK) SP6 kit. 1 µg of the purified DNA template was added together in a 20 µl reaction volume with 1× Transcription Buffer (patent protected, contains salts, buffer, dithiothreitol and other ingredients), 1× Ribonucleotide Mix (5 mM ATP, CTP, UTP; 1 mM GTP and 4 mM Cap Analogue), 1× Enzyme Mix (SP6 RNA polymerase, ribonuclease inhibitor, buffer, 50% glycerol buffer), and the volume adjusted with the supplied RNase-free water. The reaction was incubated at 37°C for 3 hours, after which 2 units of the supplied RNase-free DNase I was added and the mixture was further incubated at 37°C for 15 minutes. The reaction was terminated and the RNA recovered by the addition of nuclease-free water and the supplied Lithium Chloride Precipitation Solution (7.5 mM lithium chloride, 75 mM EDTA). This was incubated at -20°C overnight and then centrifuged at 13000 rpm for 30 minutes at 4°C. The pellet was washed in nuclease-free 70% ethanol and dried at room temperature. The dried pellet was dissolved in nuclease-free water on ice, and aliquoted into nuclease-free tubes with 1µl per tube and frozen at -70°C.

Alternatively, cRNA was synthesised with the SP6 Cap-Scribe kit (Boehringer Mannheim, Germany). The transcription reaction was set up with 1,5 µg of linearised clean DNA template together with 1× Cap-Scribe buffer, 40 units of SP6 RNA polymerase and nuclease-free water to a volume of 20 µl. This reaction mixture was incubated at 37°C for 3 hours after which 2 units RNase-free DNase I (Promega Corporation, Madison, USA) was added and incubated for a further 30 minutes at 37°C. The reaction was stopped by the addition of 15 µl of ammonium acetate stop solution (5 M ammonium acetate, 0.1 M EDTA) and 115 µl of filtered, DEPC treated water. The mixture was extracted with an equal volume of RNase-free phenol/chloroform and again with RNase-free chloroform. This aqueous phase (≈ 200 µl) was filtered through a Milex-GV 0.2 µm filter (Millipore, USA) to remove any contaminating salts. The cRNA was pelleted by the addition of isopropyl alcohol and an incubation at -20°C overnight followed by centrifugation at 13000 rpm for 30 minutes at 4°C. The pellet was washed in nuclease-free 70% ethanol and dried at

room temperature. The dried pellet was dissolved in DEPC-treated, filtered water on ice and aliquoted into nuclease-free tubes with 1 µl per tube, which were frozen at -70°C.

2.2.10 cRNA quantification

The presence of cRNA was confirmed by running an aliquot of the transcription reaction on an agarose gel. A mixture containing 1 µl cRNA, 0.07 µg/µl ethidium bromide and RNA loading buffer (80% formamide, 0.1% xylene cyanol, 0.1% bromophenol blue, 2 mM EDTA) was heated at 70°C for 2 minutes and then snap-cooled on ice. This was run on a 1% w/v agarose gel together with 0.24-9.5 Kb RNA Ladder (Life Technologies, UK). The cRNA was visualised on a transilluminator and photographed with a Polaroid direct screen instant camera.

The concentration of the cRNA was determined on a Shimadzu UV 160 A spectrophotometer. 1 µl of synthesised cRNA was diluted to 300 µl with DEPC treated water. The spectrophotometer was blanked with DEPC-treated water and the absorbancy was read at 260 nm. The cRNA concentration in µg/ml was calculated with the following equation (Sambrook *et al*, 1989):

$$A_{260} \times \text{dilution factor} \times 40 = \mu g/ml$$

2.3 Results

2.3.1 Primer design

Primers AGT1&2 produced a double point mutated construct (302SGL→AGT) of amino acid S302 and L304. Primers AGL1&2 and primers SGT1&2 produced single point mutated constructs S302A and L304T, respectively. All three sets of the complementary primers contained restriction sites designed to lie directly or close to the mutated site (Figure 2.2). All possible restriction sites not present in the wild type were modelled over the mutated regions to identify sites for reconstruction without any amino acid changes. This would produce a unique restriction site that would only

be cut if the mutation was present and would enable rapid screening of viable clones without sequencing.

```
Wild-type: 892 GGA TGT TTG TTA TCT GGT TTA CAA CAA TTT ACA GG
Amino Acid 298 Gly Cys Leu Leu Ser Gly Leu Gln Gln Phe Thr
Target Motif:              302 S   G   L
AGT mutant:892 GGA TGT TTG TTA GCT GGT ACA CAA CAA TTT ACA GG
Mutated Motif:             302 A   G   T
Primer AGT1:   GGA TGT TTG CTA GCT GGT ACA CAA CAA TTT ACA GG
```

Figure 2.2: Primer AGT1 is used here to demonstrate how a restriction site could be modelled over or near a mutated area. The restriction site *Nhe*I used in this example is underlined. Mutated amino acids are indicated in bold.

2.3.2 PCR reaction

For each new mutation, two PCR 1 reactions were carried out to create each half of the mutated construct. For example, for construct S302A, primers HTKB1and AGL2 were used in one reaction with primers AGL1 and HTKB2 in a second separate reaction (Figure 2.3).

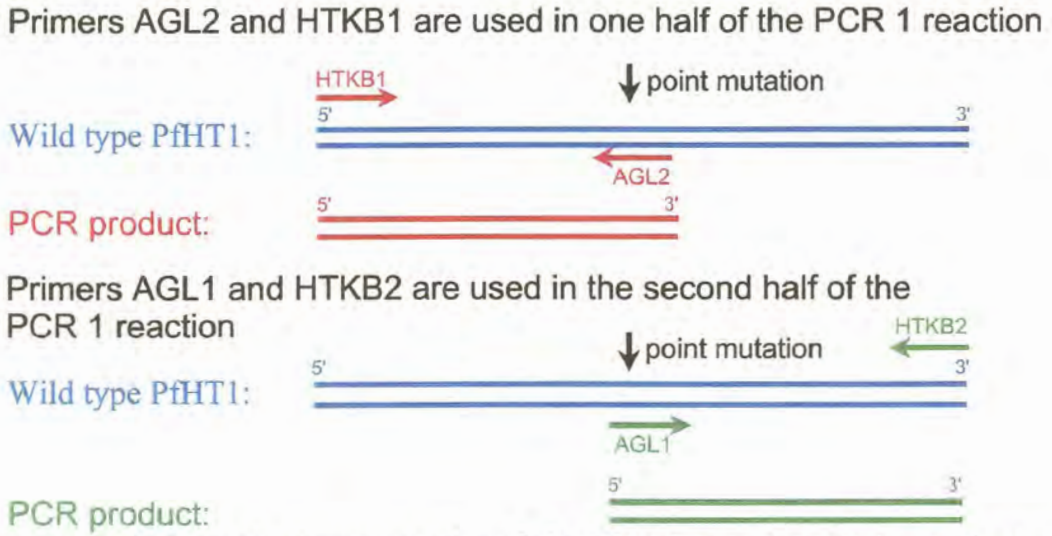

Figure 2.3: Schematic demonstration of the PCR 1 reaction. Each set of primers indicated together are included in two separate PCR reactions of 25 µl each according to the conditions set in Table 2.4.

Primers AGL1&2 and SGT1&2 with HTKB1&2 proved successful at a 55°C annealing temperature, which is 10-20°C lower than their calculated Tm's. As shown

in Figure 2.4, primers HTKB1 with AGL2 and HTKB1 with SGL2 when visualised on an agarose gel produced bands of size 0.9 Kb. Primers AGL1 with HTKB2 and SGL1 with HTKB2 when visualised on an agarose gel had produced bands of size 0.6 Kb. These bands were isolated from the agarose gels and used as template in the PCR 2 reaction (Figure 2.5).

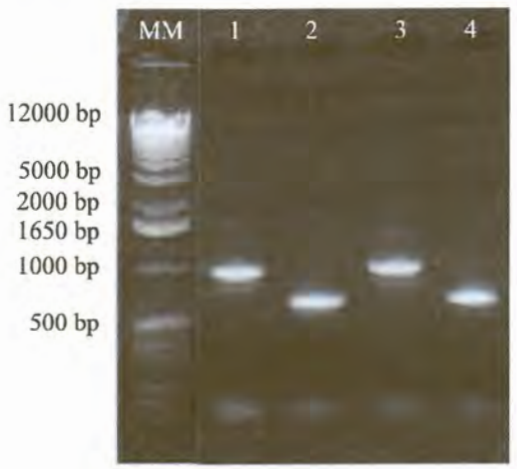

Figure 2.4: Results of the PCR 1 reaction. This PCR reaction produced the mutated motifs and the bands indicate the two halves of the full-length gene. MM indicates the 1 Kb Plus DNA Ladder. Lane1 contains product produced from primers HTKB1 and AGL2. Lane2 contains product produced from primers AGL1 and HTKB2. Lane3 contains product produced from primers HTKB1 and SGL2. Lane4 contains product produced from primers SGL1 and HTKB2.

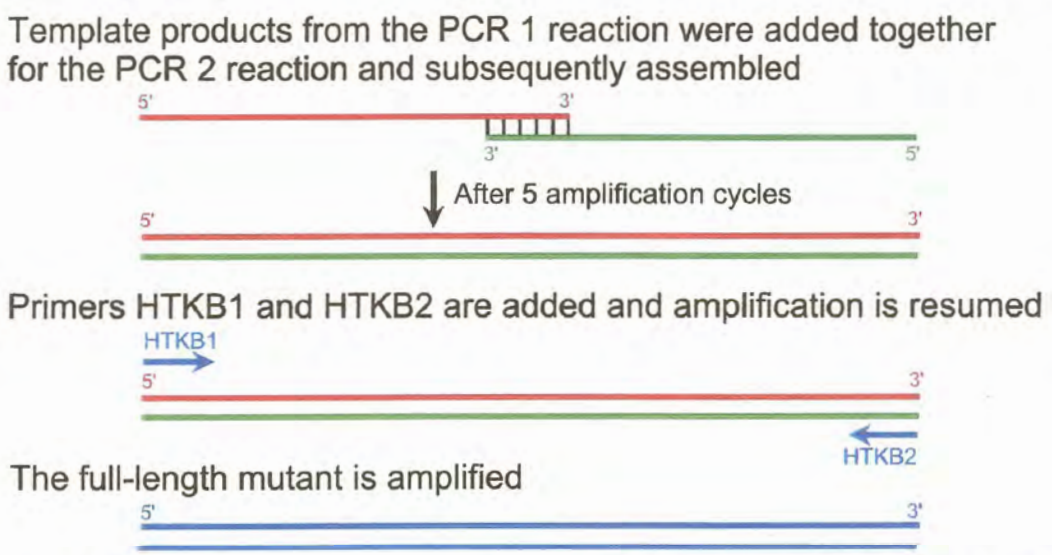

Figure 2.5: Schematic demonstration of the PCR 2 reaction with HTKB1 and 2 as primers with PCR 1 product as template.

PCR 2 proved more difficult and a few reaction parameters were varied to determine the optimum reaction conditions. Those varied were the magnesium concentration

(results not shown), the template concentration (Figure 2.6A), the annealing temperature (results not shown) and the number of cycles (Figure 2.6B). To determine the optimum number of cycles with a 1:10 dilution, a reaction volume of 50 µl was used and 12.5 µl was removed from the reaction mix after 15, 20 and 25 cycles.

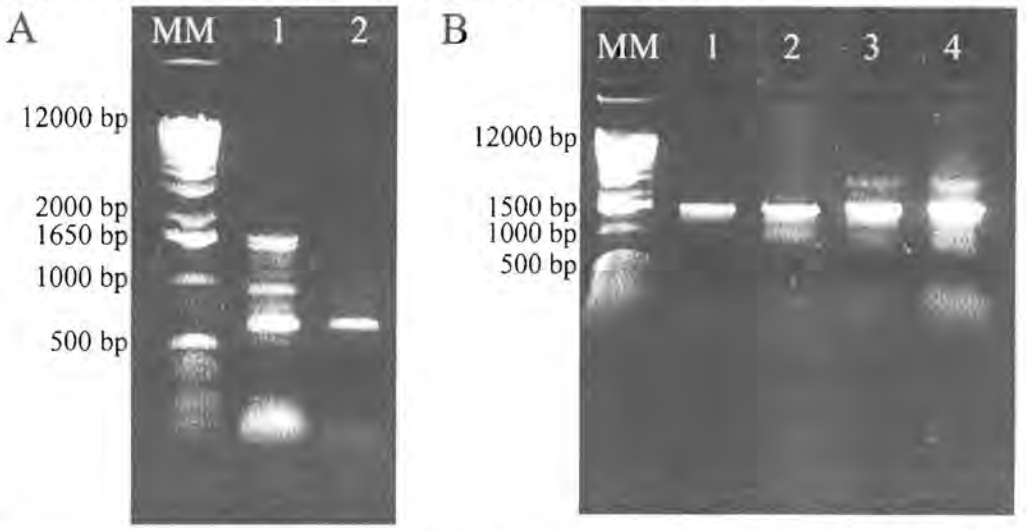

Figure 2.6: Optimisation of the PCR 2 reaction. MM in both A and B indicates the 1 Kb Plus DNA Ladder. **Figure A** represents the template concentration optimisation. Lane 1 indicates the results obtained from a 1:10 dilution and Lane 2 indicates a 1:100 dilution of the PCR 1 column cleaned templates, both amplified for 30 cycles. The expected band size is ≈ 1500 bp. **Figure B** shows product from differing number of cycles with a 1:10 dilution and gel extracted PCR 1 product as template. Lanes 1, 2, 3 and 4 are an indication of product produced after 15, 20, 25 and 30 cycles respectively.

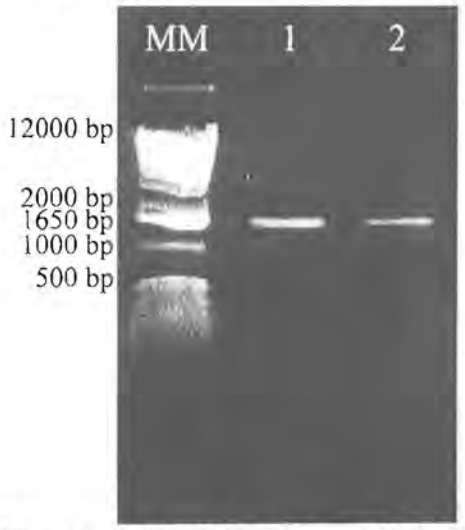

Figure 2.7: Full-length amplification of the mutated constructs. MM indicates the lane containing the 1 Kb Plus DNA Ladder. PCR 2 was conducted with 15 amplification cycles, and a 1:10 dilution of gel extracted PCR 1 product. The concentration of each mutant construct was estimated by comparison of the 100 ng 1650 bp band. Lane 1 represents 80 ng/ 5µl (16 ng) of AGL mutant construct. Lane 2 represents 40 ng/ 5µl (8 ng) of SGT mutant construct.

The PCR 1 template mixtures were first purified through a PCR Purification column (Qiagen, UK) before being used as template for PCR 2 and the outcome of the PCR 2 reaction showed multiple bands indicating either non-specific priming or over amplification (Figure 2.6A). Extracting the PCR 1 product from a gel before being used in PCR 2, and reducing the number of cycles eliminated these bands (Figure 2.6B, Lane 1). From the optimisation reactions, a 15-cycle reaction was decided on with a 1:10 dilution. Products from PCR 2 were visualised as shown in Figure 2.7.

2.3.3 Selection of correct constructs in pUC18 vector

For each mutant construct five colonies that appeared white, that resulted from the transformation into pUC18 vector, were selected from the agar plates. As shown in Figure 2.8 four out of the five colonies selected for mutant AGL produced plasmid containing an insert and all five colonies selected for mutant SGT had plasmids with inserts (expected band size ± 4.5 Kb). Plasmids the same size as the pUC18 vector used as a negative control indicated no insert present.

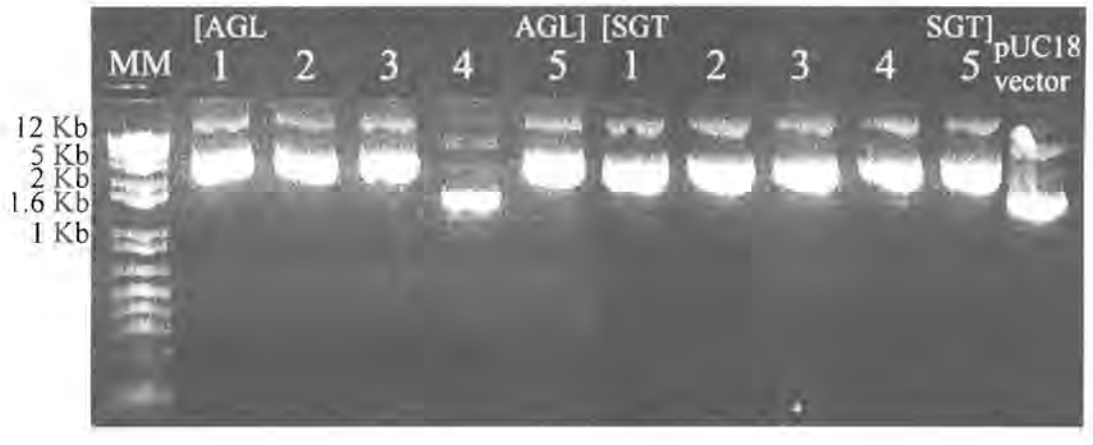

Figure 2.8: Confirmation of the presence of insert for colonies selected. The resulting plasmid isolated from five colonies selected for the AGL mutant construct and from five colonies selected for the SGT mutant construct. The pUC18 vector was used for size comparison. MM represents the 1 Kb Plus DNA Ladder.

Plasmids isolated from colonies selected for each construct were digested with restriction enzymes *Bgl*II to isolate the insert. The plasmids were also simultaneously digested with *Hha*I, which due to the many *Hha*I site in the pUC18 vector digests the

pUC18 vector into fragments smaller than 350 bp. Figure 2.9A shows the insert at 1.5 Kb. The absence of a band at this size indicates no insert in the clone. The resulting digest shown in Figure 2.9A was re-digested with the appropriate restriction enzymes to establish the presence of the mutated motif. Figure 2.9B shows the results obtained from this digest. Figure 2.9B, Lanes 1-4 show almost complete digestion of the AGL mutant construct with *Pst*I resulting in two bands of 1 Kb and 500 bp and a faint band at 1.5 Kb. Figure 2.9B, Lanes 5-9 show an incomplete digestion of the SGT mutant construct with *Kpn*I resulting in three bands of 1.5 Kb, 1 Kb and 500 bp.

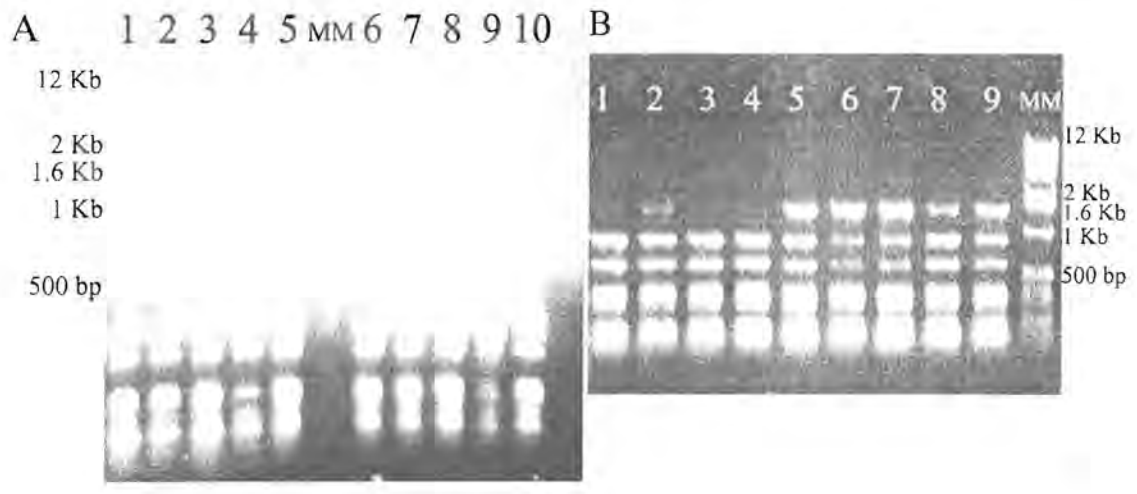

Figure 2.9: Confirmation of insert by restriction enzyme digestion. Figure A indicates the results obtained by digestion with restriction enzyme *Bgl*II and *Hha*I. Lane 1-5 represents insert from plasmids obtained from the AGL construct. Lane 4 clearly indicates the absence of insert. Lane 5-10 represents insert from plasmids obtained from the SGT construct. **Figure B** Lanes 1-4 indicates AGL construct digested with *Pst*I. Lanes 5-9 indicates SGT construct digested with *Kpn*I. MM represents the 1 Kb Plus DNA Ladder.

2.3.4 Gel extraction

Figure 2.10A shows the AGL and SGT *Bgl*II digested inserts as 1.5 Kb bands before gel extraction, and Figure 2.10B shows the resulting product after gel extraction. Also present in Figure 2.10B is a band of approximately 3 Kb, which persisted even after careful gel extraction of the band shown in Figure 2.10A.

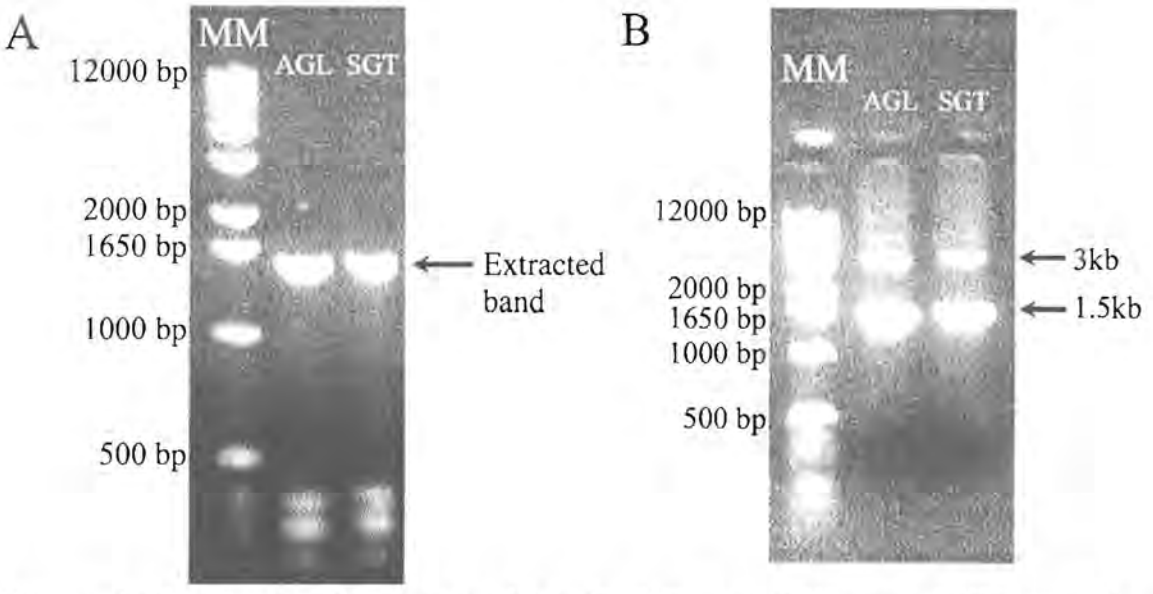

Figure 2.10: Results of gel extraction of *Bgl*II cut AGL and SGT mutant constructs. Figure A indicates the 1.5Kb insert resulting from the simultaneous digestion with *Bgl*II and *Hha*I before being extracted from the gel. **Figure B** is the resulting gel extracted product. MM represents the 1 Kb Plus DNA Ladder.

2.3.5 Selection of correct insert from pSP64T

After insertion of insert shown in Figure 2.10B into pSP64T expression vector, the vector was cloned into competent *E. coli* cells. Since no blue/white selection of colonies was possible, all resulting colonies were picked from agar plates and inoculated into LB broth containing ampicillin. 16 colonies were grown up for the AGL mutant, and 17 were grown up for the SGT mutant. Of the 16 colonies from the mutant AGL construct, 11 produced plasmid that contained insert. Of the 17 colonies from mutant SGT construct, 11 produced plasmid that contained insert. The presence of the insert in those plasmids that appeared to contain them was confirmed by linearisation.

All plasmids were digested with *Hind*III to determine the orientation of the insert. Of the 11 plasmids containing the AGL mutant construct, 4 were in the correct orientation indicated by the presence of a 1.2 Kb and 3.5 Kb band (Figure 2.11). Of the 11 plasmids containing the SGT mutant construct, 2 were in the correct orientation. All those that produced a band of 400 bp and a band of 4.3Kb were in the incorrect orientation.

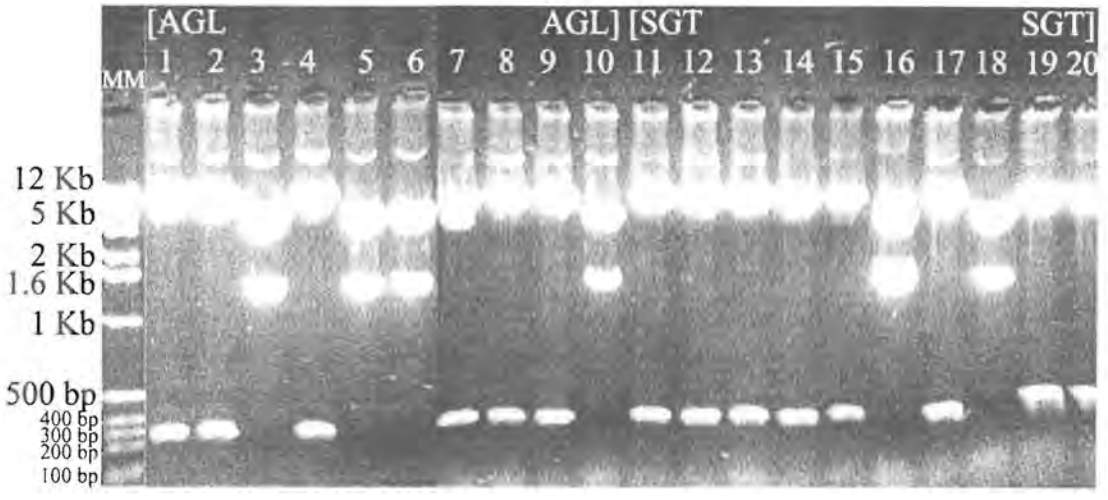

Figure 2.11: Evaluation of the correct orientation of insert in the pSP64T vector. Lanes 1-20 represent plasmids digested with *Hind*III to determine their orientation. Lanes 3, 5, 6 and 10 show plasmids from the AGL mutant containing an insert of the correct orientation. Lane 16 and 18 show plasmids from the SGT mutant containing an insert with a correct orientation. MM represents the 1 Kb Plus DNA Ladder.

2.3.6 Sequencing

The AGL and SGT mutant constructs contained in the pSP64T expression vector were sequenced before being used for cRNA transcription. The results from the analysis of the sequencing reaction over the mutated area confirmed the presences of the AGT mutant motif and the SGT mutant motif. These clones were renamed XA1.4 and XT1.10 respectively.

2.3.7 Transcription of cRNA

In order to commence cRNA transcription, the DNA template first needed to be linearised and cleaned to remove contaminating proteins and salts from the restriction digest. Figure 2.12A demonstrates DNA quality and yield after restriction enzyme digestion before and after Proteinase K digestion and phenol/chloroform extraction on a 1% w/v agarose gel. The resulting cRNA is shown in Figure 2.12B next to a 0.24-9.5 Kb RNA Ladder. The expected band size of the cRNA was approximately 1.5 Kb.

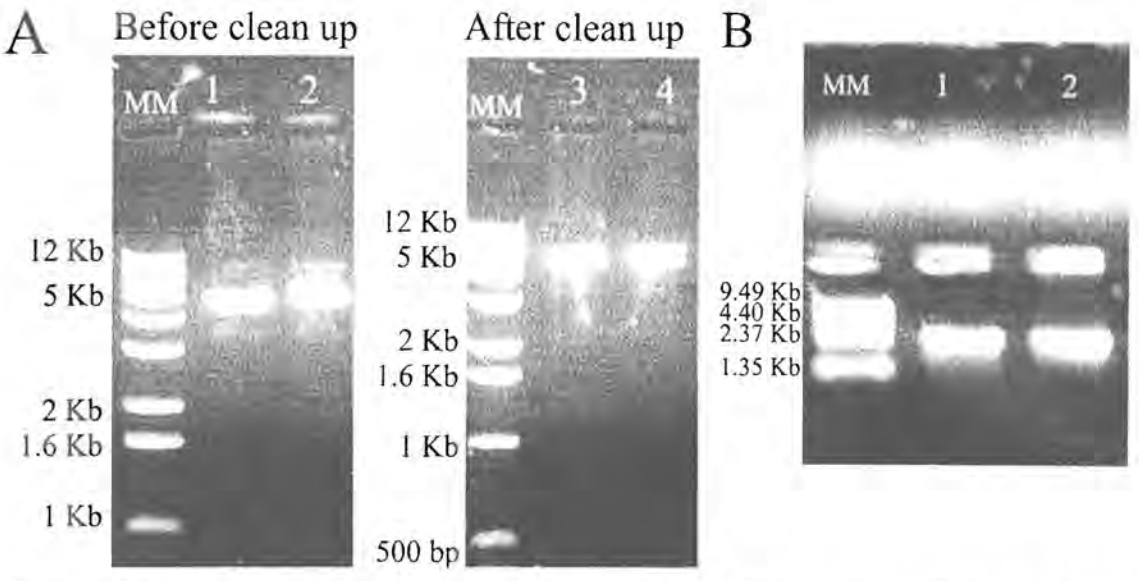

Figure 2.12: cRNA transcription DNA template and transcription product. **Figure A** shows the DNA template that was used in the cRNA transcription reaction. Lanes 1 and 2 represents the DNA template before clean-up and Lanes 3 and 4 represent the DNA template after clean-up. MM represents the 1 Kb Plus DNA Ladder. **Figure B** demonstrates the resulting cRNA from the transcription reaction on a non-denaturing agarose gel. MM represents the 0.24-9.5 Kb RNA Ladder.

The yield of cRNA after quantification with the spectrophotometer varied between 2.5 µg/µl and 5 µg/µl after being dissolved in 7-10 µl nuclease-free water. This was equivalent to a total yield of cRNA between 17.5 µg and 35 µg for every 1-1.5 µg DNA template and was close to the manufacturers predicted yield after proper use of the kit. From the spectrophotometric analysis of the cRNA, it was also observed to contain no protein or high salt contamination.

2.4 Discussion

Considering the importance of the *P. falciparum* glucose transporter PfHT1 and the role it could play in anti-malarial chemotherapy, the need for more information on this transporter is vital. Without the availability of the crystal structure of this transporter, mutational studies are presently one method to obtain structure-function information. Thus far studies on PfHT1 have revealed that it is a hexose transporter capable of transporting D-glucose and D-fructose with K_m values of 1.0 ± 0.2 mM and 11.5 ± 1.6 mM, respectively. The endofacial ligand Cytochalasin B shows high affinity for PfHT1 ($K_i \approx$ 1.4-4.3 µM) and the exofacial binding site probe 4,6-*O*-ethylidene-α-D-

glucose shows poor affinity for PfHT1 (K_i > 50 mM). Mutational studies have shown that the conserved residue Q169 in helix 5 mutated to asparagine results in the ablation of fructose transport (Woodrow *et al*, 2000).

Previous studies on the GLUT1 transporter have established a possible role for helix 7 in fructose/ glucose transport and helix 7 has also been implicated in exofacial ligand binding (Seatter *et al*, 1998). Most literature concerning helix 7 has focused on the QLS motif that is conserved within glucose transporters (GLUT1, 3 and 4) but is not present in hexose (GLUT2) or fructose (GLUT5) transporters (Table 2.1). Studies by Seatter *et al* (1998) suggested that the QLS motif confer on the transporter the ability to transport glucose at a higher affinity than the transporter would have if this motif were absent. This QLS motif in GLUT1 corresponds to a SGL motif in PfHT1. Mutation of PfHT1 helix 7 SGL motif to GLUT1 QLS resulted in no detectable uptake of either glucose or fructose (S. Krishna, unpublished results), which could be either due to a dysfunctional transporter or interrupted trafficking of the transporter to the oocyte membrane. The corresponding motif of *T. brucei* hexose transporter THT1 is an AGT motif. The affinity of THT1 for glucose is comparable to that of PfHT1, whilst its affinity for fructose is higher (K_i = 2.56 ± 0.40 mM; Tetaud *et al*, 1997) than that of PfHT1 (K_i ≈ 11.15 mM; Woodrow *et al*, 2000). Therefore the AGT motif in *T. brucei* was substituted for the SGL motif in PfHT1 in order to determine its role in glucose/ fructose binding. If this motif is responsible for fructose transport, its substitution is expected to increase the transporters ability to transport fructose. Binding of glucose to this motif can also be investigated with glucose analogues (explored in Chapter 3).

Primers were designed to incorporate mutations within the SGL motif of PfHT1. Primers of approximately 35 bases were designed to produce an SGL→AGT mutant. The length of the primers differed from the conventional length of primers of approximately 24 bases since base changes within the primer often results in lower stringency. Where bases between the primer and template are no longer complementary, binding becomes unstable at high annealing temperatures resulting in primer detachment from the template and reduced product. In this case the longer primers had a larger complementary area at the 3' end for stable priming. Additional

mutations within the helix 7 SGL motif included mutations of only one of the amino acids at a time within the motif to produce two mutants S302A and L304T intended to identify the amino acid within the motif responsible for any deviations in substrate-protein interaction (Table 2.2).

Restriction sites were included near the mutated motif. Even though primer design was limited, the primers were highly successful in the PCR 1 reactions and provided little difficulty (Figure 2.4). This was not the case for the PCR 2 reaction. Only after gel extraction of the PCR 1 products used as template for PCR 2 and optimisation of the PCR 2 reaction could the full-length gene product be recovered. For optimisation of the PCR 2 reaction, different dilutions of the template obtained from the first reaction were tested (Figure 2.6A). In Figure 2.6A, 1:10 and 1:100 dilutions of column purified PCR 1 product, which are then amplified in PCR 2, are shown. Figure 2.6A shows that a higher dilution (1:100) produces less non-specific amplification bands, but the expected band size of ≈ 1500 bp is only faintly visible. Thereafter the PCR 1 products were purified by gel extraction and used as a 1:10 dilution for PCR 2. The annealing temperature was raised to 60°C, which reduced the non-specific bands. The number of cycles used per reaction was optimised (Figure 2.6B). As shown in Figure 2.6B, excessive amplification cycles produced more non-specific amplified bands. Therefore a program of 15 cycles was decided on with a 1:10 dilution of template and an annealing temperature of 60°C.

Mutated clones in the pUC18 vector were checked for the presence of the correct mutation by restriction enzyme digestion in order to limit the number of clones to be sequenced. Partial digests of the AGL and SGT mutants are shown in Figure 2.9B. Since digestion of the inserts did occur, the presence of the mutations within the inserts was confirmed. After ligation of the mutated inserts into pSP64T, the presence of the mutated motifs was further confirmed by sequencing. The orientation of the insert in the pSP64T expression vector was determined by the use of restriction enzymes. The different sizes of bands produced by digestion with *Hind*III was used for identification of the correct orientation.

Two cRNA synthesis kits were used for the synthesis of cRNA. The Ambion kit was used at the St. Georges Hospital Medical in London. This kit was designed by a company specialising in RNA related products and the cRNA synthesised from this kit could be directly used for *in vivo* translation. The synthesis of cRNA was accomplished at the University of Pretoria using the Roche SP6 Cap Scribe. This kit did not specify that the cRNA produced could be directly used for *in vivo* translation and was specific for use in *in vitro* work. However the kit still produced cRNA in amounts equivalent to those produced by the Ambion kit and this cRNA was then was used for *in vivo* translation. The cRNA produced (Figure 2.12B) was used for microinjections into *Xenopus laevis* oocytes. The effects of the above produced mutants on glucose transport were determined by kinetic analysis in comparison to the wild type and presented in Chapter 3. In addition to these helix 7 mutants, a helix 5 mutant (Q169N) mentioned in Chapter 2.1 was also explored kinetically. This mutation resulted in the ablation of fructose transport (Woodrow *et al*, 2000).

3 CHAPTER THREE:

EXPRESSION AND KINETIC ANALYSIS OF THE PFHT1 HEXOSE TRANSPORTER IN *XENOPUS LAEVIS* OOCYTES

3.1 Introduction

The *Xenopus laevis* oocyte expression system was first used for the expression of rabbit reticulocyte 9S mRNA in 1971 and has since led to the expression of a variety of proteins. Apart from soluble proteins, the system has also been used for the expression of receptors, channel proteins and transporters (Hediger *et al*, 1987). The oocytes are ideal for expression of eukaryotic proteins since the synthesised proteins are subjected to post translational modifications such as glycosylation and are usually correctly folded and inserted into the cell membrane (Yao *et al*, 2000). Applications of the *X. laevis* expression system are shown in Figure 3.1.

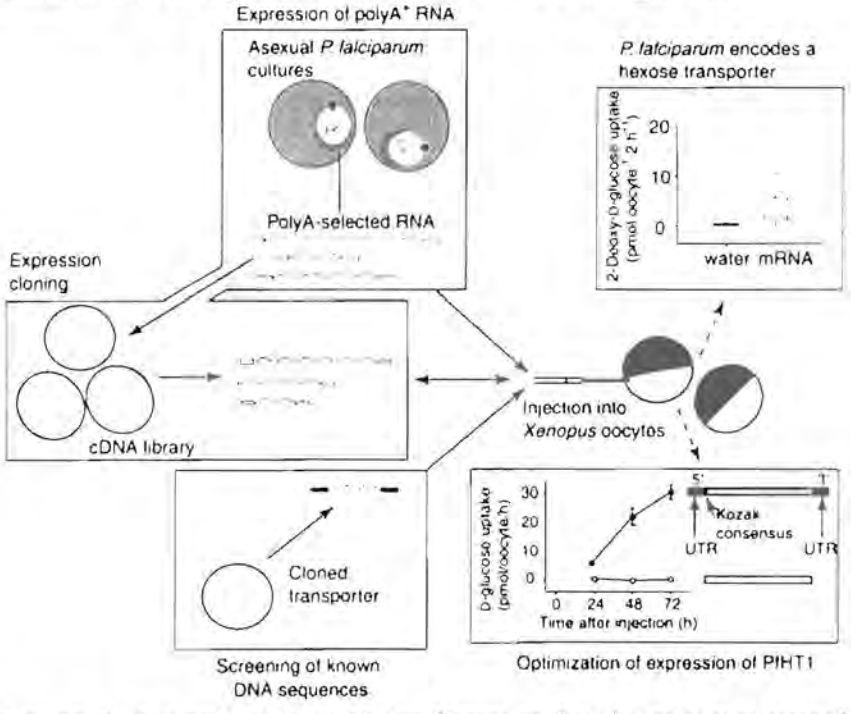

Figure 3.1: Applications of the *Xenopus laevis* oocyte expression system. *In vitro* transcribed cRNA of genomic DNA from cultured *P. falciparum*, cDNA libraries or clones are injected into *Xenopus* oocytes to reveal the possible functions and properties of translated proteins (Krishna *et al*, 2000).

The *X. laevis* frog is indigenous to South Africa, Botswana and South West Zimbabwe. The frogs are members of the family *Pipidae* and can be identified by having three claws on both their hind limbs (Figure 3.2A). For oocyte expression experiments female frogs are used and can be distinguished from males by their larger size and more prominent cloacal valves (Smart and Krishek, 1995). The oocytes are obtained from wild type or laboratory grown frogs by surgical procedures or by sacrifice of the frog. An adult frog can produce approximately 40000 oocytes that are at various stages of development. Fully-grown oocytes consist mainly of yolk proteins obtained from the maternal circulation and translation components required for the synthesis of proteins after fertilisation. Among these are three RNA polymerases sufficient to support zygotic transcription (Matthews, 1999). The oocytes grow to a diameter of >1mm and are visible with the naked eye. The ovaries of a mature female frog contain oocytes stretching over six different stages (I-VI, Figure 3.2B). Only the last two stages (stages V and VI) are used in expression studies. Stage V and VI stage cells are from 1-1.3 mm in diameter and with a light vegetal pole and a darker animal pole, which contains the nucleus. Less mature cells can be identified by the lack of pole differentiation and a uniform grey to white pigmentation. A good *Xenopus* specimen will normally contain ≥70% of stage V and VI oocytes. Under the right conditions the harvested oocytes can survive for a week and express proteins within 24h (Smart and Krishek, 1995; Yao *et al*, 2000).

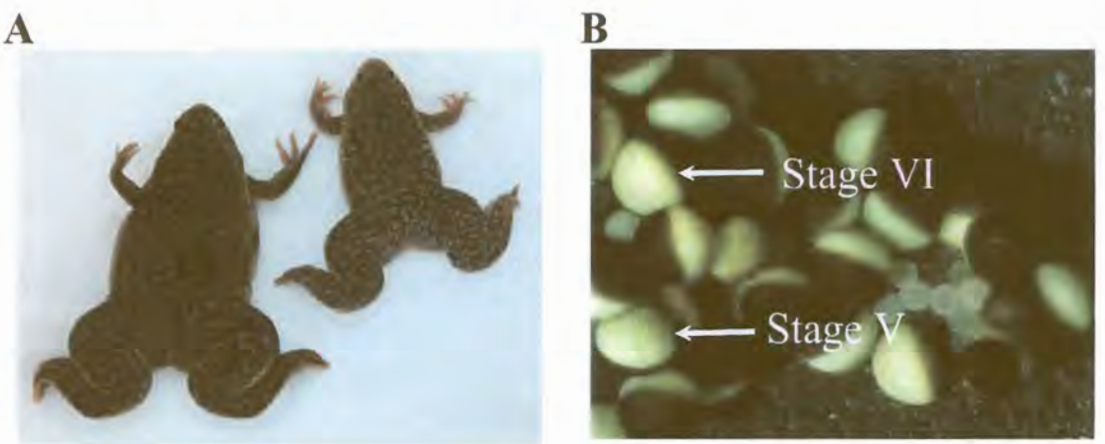

Figure 3.2: The *Xenopus laevis* frog and oocytes. Figure A demonstrates the morphology of the *Xenopus laevis* clawed frog. **Figure B** shows a typical mixture of *Xenopus* oocytes at various stages of development. The stage V oocyte is characterised by defined hemispheres. The stage VI oocyte can be distinguished from stage V by an equatorial band between the two phases. The colour of the mature oocytes can range between grey, brown, yellow and green (Yao *et al*, 2000).

The *Xenopus* oocyte expression system has been used for the heterologues expression of proteins from several different species. Heterologous expression of *P. falciparum* proteins is difficult because of *Plasmodium's* codon preferences and high A+T content (Withers-Martinez *et al*, 1999). However, the *Xenopus* oocyte expression system has been used successfully for the expression of *P. falciparum* proteins. The first reported use of this system for *P. falciparum* proteins dates back to 1982 (Gritzmacher and Reese, 1982).

Since then the successful expression of the ATP-binding cassette transporter, pfmdr1 (van Es *et al*, 1994), nucleoside, nucleobase, hexose and monocarboxylate transporter systems (Penny *et al*, 1998), as well as two different nucleoside/nucleobase transporters in *X. laevis* oocytes were reported (Parker *et al*, 2000; Carter *et al*, 2000). The isolation and expression of the *P. falciparum* hexose transporter PfHT1 in *Xenopus* oocytes was first described in 1999 (Woodrow *et al*, 1999).

Vectors such as pGEM-3Z (Promega) or pBluescript (Stratagene) are generally used for expression in *Xenopus* oocytes, but for the difficult malarial proteins it is recommended to use expression vectors such as pSP64T (Kreig and Melton, 1984) or pGEM-HE (Liman *et al*, 1992). The pSP64T vector contains an Ampicillan resistant gene, an SP6-promoter site and unique *Hind*II and *Bgl*II restriction sites situated between the 5'- and 3'-untranslated regions of the *Xenopus* β-globin gene (Appendix Ia; Yao *et al*, 2000). Studies conducted by Woodrow *et al* (2000) demonstrated the benefit of these untranslated regions as opposed to the same vector lacking them. In their work, they also included a Kozak sequence directly in front of the start codon (e.g. mRNA 5' – ACCAUG where the start codon is underlined), which is thought to be recognised by the ribosomal subunit at the start of synthesis (Lodish *et al*, 1995). In the absence of these additions, synthesis of the PfHT1 transporter was low as indicated by glucose uptake. Synthesis increased slightly with the inclusion of the 5'- and 3'-untranslated regions, and increased even more so with just the Kozak consensus in front of the PfHT1 start codon. However, inclusion of both the untranslated regions and the Kozak sequence produced the highest synthesis of transporter (Figure 3.3; Woodrow *et al*, 2000).

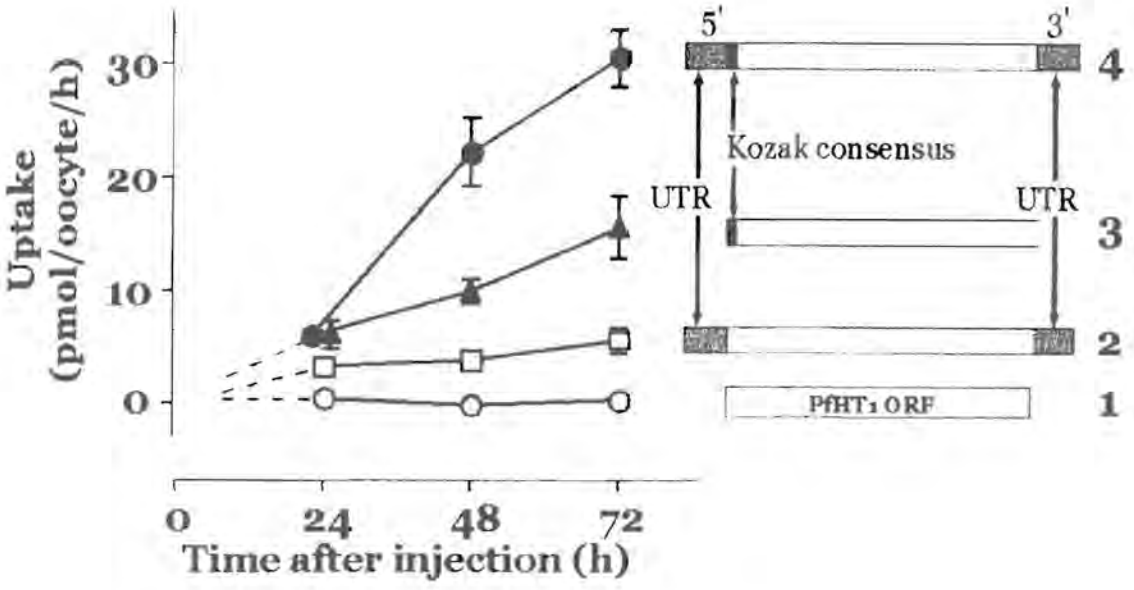

Figure 3.3: Influence of untranslated region (UTR) from *Xenopus* β-globin, and Kozak on expression of PfHT1 in *Xenopus* oocytes. ○ (1) = PfHT1 ORF. □ (2) = PfHT1 ORF UTR. ▲ (3) = PfHT1 ORF with the Kozak consensus. ● (4) = PfHT1 ORF with both the UTR and Kozak consensus (Woodrow *et al*, 2000).

In the present study three helix 7 mutant glucose transporters (described in Chapter 2) contained in the pSP64T vector namely, mutants SGL→AGT (denoted XF2.4), SGL→AGL (denoted XA1.4) and SGL→SGT (denoted XT1.10) were used as templates for synthesis of cRNA (Paragraph 2.2.9). Also included was a helix 5 mutant (denoted XmaI, described in Paragraph 2.4). Synthesised cRNA was injected into *Xenopus* oocytes and used for the estimation of kinetic parameters K_m (affinity or Michaelis constant) and K_i (half-maximal inhibition constant for carrier transport) for D-glucose and D-fructose. Estimations of K_i values for glucose analogues were also determined for each mutation. The latter kinetic parameters assist in the interpretation of the PfHT1 protein-substrate interactions.

3.2 Materials and methods

3.2.1 Harvesting of *Xenopus* oocytes

Harvesting of the *Xenopus* oocytes was conducted by two separate methods, one of which involved the sacrifice of the frog and the other one the anaesthetisation of the frog.

3.2.1.1 *Sacrifice of* Xenopus laevis

A mature female frog was placed in ice water for approximately 90 minutes to subdue her. The frog was removed from the water and decapitated by guillotine and placed dorsal side up on the operating surface. The sacs of oocytes were removed from the frog via an incision in the lower abdomen. All possible oocytes were removed to obtain maximum yield. The frog was disposed of in the appropriate manner (S. Krishna and C. J. Woodrow, personal communication). The oocytes were placed in a Petri dish containing calcium free Ringer solution (0.08 M NaCl, 1.3 mM KCl, 0.3% w/v N-2-hydroxylethylpiperazine-N'-2-ethanesulfonic acid (HEPES), pH 7.6; Smart and Krishek, 1995).

3.2.1.2 *Anaesthesia of* Xenopus laevis

A mature female frog was selected and placed in a separate container in tap water. A solution of 0.2% w/v MS-222 (3-Aminobenzoic Acid Ethyl Ester or Tricaine, Sigma, cat no A5040) was made up with 5 mM Tris-HCl (pH 7.4). This was placed in a glass container and the frog immersed in it. The degree of anaesthesia was checked every 5 minutes by turning the frog dorsal side up and checking for the "righting-reflex". Once anaesthetised the frog was washed under tap water to remove traces of anaesthetic. The frog was then placed dorsal side up on a flat bed of ice in a shallow tray. All bench surfaces were swabbed with 70% v/v ethanol and all surgical instruments were sterilised by autoclaving or with 70% v/v ethanol prior to operating. A small incision (1 cm) was made with a scalpel through the outer layer of the skin on one side of the frog. Another incision was then carefully made through the connective tissue and muscle sheet. Damage to the internal organs was avoided by lifting the exposed muscle sheet with a pair of forceps. Using a pair of forceps a section of ovary

sac-containing oocytes was carefully teased out of the incision. The sac was pinched off using absorbable surgical sutures and the oocytes were removed with scissors. The oocytes were placed in a Petri dish containing calcium-free Ringer solution. The incision was kept clear of blood and oocytes by constant spraying with distilled water and the skin and muscle layers were stitched separately using absorbable suture. The frog was recovered in a sloped container in distilled water containing 0.5% w/v NaCl for 12 hours and then left in distilled water until being returned to it's tank (Dr Eckstein-Ludwig, St. Georges Hospital Medical School, London, personal communication; Smart and Krishek, 1995).

3.2.2 Preparation of *Xenopus* oocytes

The oocytes contained in the Petri dish with calcium-free Ringer solution were manually separated into clumps with forceps and scissors. The oocytes were repeatedly washed in calcium-free Ringer solution to remove all traces of blood and cytoplasm from any ruptured oocytes. The oocytes were then defolliculated by treatment with 2 mg/ml collagenase (0.2-0.5 U/ ml, type 1A, Sigma-Aldrich, USA) for 60-120 minutes at room temperature on a shaker at approximately 50 rpm. After complete separation of the oocytes was obtained the collagenase reaction was stopped with Barth's solution (0.08 M NaCl, 1.3 mM KCl, 0.3% w/v HEPES, 0.32 mM $Ca(NO_3)_2$, 0.04 mM $CaCl_2$, 0.8 mM $MgSO_4$, 0.2% w/v $NaHCO_3$, pH 7.6; Smart and Krishek, 1995). The oocytes were repeatedly washed in Barth's solution to remove all traces of collagenase and then stored in Barth's solution containing 0.01 mg/ml penicillin and 0.01 mg/ml streptomycin (Sigma, UK) and incubated at 19°C until use.

3.2.3 Selection of *Xenopus* oocytes

Oocytes at stage V and VI were selected using a blunt and fire polished Pasteur pipette with the aid of a dissection microscope and a fibre optic lamp. Stage V and VI oocytes that had a distinct separation between the dark animal pole and light vegetal pole and without any discolouration or lesions or protrusions were selected. The much smaller and lighter Stage I oocytes, which can make selection more difficult, were

removed by repeated agitation and settlement of the oocytes in a 50 ml tube. The Stage I oocytes settled slower and were removed by vacuum suction or decanting without damage to any of the other cells. Selected stage V and VI cells were placed in a clean Petri dish containing Barth's solution with 0.01 mg/ml penicillin and 0.01 mg/ml streptomycin and incubated at 19°C until microinjection.

3.2.4 cRNA for microinjection into *Xenopus* oocytes

cRNA was prepared as described in Paragraph 2.2.9. The cRNA used for microinjections included that from wild type (PfHT1, provided by S. Krishna, St. George's Hospital Medical School, London) and the three helix 7 mutants namely, the SGL→AGT mutant (denoted XF2.4), the SGL→AGL mutant (denoted XA1.4) and the SGL→SGT mutant (denoted XT1.10). Also included in the cRNA pool was a helix 5 mutant provided by C. J. Woodrow (Woodrow *et al*, 2000). This mutant contains a point mutation at amino acid 169 (Q169N) and is denoted XmaI. No prior kinetic analysis of the helix 5 mutant had been performed other than determination of its K_m for D-glucose (Woodrow *et al*, 2000).

3.2.5 Microinjection of *Xenopus* oocytes

Sets of ten to twenty oocytes were drawn up in a blunt and fire polished Pasteur pipette and positioned on an oocyte holder (designed by S. Krishna, St. Georges Hospital Medical School, London) or in between two overlapping glass slides under a dissecting microscope illuminated by a fibre optic lamp. Glass capillaries were pulled into needles using a PUL-1 capillary puller (World Precision Instruments, UK) followed by attachment to the micromanipulator connected to a PicoPump microinjector (PV830) with PicoNozzle (World Precision Instruments, UK). RNA samples previously stored at -70°C were thawed on ice and diluted with nuclease-free water to concentrations of 0.4-0.5 ng/nl and pipetted onto parafilm. The RNA was drawn up into the needle by a suction pump attached to the microinjector. Volumes of 25-30 nl of RNA were injected into the vegetal pole of each oocyte if possible.

Alternatively RNA samples were diluted with nuclease-free water to concentrations of 2 ng/nl. The RNA was drawn up into an Eppendorf Microloader (Eppendorf, Germany) and pipetted into sterile Femtotips II (Eppendorf, Germany). The Femtotip was then connected to an Eppendorf FemtoJet microinjector (Eppendorf, Germany) and stabilised on a micromanipulator. Oocytes were injected with volumes of 5-7 nl RNA solution at a time.

Positive controls included oocytes injected with equal concentrations of wild type PfHT1 RNA or mammalian rat glucose transporter GLUT1 RNA (provided by S. Krishna, St. Georges Hospital Medical School, London), and negative controls or backgrounds were nuclease-free water-injected oocytes. Injected oocytes were collected in a Petri dish containing Barth's solution and antibiotics and incubated at 19°C for 1-4 days.

3.2.6 Uptake studies

Uptake measurements were conducted at intervals of 24, 48 and 72 hours after microinjection. Approximately 50 oocytes were injected for each cRNA and for each control (PfHT1 as positive control and water as negative control). At each time interval 6-8 oocytes were selected from each cRNA injected batch and 6 oocytes from the positive and negative controls. Oocytes were incubated in Barth's solution containing 2.5 µM D-[U-^{14}C]-glucose (Amersham Life Sciences, UK, 323 mCi/mmol) and 30 nM D-glucose (Sigma, UK) for 20 minutes and then washed three times in ice cold Barth's solution. Single oocytes were transferred into either a 1.5 ml microfuge tube and then counted on a Wallac 1450 Microbeta Plus scintillation counter (Wallac, Milton Keynes, UK) or in a 5 ml polyethylene Pony Vial (Packard, USA) and counted on a Minaxiβ Tri-Carb 4000 series liquid scintillation counter (United Technologies Packard, USA). 2 µl of uptake solution was also counted for each experiment and used to calculate pmol/ oocyte/ hour similar to calculations described in Paragraph 3.2.8. Uptakes were measured as decay per minute (DPM). Results were transferred into Microsoft Excel tables from which graphs were plotted to compare glucose uptakes for cRNA-injected and control-injected oocytes at each time interval.

3.2.7 Kinetic Assays

Once transport had been established for the mutant glucose transporters, the K_i and K_m values were determined. This analysis usually took place 36-48 hours after microinjection when expression was high and degradation of the oocytes was low. The uptake solutions used to determine the K_m for D-glucose of the mutant transporters contained 2.5 μM D-[U-^{14}C]-glucose (Amersham Life Sciences, UK, 323 mCi/mmol) in Barth's solution (pH 7.4) and 0.2-2 mM D-glucose. The uptake solutions used to determine the K_m for D-fructose of the mutant transporters contained 5.6 μM D-[U-^{14}C]-fructose (Amersham Life Sciences, UK, 289 mCi. mmol^{-1}) in Barth's solution (pH 7.4) and 1-20 mM D-fructose. Uptake solutions used to determine the K_m for 2-deoxy-D-glucose (2-DOG) and 3-*O*-methyl-D-glucose (3-OMG) contained 14.3 μM 2-deoxy-D-[U-^{14}C]glucose (58 mCi.mmol^{-1}) or 16.6 μM 3-*O*-[^{14}C]methyl-D-glucose (50 mCi.mmol^{-1}; Amersham Life Sciences, UK) in Barth's solution (pH 7.4) and 0.3-20 mM 2-DOG or 0.2-10 mM 3-OMG, respectively.

Six sets of different concentrations were used per K_m determination with 8 RNA and 6 water injected oocytes per set. Oocytes were immersed in uptake solution for 20 minutes, then removed and washed three times in ice-cold Barth's solution.

For each K_i analysis a total of 50-100 oocytes were injected with cRNA and 30-80 oocytes with water. Eight cRNA injected oocytes were used for either glucose analogues, D-fructose or the fructose analogue, 2,5-anhydro-D-mannitol (2,5-AHM) at five different concentrations each. Included in each experiment was one set of 8 cRNA injected oocytes incubated in only D-glucose (uninhibited) and a set of 6 water injected oocytes. Each uptake solution for K_i analysis contained 2.5 μM D-[U-^{14}C]-glucose and 30 nM D-glucose in Barth's solution and a range of concentrations of glucose analogues, D-fructose and 2.5-AHM. Glucose analogues included 1-deoxy-D-glucose (1-DOG), 2-deoxy-D-glucose (2-DOG), 3-*O*-methyl-D-glucose (3-OMG), 5-thio-D-glucose and 6-deoxy-D-glucose (6-DOG). D-fructose and all analogues were from Sigma or Amersham (Sigma-Aldrich, UK; Amersham, UK; Figure 3.4). Each oocyte was placed in a separate microfuge tube or pony vial and lysed in the appropriate volume of scintillation fluid and counted in a scintillation counter.

Glucose analogues

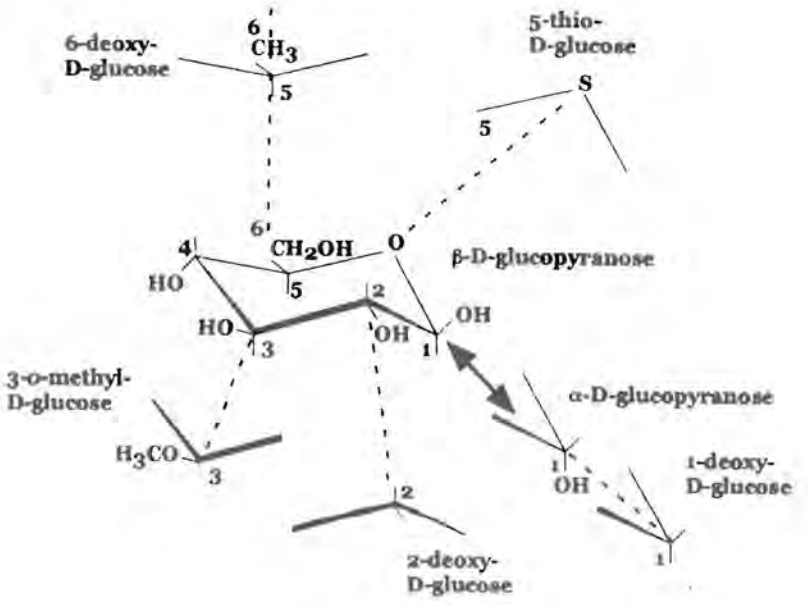

Fructose analogues

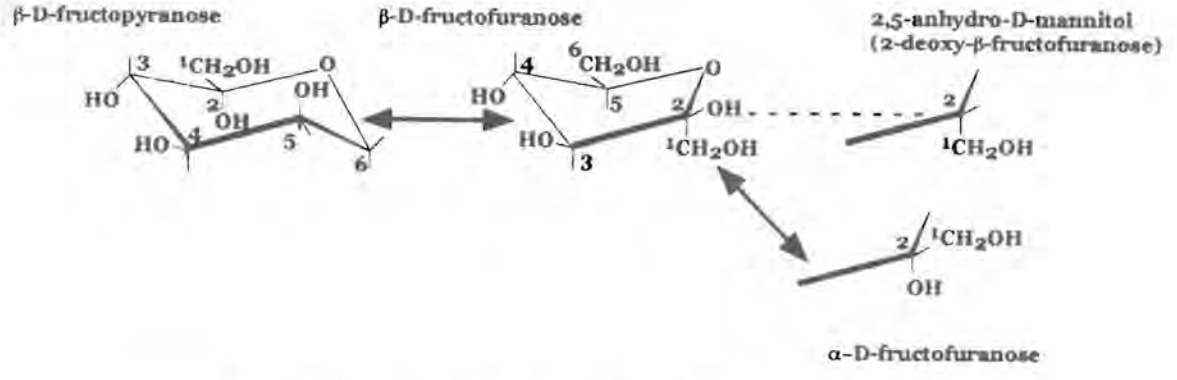

Figure 3.4: Analogues used in studies on PfHT1 and the mutated transporters Xma1, XF2.4, XA1.4 and XT1.10. Structures are represented as chair conformations. Solid arrows indicate conversions that occur under normal conditions in solution.

3.2.8 Data analysis

Initial DPM results from K_m and K_i experiments were transferred into Microsoft Excel tables to calculate the pmols/ oocyte/ hour (for K_m) and percentage of uninhibited transport (for K_i). These values were used to calculate the K_m and K_i with Prism version 2.0 (GraphPad Prism inc., USA). A Michaelis-Menten model was used for all

estimations of kinetic parameters by nonlinear regression analysis. The pmol/ oocyte/ hour value is calculated as follows:

A volume (2 µl or $2/10^6$ L) of uptake solution was counted and determined as DPM (C). *With the known concentration of inhibitor in mM* (A) *the DPM data obtained for each oocyte* (B) *was then used to determine the pmols of substrate transported into each oocyte.*

$$\frac{2\cancel{L}}{10^6} \times \frac{\text{A mmols}}{\cancel{L}} \times \frac{\text{B } \cancel{\text{DPM}}/\text{ oocyte}}{\text{C } \cancel{\text{DPM}}}$$

$\therefore 2/10^6 \times A \times B/C$ mmols/ oocyte

To get pmols: $2/10^6 \times A \times B/C$ *mmols/ oocyte* $\times 10^9$

$\therefore 2 \times 10^3 \times A \times B/C$ pmols/ oocyte

Each uptake is performed for a certain time D *(eg. 20 minutes). The time is taken as a fraction of an hour,* 60/D.

$\therefore 2 \times 10^3 \times A \times B/C \times 60/D$ pmols/ oocyte/ hour

3.3 Results

3.3.1 Uptake studies

The time course of glucose uptake induced by PfHT1 or the 302SGL→AGT, S302A and L304T PfHT1 helix 7 mutants are shown compared in Figure 3.5. Reconfiguration of the 302SGL triplet motif in helix 7 of PfHT1 to an equivalent motif (AGL) found in THT1, the *T. brucei* hexose transporter, appeared to alter the overall uptake rates of ^{14}C-glucose when compared with the wild type PfHT1 transporter 72 hours after microinjection ($P < 0.012$, n = 2, where values below 0.05 are considered statistically significant, see Figure 3.5 for an example of one experiment out of the three that were conducted.). In the example shown in Figure 3.5, the expression or efficiency of XF2.4 (the 302SGL→AGT mutant) was clearly delayed or lower compared with the wild type at 24 ($P < 0.0001$), 48 ($P < 0.0001$) and

72 ($P = 0.012$) hours after microinjection. XF2.4 produced uptake measurements that were below half that of the wild type PfHT1 at 24 hours after microinjection (25.0 ± 2.7 pmols/ oocyte/ hour compared with the wild type at 63.6 ± 4.4 pmols/ oocyte/ hour), and over half at 48 hours after microinjection (42.3 ± 2.4 pmols/ oocyte/ hour compared with the wild type at 77.4 ± 5.9 pmols/ oocyte/ hour) and 72h after microinjection (29.6 ± 4.1 pmol/ oocyte/ hour compared with the wild type at 56.7 ± 8.4 pmol/ oocyte/ hour). Uptake measurements plateau after 72h (results not shown).

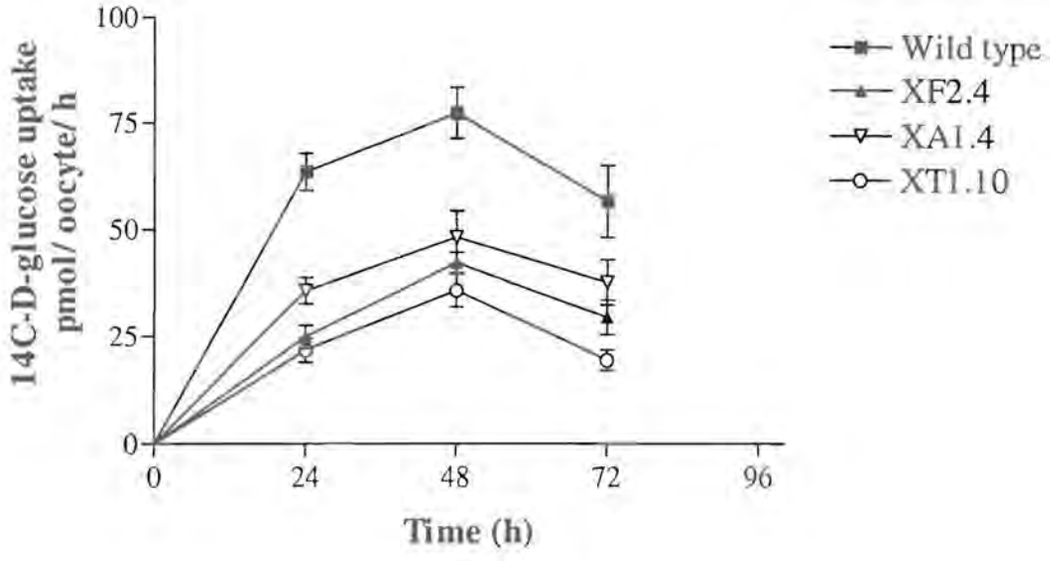

Figure 3.5: Time course assay of helix 7 mutants XF2.4, XA1.4 and XT1.10 compared with the wild type PfHT1. An equal concentration of cRNA from the wild type and each mutant was injected per oocyte. Glucose uptakes were assayed at the times indicated. Eight oocytes were used per uptake. Data displayed are mean ± SE of eight oocytes.

Uptake measurements for the time study were carried out on the S302A (XA1.4) and L304T (XT1.10) mutants in order to better define which amino acid within the XF2.4 construct was most responsible for the lower uptake measurements seen at 24, 48 and 72 hours (Figure 3.5). Uptake measurements with D-glucose proved each construct to be functional. Both XA1.4 and XT1.10 showed lower uptake ($P < 0.0010$) than the wild type at 24 hours (35.8 ± 3.1 pmol/ oocyte/ hour and 21.8 ± 2.8 pmol/ oocyte/ hour, respectively) and 48 hours (48.3 ± 6.2 pmols/ oocyte/ hour and 35.9 ± 3.9

pmols/ oocyte/ hour, respectively) after microinjection. The XA1.4 mutant had uptake values higher than XT1.10 at 24 and 48 hours after microinjection. At 72 hours the mean uptake value for XA1.4 shown in Figure 3.5 (37.8 ± 5.3 pmol/ oocyte/ hour) was not significantly different (P = 0.0780) compared with the wild type, but was significantly different (P = 0.0069) compared with XT1.10. The mean uptake measurements for XA1.4 were only significantly different to XF2.4 at 24 hours in 2 of the 3 independent experiments. The mean uptake values for XT1.10 were not significantly different to XF2.4 at any time point in 3 independent experiments.

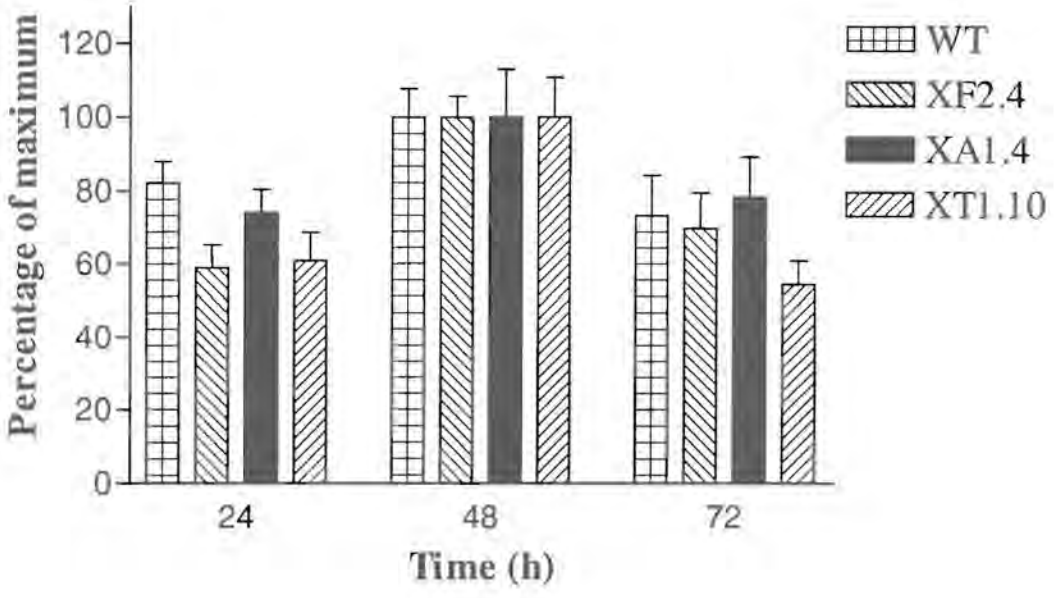

Figure 3.6: Normalization of the results represented in Figure 3.5. Values are shown as percentages of the maximum expression, which is taken at 48 hours, for each mutant and the wild type independent of each other. Data displayed are mean ± SE of eight percentages from each of the eight oocytes from Figure 3.5.

With the results in Figure 3.5 normalized as shown in Figure 3.6, it can be speculated that the XA1.4 mutant may follow a similar expression pattern to the wild type. Maximum expression is seen at 48 hours which is taken as 100%. At 24 hours XA1.4 shows 74.1 ± 6.4% of its maximum expression and the wild type is at 82.2 ± 5.7 %. At 72 hours XA1.4 shows 78.3 ± 10.9 % of its maximum expression and the wild type is at 73.3 ± 10.9 %. The XT1.10 mutant follows a similar expression pattern to that of

XF2.4. At 24 hours XT1.10 shows 60.9 ± 7.8 % of its maximum expression and XF2.4 is at 58.9 ± 6.4 %. At 72 hours XT1.10 shows 54.4 ± 6.5 of its maximum expression and XF2.4 is at 69.8 ± 9.6 %. In subsequent experiments, similar patterns were seen between the wild type and the mutants.

3.3.2 Kinetics of substrate transport of mutants in comparison to PfHT1

Table 3.1 provides K_m and K_i values obtained for PfHT1 and its various mutants. The K_m values indicate the affinity between PfHT1 and substrate. To characterise substrate-transporter interactions, a series of hexose analogues are used as competitors for transport of D-glucose, which provides a K_i value for each analogue. Uptake experiments for K_m studies involve a homogeneous solution of substrate and the rate of uptake is uniform. Uptake experiments for K_i studies involve a heterogeneous solution containing competitor (analogues) and substrate (glucose). The rate of translocation of the substrate compared with the competitor may differ; therefore K_i values are only estimates of affinity between PfHT1 and competitor.

The mutation of helix 7 SGL motif to AGT (XF2.4) supports transport of both D-glucose and D-fructose. The affinity of D-glucose for XF2.4 is not significantly different to that of the wild type ($P = 0.4825$). The affinity of glucose for XF2.4 (K_m = 0.95 ± 0.2 mM) is similar to that of the wild type (K_m = 1.0 ± 0.2 mM). XF2.4 was also capable of transporting 1-DOG, 2-DOG, 3-OMG, 5-thio-D-glucose and 6-DOG (Table 3.1). The segregated mutants S302A (XA1.4) and L304T (XT1.10) show a similar ability to transport D-fructose and D-glucose as well as the glucose analogues mentioned above. The increased affinity of glucose for the XA1.4 mutant (K_m = 0.47 ± 0.1 mM) was significantly different from the wild type ($P = 0.0410$) but not from the XF2.4 mutant ($P = 0.0600$). The increased affinity of glucose for the XT1.10 mutant (K_m = 0.68 ± 0.04 mM) was not significantly better ($P = 0.0887$) than the wild type, nor the XF2.4 mutant ($P = 0.1680$). The results therefore suggest a higher affinity of the XA1.4 for glucose to that of the wild type. The helix 5 mutant Q169N, though unable to transport D-fructose as previously reported (Woodrow *et al*, 2000), was capable of transporting D-glucose and the glucose analogues mentioned above.

3.3.2.1 Aldose analogue analysis

3.3.2.1.1 Deoxyaldose analogues.

Helix 5 mutant: For the helix 5 Q169N mutant (Xma1) the results in Table 3.1 indicate no change in affinity for 1-DOG (K_i = 13.6 ± 2.0 mM) compared with the wild type (K_i = 14.7 mM, 15.9 mM). A significant 2-3-fold decrease (P = 0.0045) in affinity was observed for 2-DOG (K_m = 3.4 ± 0.3 mM) compared with wild type (K_m = 1.3 ± 0.4 mM). A significant 3-4-fold decrease (P = 0.0087) in affinity was observed for 6-DOG (K_i = 7.9 ± 0.8 mM) compared with wild type (K_i = 2.2 ± 0.9 mM). An approximate 4-fold and significant increase (P = 0.0062) in affinity for 5-thio-D-glucose was shown for Xma1 (K_i = 0.8 ± 0.1 mM) compared with the wild type (K_i = 2.9 ± 0.4 mM).

Helix 7 mutants: DOG studies on the helix 7 mutant (302SGL→AGT; XF2.4) revealed a 2-fold decrease in affinity for 1-DOG (K_i = 26.4 ± 1.1 mM), and a 3-fold decrease in affinity for 6-DOG (K_i = 6.8 ± 1.0 mM), which are statistically significant (P = 0.0048 and 0.0273, respectively). However, its affinity for 2-DOG (K_m = 1.2 ± 0.5 mM) remained the same as the wild type. A 5-fold and significant decrease (P = 0.0039) in affinity was observed for 5-thio-D-glucose (16.1 ± 2.2 mM) compared with the wild type. Kinetic studies on the point mutation S302A together with statistical calculations showed that the 2-fold increase in K_i with 1-DOG observed for XF2.4 might be attributed to this single point mutation (K_i = 42.7 ± 5.4 mM, with P = 0.0301 when compared with the wild type) and not to the L304T mutation (K_i = 19.0 ± 2.1 mM, with P = 0.2729 when compared with the wild type). No statistically significant increase in K_i for 6-DOG was observed when compared with wild type for either S302A (K_i = 2.4 ± 0.2 mM; P = 0.9754) or L304T (K_i = 3.8 ± 0.7 mM; P = 0.2299). Both S302A and L304T mutants separately showed an increase in affinity for 5-thio-D-glucose (K_i = 11.2 ± 1.6 mM and 8.2 ± 2.0 mM) compared with the XF2.4 mutant but still a decrease in affinity compared with the wild type. Only the S302A mutant showed a statistically significant increase in affinity (P = 0.0067) for 5-thio-D-glucose when compared with the wild type. The K_i for 2-DOG obtained from XA1.4 (K_i = 0.7

± 0.2 mM) and XT1.10 (K_i = 1.2 ± 0.3 mM) was similar to the K_m value obtained from the wild type.

3.3.2.1.2 Methylaldohexoses.

The replacement of hydrogen with a larger methyl group gives an indication of the available space surrounding the carbon, and the proximity of the protein to the sugar at that site. The K_m values (7.3 mM, 5.5 mM) achieved with 3-OMG for the Q169N mutant indicated a significant decrease in affinity (P = 0.0067) of the mutant transporter for 3-OMG compared with the wild type (K_m = 1.3 ± 0.3 mM). The same is true for XF2.4 where the K_m result (K_m = 5.6 ± 0.8 mM) is 4-fold higher and significantly different (P = 0.0074) to that of the wild type. The K_i values for the XA1.4 and XT1.10 mutants for 3-OMG (K_i = 1.2 ± 0.2 mM and 1.0 ± 0.1 mM, respectively) were similar to that of the wild type (K_i = 1.4 mM, 2.7 mM; K_m = 1.3 ± 0.3 mM) and not significantly different (P = 0.6379 and 0.3553, respectively).

3.3.2.2 Ketose analogue analysis

As shown in Table 3.1 the Q169N mutant does not transport D-fructose in agreement with previously reported results (Woodrow *et al*, 2000). The mutations in helix 7 were also thought to play a role in fructose transport. For the helix 7 mutants, there appears to be a decrease in affinity for fructose as evidenced by the K_m values of all three mutants in comparison to the wild type. The XF2.4 mutant shows a 2-fold decrease in affinity (K_i = 23.1 ± 1.9 mM) and the segregated mutants XA1.4 and XT1.10 show a similar decrease (K_i = 19.9 ± 1.7 mM and 17.1 ± 3.0 mM, respectively) compared with the wild type (K_m = 11.5 ± 1.6 mM or $K_i \approx$ 11 mM). The decrease in affinity for fructose seen for XF2.4 was statistically significant (P = 0.0258) compared with the wild type, whereas XA1.4 and XT1.10 were not (P = 0.0.0630 and P = 0.2495, respectively). To confirm these results, transport of the fructose analogue 2,5-anhydro-D-mannitol (2,5-AHM) was also determined. All three helix 7 mutants XF2.4 (K_i = 1.7 ± 0.15 mM), XA1.4 (K_i = 2.2 mM, 1.2 mM) and XT1.10 (K_i = 2.7 mM, 1.0 mM) showed no significant difference in K_i for 2,5-AHM compared with the wild type (K_i = 1.4 ± 0.3 mM) with P values of 0.4791, 0.6532 and 0.6121, respectively.

Table 3.1: Kinetic analysis of helixes 7 and 5 mutants compared to the wild type on transport of glucose, fructose and analogues . All values are in mM. PfHT1 kinetic results have been previously reported (Woodrow, *et al*, 2000) except for one 5-thio-D-glucose value and one 1-DOG value, which were needed for a SE calculation. Xma1 is the Q169N mutant of helix 5 that has been previously reported but on which no kinetic studies had been done.

*Means ± SE of three independent experiments unless otherwise indicated.

†Xma1 glucose K_m and ketose analogue results were obtained from previous experiments (Woodrow, *et al*, 2000).

Substrate	PfHT1 (wild type)	*Helix 5 mutant* Xma1† (Q169N)	*Helix 7 mutant* XF2.4 (302SGL→AGT)	*Helix 7 mutant* XA1.4 (S302A)	*Helix 7 mutant* XT1.10 (L304T)
Aldose analogues D-glucose	$K_m = 1.0 \pm 0.2$*	†$K_m = 1.2 \pm 0.2$	$K_m = 0.93 \pm 0.3$	$K_m = 0.47 \pm 0.2$	$K_m = 0.68 \pm 0.07$
C1-position 1-deoxy-D-glucose	$K_i = 14.7, 15.9$	$K_i = 13.6 \pm 3.4$	$K_i = 26.4 \pm 1.9$	$K_i = 40.0 \pm 6.4$	$K_i = 19.0 \pm 3.7$
C2-position 2-deoxy-D-glucose	$K_m = 1.3 \pm 0.4$	$K_m = 3.4 \pm 0.5$	$K_m = 1.2 \pm 0.8$	$K_i = 0.7 \pm 0.3$	$K_i = 1.2 \pm 0.5$
C3-position 3-*O*-methyl-D-glucose	$K_m = 1.3 \pm 0.3$ $K_i = 1.4, 2.7$	$K_m = 7.3, 5.5$	$K_m = 5.6 \pm 1.6$ (n = 4)	$K_i = 1.2 \pm 0.4$	$K_i = 1.0 \pm 0.2$
C5-position 5-thio-D-glucose	$K_i = 2.9 \pm 0.7$	$K_i = 0.8 \pm 0.1$	$K_i = 16.1 \pm 3.7$	$K_i = 11.2 \pm 2.7$	$K_i = 8.1 \pm 3.3$
C6-position 6-deoxy-D-glucose	$K_i = 2.2 \pm 0.9$	$K_i = 7.9 \pm 1.5$	$K_i = 6.8 \pm 1.8$	$K_i = 2.4 \pm 0.4$	$K_i = 3.8 \pm 1.1$
Ketose analogues D-fructose	$K_m = 11.5 \pm 1.6$ $K_i = 10.6, 11.7$	†No trans.	$K_i = 23.0 \pm 3.2$	$K_i = 19.9 \pm 3.0$	$K_i = 17.1 \pm 5.2$
C2-position 2,5-anhydro-D-mannitol	$K_i = 1.4 \pm 0.3$	†$K_i = 28$	$K_i = 1.7 \pm 0.2$	$K_i = 2.2, 1.2$	$K_i = 2.7, 1.0$

3.4 Discussion

Three mutations in the PfHT1 helix 7 motif SGL and one in helix 5 (Q169N) were investigated. These two helices have previously been implicated in substrate binding or glucose/ fructose differentiation. The most significant difference up to date between the PfHT1 and GLUT1 transporters is PfHT1s ability to transport fructose as well as glucose (Woodrow *et al*, 1999). Studies with mammalian glucose transporters (GLUT1, 3 and 4) and hexose transporters (GLUT2 and 5) have implicated helix 7 as being involved in glucose/ fructose recognition and translocation (Arbuckle *et al*, 1996; Seatter *et al*, 1998). Cysteine-scanning mutagenesis studies on GLUT1 helix 5 have indicated 6 amino acids accessible to external medium all of which were clustered along one face of the putative α-helix (Mueckler *et al*, 1999). Similar studies were conducted with GLUT1 helix 7. Several amino acids in GLUT1 helix 7, predicted to lie near the exofacial side of the cell membrane, were shown to be accessible to outside medium. However these amino acids did not cluster along one face of the putative α-helix. This provided evidence for the likely positioning of helix 7 within the glucose permeation pathway as shown in Chapter 2, Figure 2.1B (Hruz and Mueckler, 1999).

In this study, the uptake measurements of the helix 7 and helix 5 mutants were performed on cRNA injected oocytes with D-glucose, D-fructose and hexose analogues. The XF2.4, XA1.4 and XT1.10 mutants produced lower uptake measurements compared with the wild type at 24, 48 and 72 hours (Figure 3.5). Since the K_m values for the helix 7 mutants are all similar to the wild type (Table 3.1), the lower uptake measurements seen at 24, 48 and 72 hours for XF2.4, XA1.4 and XT1.10 were not due to a decrease in affinity (Figure 3.5). Two possibilities exist that could explain this lower uptake. The mutations could be affecting the transporters ability to change its conformation, decreasing translocation of the substrate from the external medium to the inside (Chapter 1, Section 1.6.2.1), therefore the transporters efficiency is affected. If the mutant's ability to translocate substrate across the membrane is similar to the wild type, the lower uptake measurements could be as a result of a lower expression of the mutant transporters compared with the wild type so

that there are less mutant transporters compared with wild type transporters present on the membrane at any given time.

Since the XF2.4 mutant, which contains a double point mutation, was segregated into two single mutations S302A (XA1.4) and L304T (XT1.10), one may be able to determine if a single amino acid within the XF2.4 construct was responsible for the lower uptake seen for the mutant at 24, 48 and 72 hours. As shown in Figure 3.5, both the S302A and L304T mutants had similar uptakes to the XF2.4 mutant at 24, 48 and 72 hours after microinjection. However, the XT1.10 mutant had significantly lower ($P < 0.04$) uptakes than the XA1.4 mutant at 24, 48 and 72 hours. The expression patterns shown in Figure 3.6 suggest that the XA1.4 mutant follows a similar expression pattern to the wild type whilst the XT1.10 mutant follows a similar expression pattern to the XF2.4 mutant. This suggests that the L304T mutant may be in some way more responsible for the lower uptakes seen in Figure 3.5. However, both mutants collectively appear to have an effect on the transporters efficiency or expression. These results were reproducible in two further experiments.

For the kinetic studies (Paragraph 3.3.2), results obtained with glucose analogues with PfHT1 mutants were also compared with results obtained for the wild type to see what influence the mutation had over the already existing changes in affinity produced by the glucose analogues. These changes in affinity between mutant transporters and substrate will give insight into how a specific amino acid interacts with different carbon atoms on the glucose substrate. Those analogues that produced statistically significant changes in affinity are discussed below.

Deoxy-D-glucose (DOG) analogues provide insight into which ones out of the six possible hydrogen bonding sites on glucose are required for substrate-protein interactions via hydrogen bonds. These potential hydrogen-bonding sites are interrupted by removal of the hydroxyl group (on carbons 1-4 and 6) and by replacing the oxygen on C-5 with a sulphur atom. K_m is an indication of affinity between transporter and substrate. K_i is similar to K_m but provides only an estimate of affinity between transporter and substrate as discussed in Paragraph 3.3.1.

Looking at the helix 5 mutant (Q169N) in comparison with the results obtained for the wild type (Woodrow *et al*, 2000), Q169 did not appear to be involved in binding to the C-1 oxygen, as the K_i was no different to that obtained for the wild type. A statistically significant decrease in affinity was observed for 2-DOG, which suggests that the oxygen at this carbon is involved in hydrogen bonding to the helix 5 Q169 amino acid. The 3-DOG analogue was not used, but the 3-OMG analogue did produce a 5-fold decrease in affinity compared with the wild type, which is discussed below. A 4-fold increase in affinity between XmaI and 5-thio-D-glucose was produced, which could suggest that asparagine in helix 5 hydrogen bonds more strongly to the C-5 sulphur of 5-thio-D-glucose than the glutamine did that it replaced (Appendix II for amino acid structures). Both oxygen and sulphur have an equal potential to form hydrogen bonds as a result of an equal number (2) of lone-pair (valence) electrons. Sulphur differs to oxygen in that it is able to form a further 4 covalent bonds as a result of its empty 3d orbital in its outer electron shell. Whether this has caused the increase in affinity between XmaI and 5-thio-D-glucose is uncertain. A 4-fold decrease in affinity compared with the wild type was observed with 6-DOG, which suggests an importance for the C-6 hydroxyl group for hydrogen bonding to helix 5.

The introduction of a much larger methyl group on D-glucose C-3 gives an indication of the available space surrounding the carbon, and the proximity of the protein to the sugar at C-3. A 5-fold decrease in affinity between XmaI and 3-OMG compared with the wild type and 3-OMG was observed. This suggests that introduction of an asparagine in place of a glutamine (Q169N) decreased the ability of the transporter to transport 3-OMG. This is interesting since asparagine is one C-atom shorter than glutamine, which is expected to create more space for the accommodation of the methyl group. The introduction of a methyl group also increases the potential for hydrogen bonding. The higher potential for hydrogen bonding could increase the affinity of the transporter for the substrate. However, since affinity decreased instead, this is not the case. The additional hydrogens, introduced by 3-OMG, also increase the positive charge at C-3, which could have an adverse affect on the affinity of the transporter for the substrate. The relevance of glutamine in spatial interactions with 3-OMG can only be resolved by mutating it to larger residues such as arginine, lysine or histidine.

The results obtained for Q169 seem to indicate that this amino acid is important for hydrogen bonding to C-2, C-3, C-5 and C-6. However, when this amino acid was mutated to asparagines it resulted in the ablation of fructose transport. Therefore the importance of this amino acid in interactions with the substrate could be extensive, and hence it is probable that it interacts with the glucose substrate at all these carbon atoms.

For the helix 7 mutants, the S302 amino acid may be involved in hydrogen bonding to C-1, which when mutated to alanine decreases the affinity between PfHT1 and 1-DOG by almost a third (Table 3.1). Studies on the double mutation in helix 7 (302SGL→AGT; XF2.4) suggested an importance of C-6 (3-fold decrease in affinity with 6-DOG). However the affinity is not affected when the XF2.4 mutant is segregated into XA1.4 and XT1.10, which have K_i values similar to the wild type. Therefore the importance of D-glucose C-6 in hydrogen bonding to helix 7 at this motif is debatable, or perhaps both mutations need to be present for transport to be affected negatively. There is a 6-fold decrease in affinity between XF2.4 and 5-thio-D-glucose compared with the wild type. However, it appears that both amino acids (302S and 304L) may be needed for the helix 7 interactions with D-glucose substrate at C-5. Both separately cause a decrease in affinity for substrate when mutated, but only the S302A mutation causes a statistically significant decrease in affinity when compared with the wild type. Therefore the S302A mutant is probably more responsible for the decrease in affinity seen between XF2.4 and 5-thio-D-glucose. Oxygen is more flexible around its covalent bonds and therefore will allow the glucose to be more flexible to fit into the transporters binding site. Therefore the introduction of a sulphur atom at this site may cause the glucose to be more rigid and unable to interact properly at this helix 7 site within the transporter.

There is a 4-fold decrease in affinity between XF2.4 and 3-OMG compared with the wild type. The amino acids alanine and threonine that replace serine (S302) and leucine (L304), respectively, are shorter by one carbon. For S302A there is a loss of a hydroxyl group, which may have formed a hydrogen bond to the substrate at C-3. For the L304T mutant there is a gain of a hydroxyl group, which might interfere

negatively as a result of the increase in positive charges created by the additional hydrogens from the methyl group. As for their properties, S302A results in the exchange of a polar side chain to a non-polar side chain, and L304T results in the opposite. When these two mutations are separated the decrease in affinity is abolished, the reasons for which are unclear. Therefore both are needed for the decrease in affinity to occur between XF2.4 and 3-OMG.

Previous studies with PfHT1 showed hydrogen bonding to glucose to be important at position C-1 and C-3 with a more than 10-fold increase in K_i with 1-DOG and 3-DOG compared with D-glucose (Woodrow *et al*, 2000). The results of this study on helix 7 with glucose analogues suggest possible hydrogen-bonding interactions of the SGL motif with D-glucose C-1, C-3, C-5 and C-6. However, there are a few points to be considered when reviewing the results from this study. The decrease in affinity seen for XF2.4 and 3-OMG might not be as a result of loss of hydrogen bonding but rather as a result of disfavour of the transporter for the larger methyl group. Also, when the amino acids S302 and L304 were tested separately with 3-OMG, the decrease in affinity observed with XF2.4 was not reproduced. Therefore, the importance of glucose C-3 in hydrogen bonding might be better resolved with an analogue such as 3-DOG where the oxygen is absent. C-6 investigated with 6-DOG only produced a change in the double point mutation XF2.4 and not when the mutations were separated. This questions the validity of the decrease in affinity between XF2.4 and 6-DOG. Overall, when looking at the degree to which affinity was affected by the different analogues, it appears that C-1 and C-5 are more important in hydrogen bonding to helix 7.

GLUT1 helix 7 has previously been suggested by Arbuckle *et al* (1996) to be important in fructose transport. Therefore it was hypothesised that the PfHT1 SGL motif in helix 7 could be important for D-fructose transport, and that mutation of this motif might affect affinity for D-fructose. PfHT1 transports D-fructose only in its furanose form, and a strong inhibitor of D-fructose is 2,5-anhydro-D-mannitol (2,5-AHM), which is fixed in the furanose form and differs from D-fructose only in the absence of a 2-hydroxyl group. The use of this fructose analogue provides a good indication of the ability of the helix 7 mutants to transport D-fructose. Only one of the

helix 7 mutant constructs (XF2.4) showed a statistically significant decrease in affinity (P = 0.0258) for D-fructose compared with the wild type. However, all three helix 7 mutants (XF2.4, XA1.4 and XT1.10) showed no difference in affinity for 2,5-AHM compared with the wild type. Therefore it cannot be said for certain that these helix 7 mutations have any affect on the transport of fructose.

4 CHAPTER FOUR

MEMBRANE PROTEIN ISOLATION FROM *XENOPUS* OOCYTES AND PROTEIN GEL DETECTION

4.1 Introduction

4.1.1 Expression and isolation of *Plasmodium* proteins

Xenopus laevis oocytes have been used for expression of many proteins, including a few *P. falciparum* proteins (Woodrow *et al*, 1999; Krishna *et al*, 2001). However other expression systems have also been used for the expression and isolation of *Plasmodium* proteins, including *Escherichia coli* (Degen *et al*, 2000; Krause *et al*, 2000; Rohdich *et al*, 2001), yeast *Saccharomyces cerevisiae* (Wang *et al*, 2001) mammalian cells (Gamain *et al*, 2001), Chinese Hamster Ovaries (CHO; van Es *et al*, 1994; Buffet *et al*, 1999) and the slime mould, *Dictyostelium discoideum*. The latter system was used for the expression and purification of the nearly full-length circumsporozoite protein and has the closest codon preferences to *P. falciparum* than any of the other expression systems (van Bemmelen *et al*, 2000).

Plasma membrane proteins have been successfully isolated from *Xenopus* oocytes by repeated sedimentation in discontinuous sucrose gradients (Bretzel *et al*, 1986) and by varying high and low speed centrifugation steps (Camacho and Lechleiter, 1993). *P. falciparum* proteins such as the Ca^{2+}-ATPase (PfATP4) have also been successfully isolated from *Xenopus* oocytes by the centrifugation method (R. Webb, St. George's Hospital Medical School, London, personal communication; Krishna *et al*, 2001) and used for Western blots. The method can therefore be very useful for the detection of dysfunctional recombinant mutant proteins that may have been inserted into the *Xenopus* oocyte membrane, but are undetectable using uptake assays. Reports on point mutated *P. falciparum* proteins expressed in *Xenopus* oocytes have been successful (Woodrow *et al*, 2000) but when dealing with chimaera proteins made by

the joining of a protein from two different species, the results can prove more difficult (K. Nel, University of Pretoria, South Africa, personal communication).

4.1.2 Chimaera proteins

Chimaera proteins are created from the joining of two or more regions from different proteins to create a new one (Lodish *et al*, 1995). This can either be done using completely different proteins, such as the attachment of the green fluorescent protein (GFP) to glucose transporters to monitor their trafficking within a cell (Oatey *et al*, 1997; Inukai *et al*, 1995; Powell *et al*, 1999), or with similar proteins such as those in the human glucose and fructose transporter family (Arbuckle *et al*, 1996).

The design and experimentation with chimaera proteins can give useful insight into the structure-function relationship of a transporter protein. Arbuckle *et al* (1996) and also Wu *et al* (1998) applied chimaeras in their studies to elucidate the fundamental difference between the mammalian glucose transporter GLUT3 and the mammalian hexose transporter GLUT2. Arbuckle *et al* (1996) created eight chimaera proteins from GLUT2 and GLUT3, all of which were functional, to identify the region or regions responsible for GLUT2's ability to transport fructose as well as glucose, and GLUT3's inability to. Each chimaera included a mixture of complete helixes, thereby enabling the differences between GLUT2 and GLUT3 to be targeted to a specific helix. This method was relatively simple and enabled the researchers to pin point helix 7 as the region where differences that enable fructose transport in GLUT2 may lie. Buchs *et al* (1998) applied the same technique to chimaeras of GLUT3 and the mammalian fructose transporter GLUT5. Eight chimaeras were made, four of which were not functional. Research studies by Noel and Newgard (1997) also involved experimentation with GLUT1/GLUT2 chimaeras, except that it focused on the importance of the C-terminal tail for transport of fructose. All the above studies involved chimaera proteins made between proteins from the same group of transporters and from the same species. Coady *et al* (2000) applied a similar technique to different transporters namely, the Na^+/glucose and Na^+/*myo*-inositol co-transporters. These mammalian proteins transport different substrates, but fall within the same family. Twelve chimaeras were created, only two of which remained

functional, demonstrating the difficulty in maintaining functionality with increasing diversity between proteins (Coady *et al*, 2000).

An attempt was made to apply this technique to the *P. falciparum* hexose transporter PfHT1. No other *P. falciparum* sugar transporters have been reported yet. Chimaeras were therefore constructed between the *P. falciparum* and the mammalian glucose transporter GLUT1. Chimaeras of human and parasite glucose transporters were anticipated to establish differences between the two transporters that could be exploited for anti-malarial drug design. In the event that the chimaera transporters proved dysfunctional, isolation of the chimaera protein from the plasma membrane and Western blots would distinguish between problems with the expression or the trafficking of the protein from the ER/ Golgi to the plasma membrane or assembly of a functional protein. However, trafficking and assembly will be indistinguishable from one another.

4.2 Materials and method

4.2.1 Construction of Chimaeras

4.2.1.1 Chimaera design

Two chimaera proteins were designed by K. Nel under the supervision of Professor A. I. Louw (University of Pretoria, South Africa), and were designated the names Chimaera 1 and Chimaera 2. The amino acid sequence from the *P. falciparum* hexose transporter PfHT1 was aligned with the amino acid sequence from the rat glucose transporter (*Rattus novegicus*, GenBank Accession number M13979), which is identical to the human glucose transporter GLUT1 (*Homo Sapiens*, GenBank Accession number K03195). Chimaera 1 contained the first 6 helices from PfHT1 and the last 6 helices from the rat glucose transporter. Chimaera 2 contained all 12 helices from PfHT1 and the C-terminal tail region from the rat glucose transporter (Figure 4.1, helical alignments in Appendix IIIa).

Chimaera 1

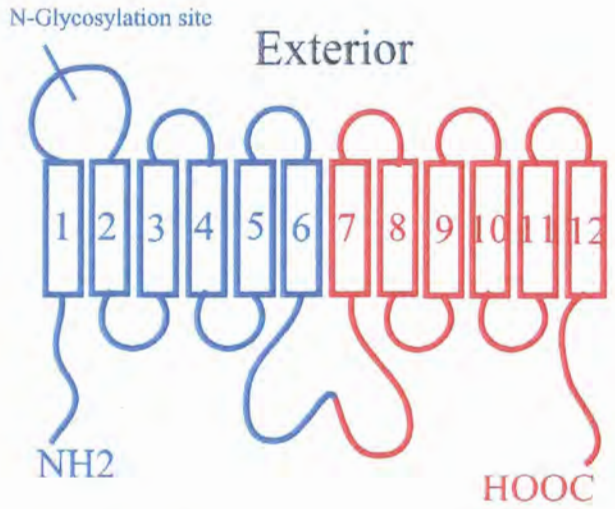

Chimaera 2

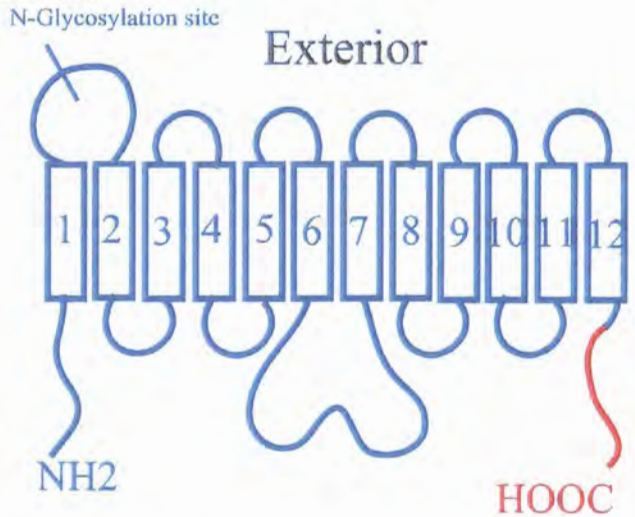

Figure 4.1: Schematic representation of Chimaera 1 and 2. Helices and joining strands in blue indicate regions from the *P. falciparum* hexose transporter PfHT1. Those in red indicate regions from the mammalian glucose transporter GLUT1. There is 29.8% identity between the mammalian and *P. falciparum* sugar transporters (Woodrow *et al*, 1999). The mammalian C-terminal tail is longer (42 amino acids) than that for PfHT1 (29 amino acids), whereas the N-terminal is shorter (GLUT1: 12 amino acids, PfHT1: 28 amino acids).

The rat glucose transporter gene was a gift from G. Gould (University of Glasgow, UK) and was contained in the pSP64T expression vector. The chimaeras were constructed by overlapping PCR as described in Paragraph 2.2.2. PCR 1 for Chimaera 1 used primers Mal/Rat F and R, and Chimaera 2 used primers Mal/Rat Tail F and R. PCR2 for both chimaeras used Mal 5' F and Rat 3' R for the amplification of the full-length gene (Table 4.1). PCR reactions were performed with 1.25 U ExTaq (Takara

Shuzo, Japan) and PCR conditions as described in Table 2.4. The PCR products were electrophoresed and isolated from agarose gel. The chimaera PCR products were then ligated into the pGEM®-T easy vector (Appendix Ib) and transformed into competent SURE *E. Coli* cells. The sequence of the chimaeras were verified with sequencing as described in Paragraph 2.2.8 with the T7 reverse primer in addition to the primers mentioned in Paragraph 2.2.8.

Table 4.1: Primer sequences for the primers used to construct Chimaera 1 and Chimaera 2. Mal = *P. falciparum* glucose transporter (in uppercase), Rat = rat glucose transporter (in lowercase), F = forward, R = reverse. Start and stop codons are in bold, *Bgl*II sites are underlined, and the Kozak sequence is given in italics.

Primer Name	Primer Sequence 5'-3'
Mal/Rat F	CAGATAATGTCGATGAACCAcaggagatgaaagaagag
Mal/Rat R	ctcttctttcatctcctgTGGTTCATCGACATTATCTG
Mal/Rat Tail F	TTATCAAAGAAACcaaaggccggaccttc
Mal/Rat Tail R	gaaggtccggcctttgGTTTCTTTGATAA
Mal 5' F	AAAGATCT*CACC***ATG**ACGAAAAGTTCGAAGGATATATGTAGTG
Rat 3' R	aaagatct**tca**cacttgcgagtcagctcccagag

4.2.1.2 Ligation into pGEM®-T Easy Vector

The chimaera DNA from PCR reactions was inserted into the pGEM®-T Easy Vector (Promega, USA) according to the manufacturers instructions. Briefly a 3:1 insert to vector ratio was used for ligation, which resulted in 25 pmol of vector and 75 pmol of insert DNA. The vector and insert were added together with a 1× T4 DNA Ligase Buffer (30 mM Tris-HCl, pH 7.8; 10 mM $MgCl_2$; 10 mM DTT; 1 mM ATP) and 2 Weis units of T4 DNA Ligase (Promega, USA). The reaction was made up to a final volume of 10 µl with distilled, deionised water. The reaction was then incubated overnight at 4°C, and stopped by inactivation of the T4 DNA Ligase enzyme at 70°C for 3 minutes.

4.2.1.3 *Transformation into competent SURE E. coli cells*

A few methods were tried for the preparation of competent cells and the calcium/ magnesium-based method yielded the best results (Hanahan *et al*, 1991).

SURE *E. coli* cells (Stratagene, La Jolla, CA, USA) were streaked on M9 minimal medium agar plates (0.05 M Na_2HPO_4-$2H_2O$, 0.02 M KH_2PO_4, 8 mM NaCl, 0.02 M NH_4Cl, 2 mM $MgSO_4$, 0.01 M D-glucose, 0.1 mM $CaCl_2$, 1 mM thiamine hydrochloride, 1.5% w/v agar, pH 7.4) and left to grow overnight at 30°C. Cells were picked from the M9 plates and streaked onto LB medium agar (1.5% w/v agar) containing 12.5 µg/ml tetracycline and grown overnight at 30°C. Colonies were picked from the plate and vortexed in 1 ml SOB medium (2% w/v Trypton, 0.5% w/v yeast extract, 10 mM NaCl, 2,5 mM KCl, pH 6.8-7.2). The 1 ml SOB with bacteria was inoculated into 49 ml SOB medium in a 500 ml flask and grown at 30°C while shaking at 250 rpm until an OD_{600} of 0.3 was reached indicating an early exponential phase of growth. The cells were transferred to a 50 ml centrifuge tube and incubated for 10 minutes on ice. The cells were then centrifuged at 1000g for 15 minutes at 4°C. The supernatant was removed and the cells resuspended in one-third the volume CCMB80 medium (80 mM $CaCl_2$-$2H_2O$, 20 mM $MnCl_2$-$4H_2O$, 10 mM $MgCl_2$-$6H_2O$, 10 mM K-acetate, 10% v/v glycerol, pH 6.8) and incubated on ice for 20 minutes. The cells were centrifuged at 1000g for 10 minutes and the supernatant removed. The cells were resuspended in a twelfth the original volume of CCMB80 medium and aliquoted into microfuge tubes and frozen at -70°C.

The pGEM-T Easy Vector containing insert was transformed in competent SURE *E. coli* cells by the heat shock method (Sambrook *et al*, 1989). Competent SURE *E. coli* cells were thawed on ice from storage at -70°C. In 5 ml plastic tubes, 2 µl of the deactivated ligation reaction mix was added to 100 µl of competent cells on ice. The same concentration of pBlueScript vector was used as a positive control, and 100 µl of competent cells without plasmid was used as a negative control. The cells were incubated on ice for 30 minutes. A heat-shock step followed, which involved immersing the cells into a 42°C water bath for 90 seconds and then transferring them immediately to ice for a 2-minute incubation. Preheated SOC medium (900 µl, 2%

w/v Trypton, 0.5% w/v yeast extract, 10 mM NaCl, 2,5 mM KCl, 20 mM D-glucose, pH 6.8-7.2) was added to the cells and incubated at 30°C for 1 hour while shaking at 250 rpm. The transformation reaction (100 µl) was plated on LB agar plates (1.5% w/v agar) containing 100 µg/ml ampicillin. The plates were first prepared with 32 µl of 20 mg/ml X-gal and 4 µl of 0.4 mM IPTG for blue/white selection. The plates were incubated at 30°C overnight.

4.2.2 Expression in *Xenopus* oocytes

For injection into *Xenopus* oocytes cRNA was prepared of Chimaera 1 and 2 and GLUT1 as described in Paragraph 2.2.9. *Xenopus* oocytes were assayed as described in Chapter 3. Uptake measurements were performed on batches of 6 oocytes from each cRNA injected and water injected controls at approximately 24, 48, 72 and 96 hours after injection. Oocytes were incubated in Barth's solution containing 2.5 µM D-[U-^{14}C]-glucose (Amersham Life Sciences, UK, 323mCi/mmol) and 30 nM D-glucose (Sigma-Aldrich, UK) for 20 minutes and then washed three times in ice cold Barth's solution. Each oocyte was lysed in scintillation fluid in a 1.5 ml microfuge tube and then counted on a Wallac 1450 Microbeta Plus scintillation counter as decays per minute (DPM). Results were analysed with Microsoft Excel software.

4.2.3 Isolation of membrane proteins

Surface membrane proteins were isolated from Chimaera 1 and 2, GLUT1 cRNA injected and water injected oocytes 72 hours after injection and one hundred oocytes were used for each. A protein isolation procedure was followed published by Krishna *et al* (2001). Each batch of oocytes was separated into 1.9 ml microfuge tubes with 10 oocytes per tube. 500 µl of homogenisation buffer (83 mM NaCl, 1 mM $MgCl_2$, 10 mM HEPES, pH 7.9) was added to each microfuge tube. One Complete Protease Inhibitor Cocktail tablet (Roche, Germany) was added to every 10 ml homogenisation buffer before adding to oocytes. The oocytes were homogenised with 20 hand driven strokes with a homogeniser on ice. The homogenised solutions were centrifuged at 1000g for 5 minutes at 4°C to remove the yolk granules and melanosomes. The supernatant was removed and collected and 500 µl of homogenisation buffer was

added to the pellet and homogenised again and centrifuged at 1000g for 5 minutes at 4°C. The supernatant was collected and combined with the supernatant from the previous centrifugation. The pooled supernatants were centrifuged at 1000g for 5 minutes at 4°C to remove residual yolk protein. The resulting supernatant was centrifuged at 100 000g for 90 minutes at 4°C. The pellet was resuspended in homogenisation fluid; aliquoted into microfuge tubes and frozen at -70°C. Protein concentrations were determined with the Modified Lowry Kit for Protein Determination (Sigma-Aldrich, UK) and read on a Shimadzu UV 160 A spectrophotometer at 750 nm.

4.2.4 Protein separation using SDS-polyacrylamide gel electrophoresis (SDS-PAGE)

A Mini-Protean II Electrophoresis Cell (Bio-Rad, UK) was used for the separation of the protein samples collected from the membrane protein isolation step. Ten ml of separation gel (8% w/v acrylamide; 0.375 M Tris buffer, pH 8.8; 0.06% v/v TEMED; 0.1% w/v sodium dodecyl sulphate, 0.1% w/v ammonium persulphate) was made and poured between a glass sandwich set on a casting stand. The gel was covered with butanol and left to set. Once set the butanol was removed from the gel and a 10 well comb was placed on top of the gel. Five ml stacking gel (5% w/v acrylamide; 0.126 M Tris buffer, pH 6.8; 0.1% v/v TEMED; 0.1% w/v sodium dodecyl sulphate, 0.1% w/v ammonium persulphate) was made and poured around the comb and the gel was left to set. The glass sandwich containing the gel was placed in the electrophoresis tank and 1× PAGE running buffer (0.4 M Tris base, pH 8.3, 14.41% w/v glycine, 0.1% sodium dodecyl sulphate) was poured into the tank. Approximately 150 ug of each protein sample was loaded into each well alongside 10 µl BenchMark™ Prestained Protein Ladder (Life Technologies, UK). The gel was run at 200 Volts for 45 minutes. The gels were either stained in Coomassie Brilliant Blue R250 Stain (Sigma-Aldrich, UK) or used for Western blots. Gels not used for Western blots were stained in 0.1% w/v Coomassie Brilliant Blue for 2 hours and then transferred to a 1:10 dilution of Coomassie Brilliant Blue and stained overnight. The gels were then destained in 10% v/v acetic acid for 1-2 hours. The stained gels were dried at 60°C on Whatman paper

on a Hoefer GD 2000 Vacuum Gel Dryer System (Amersham Pharmacia Biotech, USA).

4.2.5 Western blots

Gels were sandwiched between nitrocellulose paper and blotting paper and placed in a Mini Trans-Blot Electrophoresis Transfer Cell (Bio-Rad, UK) and run at 100 Volts for 1 hour. Gels were removed and placed in Coomassie Brilliant Blue as in Paragraph 4.2.4 to check the transfer from the gels. The nitrocellulose blots were blocked in Tris buffered saline (TBS)/ Tween (0.145 M NaCl; 0.05 M Tris/ HCL, pH 7.5; 1% v/v Tween) with 5% w/v powdered milk for 30 minutes. The nitrocellulose blots were then transferred to TBS/ Tween buffer containing 1:5000 dilution of rabbit anti-GLUT-1 polyclonal antiserum (Chemicon International, CA, USA) and incubated for 1-2 hours on a rotator. The blots were washed 3 times in TBS/ Tween for 5 minutes each wash. The blots were then incubated in TBS/ Tween containing a 1:500 dilution of anti-rabbit alkaline phosphate conjugated secondary antibody for 1 hour. The blots were washed 3 times in TBS/ Tween for 5 minutes each wash. Two tablets of Sigma Fast™ 5-bromo-4-chloro-3-indolyl phosphate/nitro blue tetrazolium (Sigma-Aldrich, UK) were dissolved in distilled water and the blots were soaked in the solution for 5-10 minutes. The blots were then rinsed in distilled water and left in the dark to dry.

4.3 Results

4.3.1 Expression in *Xenopus* oocytes

Uptake measurements of D-[U-^{14}C]-glucose were conducted 24, 48, 72 and 96 hours after injection. As seen in Figure 4.2, 96 hours after injection the counts for Chimaera 1 and Chimaera 2 are similar to those obtained for the water-injected controls, which remained low (≈ 100 counts per minute). The uptake measurements obtained for the GLUT1 injected oocytes were high (2000-4500 counts per minute).

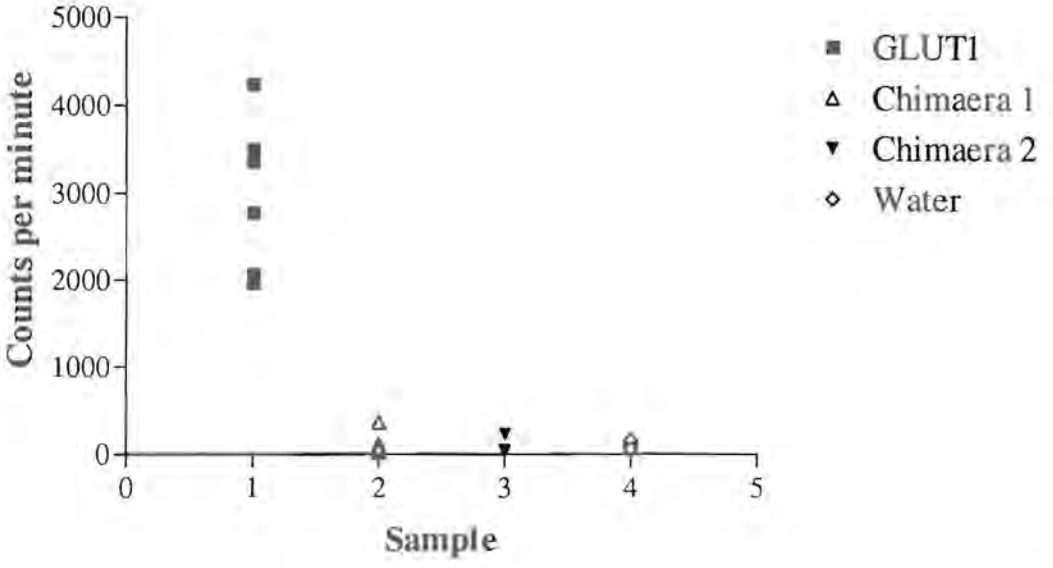

Figure 4.2: Uptake measurements of D-[U-^{14}C]-glucose by chimaeras compared to GLUT1 96 hours after injection. The *Xenopus* oocytes injected with GLUT1 cRNA showed uptake measurements 200-400 fold higher than those obtained for Chimaera 1and 2 cRNA injected oocytes, which were as low as water-injected oocytes.

4.3.2 SDS-PAGE gel and Western blots

The SDS-PAGE gels stained with Coomassie Blue revealed lanes cluttered with membrane proteins originating mainly from endogenously expressed *X. laevis* proteins (Figure 4.3). The expected size for the chimaera proteins was around 60 kDa and the expected size for the GLUT1 protein was 56.4 kDa (Woodrow *et al*, 1999). Each lane for the cRNA and water injected oocytes showed similar patterns of protein separation and no distinct band was visible around 60 kDa for the cRNA injected oocytes compared to the water-injected oocytes.

The Western blot revealed a distinct staining around 60 kDa for the GLUT1 injected oocyte with a smear below 60 kDa (Figure 4.4). The primary rabbit anti-GLUT1 antibody recognises the C-terminal section of GLUT1 in human and rat tissue. Since the chimaeras both have C-terminals from the rat glucose transporter the antibody will bind to either chimaera protein if present on the nitrocellulose as well as to the GLUT1 positive controls. No bands were detected for Chimaera 1 or 2 or for the water injected control.

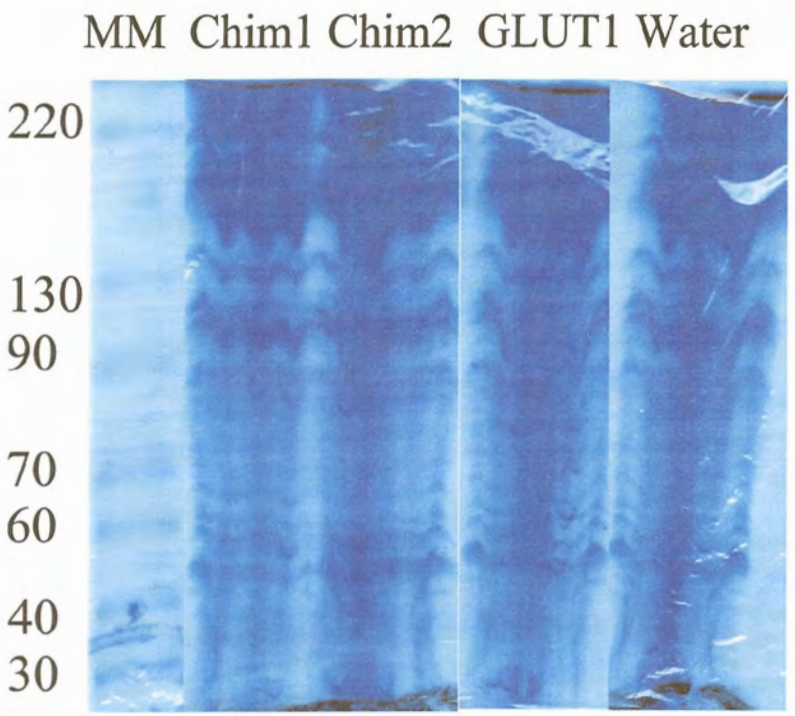

Figure 4.3: SDS-PAGE gel stained with Coomassie Blue. Molecular markers (MM) are in kDa and the 70 kDa band is stained pink for easy identification. Chim1 and Chim2 stand for Chimaera 1 and 2, respectively.

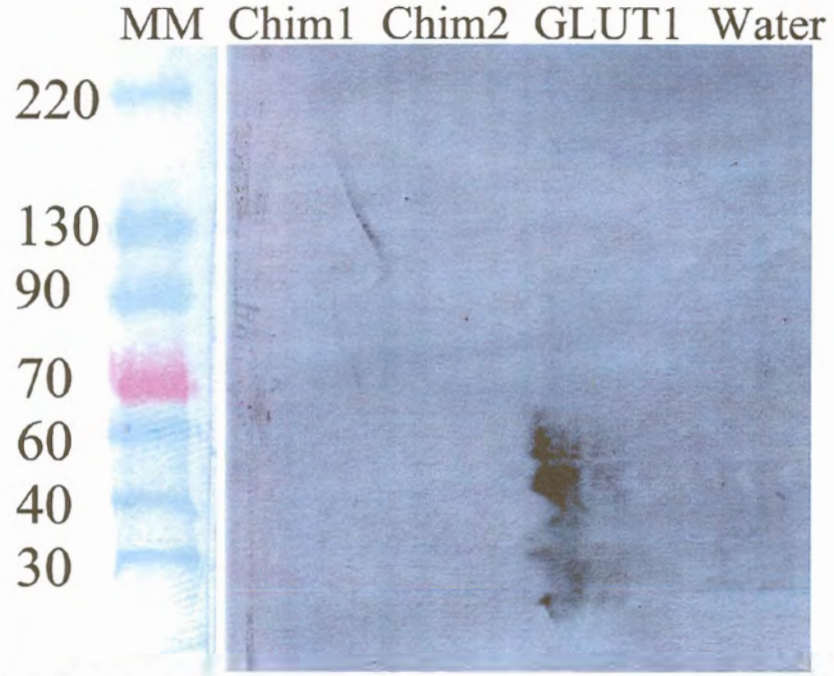

Figure 4.4: Western blots of chimaera proteins and GLUT1. Molecular markers (MM) are in kDa and the 70 kDa band is stained pink for easy identification. Chim1 and Chim2 stand for Chimaera 1 and 2 respectively. The lane containing membrane proteins isolated from GLUT1 cRNA injected oocytes has a smear from 60 kDa and below.

4.4 Discussion

The fate of chimaera proteins originating from a conjugation of sugar transporters from distinctly different species such as the malaria parasite and its host, are multifaceted. In the case where expression of the proteins in an exogenous expression system is unsuccessful, the problem may lie in various areas. A chimaera containing the first 6 helices of the PfHT1 hexose transporter and the last 6 helices of the rat glucose transporter; and a chimaera containing all 12 helices of the PfHT1 hexose transporter and the tail of the rat glucose transporter were constructed. Injection of the chimaeras into *Xenopus* oocytes and uptake measurements with D-glucose revealed no transport of substrate by the chimaera proteins. This could indicate a number of possibilities. Since the protein is made from two transporters that differ slightly in their substrate selectivity, the lack of transport indicated by the chimaera proteins could originate from disfunctionality of the chimaera as a result of this difference in substrate selectivity between the two parent proteins. Another possibility is that the protein is expressed and folded in the ER but is not trafficked to the oocyte membrane due to a lack of some signal sequence removed by the construction of the chimaera. More likely in the case of a chimaera protein originating from two phylogenetically distinct species, the protein may be expressed and not folded properly and instead aggregates within the cell and is destroyed. Whether the protein is inserted or not into the oocyte membrane can easily be resolved with membrane protein isolation and Western blots.

Membrane protein isolation from the cRNA and water-injected oocytes and their subsequent separation on a SDS-PAGE gel revealed a collection of membrane proteins ranging in size from approximately 20 kDa and larger. The protein bands from the cRNA injected oocytes were identical to those obtained from the water injected oocytes which indicates that they originate from the endogenously expressed *X. laevis* membrane proteins. If any protein is present originating from the injected cRNA, it is lost within the high concentrations of endogenous protein.

The Western blots revealed binding of GLUT1-specific antibody to the nitrocellulose in the lane corresponding to the GLUT1 injected oocytes. This resulted in a smear

from 60 kDa and smaller that could indicate that the expected 60 kDa GLUT1 protein was slightly degraded possibly during the membrane protein isolation step. However no similar bands were obtained for either Chimaera 1 or Chimaera 2 cRNA injected oocytes. No bands were expected for the water-injected oocyte used as negative controls. This indicates that whereas the GLUT1 protein was functionally inserted into the oocyte membrane, the chimaera proteins were not inserted at all.

The trafficking mechanisms within the malaria parasite differ is some ways from higher eukaryotes as reviewed in Chapter 1. It is fairly agreed upon that the parasite has a functional ER at the nucleus periphery. The presence of a Golgi apparatus is less well defined and Golgi functions have been found scattered throughout the cell as well as in the TVM. This difference in trafficking may cause certain malaria proteins expressed in exogenous expression systems to not be trafficked to their proper destinations. However in the case of PfHT1, the wild type transporter is inserted functionally into the *Xenopus* oocyte membrane (Woodrow *et al*, 1999), as is the GLUT1 glucose transporter seen in Figure 4.2. Therefore the absence of the chimaera proteins in the oocyte membrane made from these two parent transporters must be as a result of misfolding of the chimaera within the ER.

Chimaera proteins can be useful in identifying regions between different proteins that are important for the proteins functions. However most chimaeras, except for GFP conjugated chimaera proteins, are usually made from two proteins originating from the same species. In the case of the chimaeras designed here they originated from two species that are distantly related. Parasitic protozoa such as *P. falciparum* and *T. brucei* may have sugar transporters that belong to the same superfamily as GLUT1, but are evolutionary distant (Walmsley *et al*, 1998). The idea behind the design of Chimaera 1 and Chimaera 2 was centred on a direct approach to elucidate differences between the malaria parasites hexose transporter and its hosts transporter GLUT1 by combining the two transporters.

Deletion of most of the C-terminus (37 out of 42 amino acids) of GLUT1 by Oka *et al* (1990) still resulted in the transporter being inserted in CHO cell membranes determined by Western blots. However the transporter was no longer able to transport

glucose into the cell and was hypothesised to be locked in an inward facing form due its ability to bind the endofacial ligand cytochalasin B but not the exofacial ligand ATB-BMPA. Chimaera 2 was constructed with the 12 helices from PfHT1 truncated 4 amino acids after the 12th transmembrane helix and joined to the last 36 amino acids of the rat glucose transporter tail, the same amino acids deleted in the experiments conducted by Oka *et al* (1990). This leaves 7 amino acids (residues 449-455) left out from the GLUT1 tail that lie directly after the GLUT1 12th transmembrane helix. Had these amino acids been included in Chimaera 2, this protein may have been inserted into the oocyte membrane. Alternatively, if seven amino acids directly after PfHT1 helix 12 had been included instead of only four, the transporter may have been inserted in the membrane or may have even been functional. These amino acids may be important for the correct folding or insertion into the ER membrane during expression into the ER lumen.

It appears that in order for studies of this nature to be successful, the chimaeras need to be constructed from parts originating from the same species or genus. Until an additional sugar transporter is identified from *P. falciparum* or any other *Plasmodium* species, chimaeras of this nature may not be successfully expressed. For a parasite to survive inside its host it must adapt to many challenges, one being the challenge to obtain nutrients in competition with its hosts own nutrient requirements. In the case of glucose transporters this could result in such evolutionary differences between host and parasite transporters that they will not function when combined in a chimaera form. Further glucose transporters for *Plasmodium* species, or in particular *P. falciparum*, will have to be identified before such chimaera experiments would be successful.

5 CHAPTER FIVE:

CONCLUDING DISCUSSION

At present, about 500 million people are affected by malaria globally, and there are up to 3 million malaria deaths per year. Malaria is generally endemic in the tropics, with extensions into the subtropics (Bradley, 1996). Early diagnosis and correct treatment form the basic elements of any malaria control program. The need to discover and validate new targets to generate new drug candidates has elevated because of the emergence of resistance to widely used antimalarial drugs, such as chloroquine (Hastings and D'Alessandro, 2000). Several enzymes from a number of biochemical pathways in the human malaria parasite *P. falciparum* have been identified and proposed as potential drug targets, although few of them have been validated (Chapter 1, Table 1.1).

One of these potential drug targets, a putative glucose transporter named PfHT1, was isolated, cloned and expressed in *Xenopus* oocytes (Woodrow *et al*, 1999). PfHT1 transports D-glucose at a higher affinity than GLUT1 and also transports D-fructose with a relatively high affinity. The most important carbons on glucose with which PfHT1 interacts are C-3 and C-4. The most interesting observation to date is the discovery that mutation of Q169 resulted in no fructose being transported by PfHT1 (Woodrow *et al*, 2000).

GLUT1 is the most studied glucose transporter to date, and along with most transporters within the major facilitative superfamily, is predicted to form 12 transmembrane helices (Mueckler *et al*, 1985). Without the availability of a crystal structure, indirect approaches remain the best means for obtaining structure-function information on transporters within this family. From indirect approaches a number of interesting details of GLUT1 have emerged. Five of the 12 transmembrane helices are thought to be amphipathic and form an aqueous pore through which the hydrophilic substrate is proposed to cross the lipid membrane. Hence most studies have concentrated on these five key helices as discussed in Chapter 2, Paragraph 2.1.

Mutational studies provide information into structure-function relationships and extensive studies have already been carried out on mammalian GLUT1. Cysteine-scanning mutagenesis studies on GLUT1 helix 7 have provided insight into which of the helix 7 amino acids are exposed to the substrate for interaction. The highly conserved QLSQQLSGINAVFY region in helix 7 has been the main subject for investigation, and has revealed five amino acids within this region as essential for protein-substrate interaction namely, Q282, Q283, I287, V290 and F291 (Olsowski *et al*, 2000; Olsowski *et al*, 1998). GLUT1 helix 7 residues that have been suggested to be involved in substrate binding, such as Q282 and Q283, are located in the centre of the transmembrane helix, and it has therefore been suggested that helix 7 may move up in the membrane to accept exofacial ligands (Hashiramoto *et al*, 1992). Glutamine 161 in GLUT1 helix 5 that corresponds to glutamine 169 in PfHT1 (Q169) was predicted to form part of the exofacial ligand binding site of GLUT1. Glutamine 161 (in GLUT1 helix 5) when mutated to leucine reduced the transport activity by 50-fold as discussed in Chapter 2 (Mueckler *et al*, 1994). Studies such as these on PfHT1 would provide valuable information on key amino acids that are involved in ligand binding.

Site directed mutagenesis studies have already been applied to PfHT1 and resulted in the discovery that mutation of Q169 to asparagine ablated PfHT1s ability to transport fructose (Woodrow *et al*, 2000). In this study, a site directed mutagenesis approach was applied to identify key amino acid residues within helix 5 and 7 responsible for PfHT1-hexose interactions. The amino acids that were focused on were Q169 in helix 5, and S302 and L304 in helix 7. These amino acids were mutated to residues differing in atomic composition and size to the original. Results concerning the helix 5 amino acid (Q169) had already been published (Woodrow *et al*, 2000), but kinetic studies had not yet been completed. Studies on the helix 7 amino acids were novel. The helix 7 amino acids are contained within a motif (SGL), whose equivalent in GLUT1 (QLS, Figure 2.1A) has been implicated in differential transport of fructose and glucose. An attempt was made to mutate the PfHT1 SGL motif to the GLUT1 QLS motif. These attempts failed to produce a functional transporter (Krishna, St. George's Hospital Medical School, London, unpublished results) and therefore an alternative was needed. The *T. brucei* equivalent motif (AGT) was decided on since a

correlation can be drawn between these two parasites. *P. falciparum* and *T. brucei* share similar living conditions within their vertebrate hosts and may have evolved similarly due to pressure exerted by harsh living conditions and also by a common necessity to obtain glucose from their hosts. The mutations were achieved by PCR reactions discussed in Chapter 2 and the resulting mutants were cloned into a *Xenopus* expression vector (pSP64T). Kinetic parameters K_i and K_m were obtained from uptake experiments with the mutant transporters and glucose, fructose and their analogues and are presented in Chapter 3.

The involvement of the helix 7 tripeptide motif (SGL) in PfHT1 in the discrimination between glucose and fructose substrate is now questionable. It was thought that this motif was associated with fructose transport. Based on the results obtained in this study in comparison with those obtained by Seatter *et al* (1998), it appears that the conserved QLS motif in mammalian glucose transporters is only important for D-glucose transport. Transporters with this motif cannot transport D-fructose, whereas those without it can. This is most evident when replacement of GLUT2 HVA by QLS resulted in a notable decrease in D-glucose transport inhibition by D-fructose (Seatter *et al*, 1998). It would have been interesting to see what effect substitution of GLUT1 279QLS for PfHT1 302SGL would have had on the PfHT1 transporters activities and properties. However, such a mutation resulted in no transport of any substrate across the *Xenopus* oocyte membrane. This could be due to either misfolding of the mutant protein or to disruption of the mutant protein's trafficking to the oocyte membrane (Krishna, St. Georges Hospital Medical School, London, unpublished results).

With the PfHT1 helix 7 SGL motif mutated to the *T. brucei* THT1 AGT motif, a lower uptake was observed after 24, 48 and 72 hours after microinjection (Chapter 3, Figure 3.5). The S302A and L304T separately also produced lower uptakes at 24, 48 and 72 hours after microinjection. From Figure 3.5 (Chapter 3) it can be postulated that both the S203A and L304T mutations were causing the lower uptake seen for XF2.4. However, the L304T mutant may have a greater effect on lowering the uptake measurements seen for XF2.4 as it has a significantly lower ($P < 0.04$) uptake measurement compared with S302A. From Figure 3.6 (Chapter 3) it can be postulated that XT1.10 may follow a similar expression pattern to XF2.4 when one compares the

percentages of the maximum expression (48h), particularly at 24 and 48 hours. The same can be said for XA1.4 that appears to follow a similar expression pattern to the wild type at all time points.

The results obtained from kinetic analysis of the mutants are summarised in Chapter 3 Table 3.1. The results suggest that the helix 5 residue (Q169) may interact with glucose at C-2, C-3, C-5 and C-6. Mutation of this amino acid results in the ablation of fructose transport as previously reported, but it appears that this amino acid is not as important for glucose transport. This glutamine may either be interacting directly with glucose or it may be interacting with another amino acid which itself interacts directly with the glucose.

Mutation of the two amino acids in helix 7 (S302 and L304, XF2.4) produced a significant change in fructose transport. However, no significant change in fructose transport was observed with the single mutants. However, all three helix 7 mutants (XF2.4, XA1.4 and XT1.10) showed no difference in affinity for 2,5-AHM compared with the wild type. Therefore the involvement of the PfHT1 SGL motif in fructose transport does not appear to be important.

It is already proposed that PfHT1 hydrogen bonds to C-1 and C-3 (Woodrow *et al*, 1999). Analogue studies with the helix 7 mutants produced changes in affinity between PfHT1 and 1-DOG, 3-OMG, 5-thio-D-glucose and 6-DOG. However the significances of the results for 1-DOG and 5-thio-D-glucose were greater than those for 3-OMG and 6-DOG. It therefore appears that the helix 7 SGL motif interacts more strongly with C-1 and C-5. If one looks at the two amino acids (S302 and L304) separately, it becomes apparent from the results in Table 3.1 that the significant changes seen for XF2.4 can be attributed to the amino acid S302. Therefore it can be said that S302 may interact with glucose at C-1 and C-5. The significance of the results obtained with the C-3 or C-6 analogues (3-OMG and 6-DOG, respectively) could be further investigated using alternative analogues such as 3-DOG, which has the hydroxyl removed at C-3, and D-xylose, which has C-6 removed. This may clarify whether the PfHT1 transporter forms any interactions with these two carbon atoms in glucose.

Another approach to structure-function studies was explored using chimaeras constructed from the rat GLUT1 and *P. falciparum* PfHT1. Two chimaeras were constructed, one consisting of the first 6 helices from PfHT1 and the last 6 helices from GLUT1, and the other consisting of all 12 helices from PfHT1 and the GLUT1 tail. Neither chimaera produced uptake measurements with D-glucose. Western blots revealed that the transporters were not inserted into the oocyte membrane. Therefore the chimaeras were either not expressed or folded properly, or they were not trafficked through the ER and Golgi apparatus of the *Xenopus* oocyte. The literature confirms the difficulties experienced when trying to express chimaeras of varying diversity between the counterparts. Here the chimaeras were made from two species that are placed very far apart on the evolutionary tree (Walmsley *et al*, 1998).

Chimaera 2 was constructed with the 12 helices from PfHT1 truncated 4 amino acids after the 12th transmembrane helix and joined to the last 37 amino acids of the rat glucose transporter tail. In an experiment conducted by Oka *et al* (1990), 37 amino acids of the GLUT1 tail were truncated, which resulted in the transporter being unable to transport substrate into CHO cells (Chapter 4). This same transporter constructed by Oka *et al* did however contain 7 amino acids that lie directly after helix 7. With these 7 amino acids the transporter was inserted correctly into the oocyte CHO membrane, yet without the rest of the tail the transporter would not transport glucose into the cell. Therefore, if 7 or more amino acids directly after PfHT1 helix 12 had been included instead of only four this protein may have been inserted into the oocyte membrane. These 7 amino acids directly after PfHT1 helix 12 may be important for the correct expression or functioning of the transporter.

The mutational and chimaera studies conducted here and the results obtained open the way for further investigations into PfHT1 helices that could be important for protein-substrate interactions. These results could be extended by studies with additional analogues such as those used by Woodrow *et al* (2000). The use of only one glucose analogue per C-atom position may not be extensive enough to give conclusive results. The importance of the amino acids investigated in helix 5 and 7 could also be further investigated by mutating them to a variety of alternative amino acids that differ in

polarity and size. Investigations into the affect of alternative amino acids in place of Q169 are already underway (Krishna, St. George's Hospital Medical School, London, personal communication). If one were to consider the extent to which GLUT1 has been studied and that this transporter is still being studied, there is still a lot of potential for investigation into structure/ function relationships of PfHT1.

REFERENCES

- Abath, F.G.C., Montenegro, S.M.L., Gomes, Y.M. (1998) Vaccines against human parasitic diseases: an overview. *Acta Tropica* **71**, 237-254.
- Adams, R.L.P., Knowler, J.T., Leader, D.P. (1992) The Biochemistry of the Nucleic Acids, 11th Edition. Chapman and Hall.
- Aikawa, M. 1971, Plasmodium: the fine structure of malaria parasites, *Experimental Parasitology* **30**, 284-320.
- Aitman, T.J., Cooper, L.D., Norsworthy, P.J., Wahid, F.N., Gray, J.K., Curtis, B.R., McKeigue, P.M., Kwiatkowski, D., Greenwood, B.M., Snow, R.W., Hill, A.V., Scott, J. (2000) Malaria susceptibility and CD36 mutation. *Nature* **405**, 1015-1016.
- Alvarez, J., Lee, D.C., Baldwin, S.A., Chapman, D. (1987) Fourier transform infrared spectroscopic study of the structure and conformational changes of the human erythrocyte glucose transporter. *The Journal of Biological Chemistry* **262**(8), 3502-3509.
- Arbuckle, M.I., Kane, S., Porter, L.M., Seatter, M.J., Gould, G.W. (1996) Structure-function analysis of liver-type (GLUT2) and brain-type (GLUT3) glucose transporters: Expression of chimeric transporters in *Xenopus* oocytes suggests an important role for putative transmembrane helix 7 in determining substrate selectivity. *Biochemistry* **35**, 16519-16527.
- Baldwin, S.A. (1992) Mechanisms of active and passive transport in a family of homologous sugar transporters found in both prokaryotes and eukaryotes. *Molecular Aspects of Transport Proteins*. Elsevier Science Publishers.
- Baldwin, S.A., Baldwin, J.M., Lienhard, G.E. (1982) Monosaccharide transporter of the human erythrocyte. Characterization of an improved preparation. *Biochemistry* **21**(16), 3837-3842.
- Bannister, L.H., Hopkins, J.M., Fowler, R.E., Krishna, S., Mitchell, G.H. (2000) A brief guide to the ultrastructure of *Plasmodium falciparum* asexual blood stages. *Parasitology Today* **16**(10), 427-433.

- Barrett, M.P., Tetaud, E., Seyfang, A., Bringaud, F., Baltz, T. (1998) Trypanosome glucose transporters. *Molecular and Biochemical Parasitology* **91**, 195-205.
- Benting, J., Mattei, D., Lingelbach, K. (1994) Brefeldin A inhibits transport of the glycophorin-binding protein from *Plasmodium falciparum* into the host erythrocyte. *Biochemical Journal* **300**, 821-826.
- Bianco C, Patrick R, Nussenzweig V. (1970) A population of lymphocytes bearing a membrane receptor for antigen-antibody-complement complexes. I. Separation and characterization. *J Exp Med.* **132**(4), 702-20.
- Bozdech, Z., Van Wye, J., Haldar, K., Schurr, E. (1998) The human malaria parasite *Plasmodium falciparum* exports the ATP-binding cassette protein PFGCN20 to membrane structures in the host red blood cell. *Molecular and Biochemical Parasitology* **97**(1-2), 81-95.
- Bradley, T. (1996) Leicester University, United Kingdom, http://www-micro.msb.le.ac.uk/224/Bradley/History.html
- Bretzel, G., Janeczek, J., Born, J., John, M., Tiedemann, He., Tiedemann, Hi. (1986) Isolation of plasma membranes from *Xenopus* embryos. *Roux's Arch Developmental Biology* **195**, 117-122.
- Bringaud, F. and Baltz, T. (1993) African trypanosome glucose transporter genes: organisation and evolution of a multigene family. *Molecular Biology Evolution* **13**, 1146-1154.
- Brown, G.V., Beck, H-P, Molyneux, M. Marsh, K. (2000) Molecular approaches to epidemiology and clinical aspects of malaria. *Parasitology Today* **16**(10), 448-450.
- Buchs, A.E., Sasson, S., Joost, H.G., Cerasi, E. (1998) Characterisation of GLUT5 domains responsible for fructose transport. *Endocrinology* **139**(3), 827-831.
- Buffet, P.A., Gamain, B., Scheidig, C., Baruch, D., Smith, J.D., Hernandez-Rivas, R., Pouvelle, B., Oishi, S., Fujii, N., Fusai, T., Parzy, D., Miller, L.H., Gysin, J., Scherf, A. (1999) *Plasmodium falciparum* domain mediating adhesion to chondroitin sulfate A: a receptor for human placental infection. *Proceedings of the National Academy of Science of the USA* **96**(22), 12743-12748.
- Cairns, M.T., Alvarez, J., Panico, M., Gibbs, A.F., Morris, H.R., Chapman, D., Baldwin, S.A. (1987) Investigation of the structure and function of the human

erythrocyte glucose transporter by proteolytic dissection. *Biochemica et Biophysica Acta* **905**, 295-310.

- Camacho P, Lechleiter JD. (1993) Increased frequency of calcium waves in Xenopus laevis oocytes that express a calcium-ATPase. *Science*. **260**(5105), 226-229.
- Carayannopoulos, M.O., Chi, M.M-Y., Cui, Y., Pingsterhaus, J.M., McKnight, R.A., Mueckler, M., Devaskar, S.U., Moley, K.H. (2000) GLUT8 is a glucose transporter responsible for insulin-stimulated glucose uptake in the blastocyst. *Proceedings of the National Academy of Science, USA* **97**(13), 7313-7318.
- Carter, N.S., Mamoun, C.B., Liu, W., Silva, E.O., Landfear, S. M., Goldberg, D. E., Ullman, B. (2000) Isolation and functional characterisation of the PfNT1 nucleoside transporter gene from *Plasmodium falciparum*. *Journal of Biological Chemistry* **265**(14), 10683-10691.
- Chin, J.J., Jung, E.K.Y., Jung, C.Y. (1986) Structural basis of human erythrocyte glucose transporter function in reconstructed vesicles. *The Journal of Biological Chemistry* **261**(16), 7101-7104.
- Clark, I.A. and Chaudhri, G. (1988) Tumour necrosis factor may contribute to the anaemia of malaria by causing dyserythropoiesis and erythrophagocytosis. *British Journal of Haematology* **70**, 99-103.
- Clark, I.A. and Cowden, W.B. (1999) Why is the pathology of *falciparum* worse than that of *vivax* malaria? *Parasitology Today* **15**(11), 458-461.
- Clark, I.A. and Scholfield, L. (2000) Pathogenesis of malaria. *Parasitology Today* **16**(10), 451-454.
- Clark, I.A., Rockett, K.A., Cowden, W.B. (1991) Proposed link between cytokines, nitric oxide and human cerebral malaria. *Parasitology Today* **7**, 205-207.
- Clyde DF, Most H, McCarthy VC, Vanderberg JP. (1973) Immunization of man against sporozite-induced falciparum malaria. *Am J Med Sci.***266**(3), 169-77.
- Coady, M.J., Jalal, F., Bissonnette, P., Cartier, M., Wallendorff, B., Lemay, G., Lapointe, J-Y. (2000) Functional studies of a chimeric protein containing portions of the Na^+/glucose and Na^+/*myo*-inositol cotransporters. *Biochemica et Biophysica Acta* **1466**, 139-150.

- Concha, I.I., Velasquez, F.V., Martinez, J.M., Angulo, C., Droppelmann, A., Reyes, A.M., Slebe, J.C., Vera, J.C., Golde, D.W. (1997) Human erythrocytes express GLUT5 and transport fructose. *Blood* **89**(11), 4190-4195.
- Cooke, B.M. and Cowman, A.F. (2000) Molecular approaches to malaria. *Parasitology Today* **16**(5), 177-178.
- Cooke, B.M., Wahlgren, M., Coppel, R.L. (2000) *Falciparum* malaria: sticking up, standing out and out-standing. *Parasitology Today* **16**(10), 416-420.
- Curtis, C.F. and Lines, J.D. (2000) Should DDT be banned by international treaty? *Parasitology Today* **16**(3), 119-121.
- Deans, J.A., Thomas, A.W., Alderson, T., Cohen, S. (1984) Biosynthesis of a putative protective *Plasmodium knowlesi* merozoite antigen. *Molecular and Biochemical Parasitology* **11**, 189-204.
- Degen, R., Weis, N., Beck, H.P. (2000) *Plasmodium falciparum*: cloned and expressed CIDR domains of PfEMP1 bind to chonroitin sulfate A. *Experimental Parasitology* **95**(2), 113-121.
- Deitsch, K.W. and Wellems, T.E. (1996) Membrane modifications in erythrocytes parasitised by *Plasmodium falciparum*. *Molecular and Biochemical Parasitology* **76**, 1-10.
- Desai, S.A., Krogstad, D.J., McCleskey, E.W. (1993) A nutrient-permeable channel on the intraerythrocytic malaria parasite. *Nature* **362**(6421), 643-646.
- Divo, A.A., Geary, T.G., Davis, N.L., Jensen, J.B. (1985) Nutrient requirements of *Plasmodium falciparum* in culture. I. Exogenously supplied dialyzable components necessary for continuous growth. *Journal of Protozoology* **32**, 59-64.
- Doolan, D.L. and Hoffman, S.L. (2001) DNA-based vaccines against malaria: status and promise of the Multi-Stage Malaria DNA Vaccine Operation. *International Journal for Parasitology* **31**, 753-762. Patience
- Ducarme, P., Rahman, M., Lins, L., Brasseur, R., (1996) The erythrocyte/brain glucose transporter (GLUT1) may adopt a two-channel transmembrane α/β structure. *Journal of Molecular Modelling* **2**, 27-45.
- Elford, B.C., Cowan, G.M., Ferguson, D.J.P. (1995) Parasite-regulated membrane transport processes and metabolic control in malaria-infected erythrocytes. *Biochemical Journal* **308**, 361-374.

- Elmendorf, H.G. and Haldar, K. (1993) Identification and localisation of ERD2 in the malaria parasite *Plasmodium falciparum*: Separation from sites of sphingomyelin synthesis and implications for organization of the Golgi. *The EMBO Journal* **12**(12), 4763-4773.
- Elmendorf, H.G. and Haldar, K. (1994) *Plasmodium falciparum* exports the Golgi marker sphingomyelin synthase into a tubovesicular network in the cytoplasm of mature erythrocytes. *The Journal of Cell Biology* **124**, 449-462.
- Etlinger, H.M Caspers P., Matile H., Schoenfeld H.J., Stueber D., Takacs B. (1991) Ability of recombinant or native proteins to protect monkeys against heterologous challenge with *Plasmodium falciparum*. *Infectious Immunology* **59**, 3498-3503.
- Fernandez-Reyes D., Craig, A.G., Kyes, S.A., Peshu, N., Snow, R.W., Berendt, A.R., Marsh, K., Newbold, C.I. (1997) A high frequency African coding polymorphism in the N-terminal domain of ICAM-1 predisposing to cerebral malaria in Kenya. *Human Molecular Genetics* **6**, 1357-1360.
- Feugeas, J-P., Neel, D., Pavia, A.A., Laham, A., Goussault, Y., Derappe, C. (1990) Glycosylation of the human erythrocyte glucose transporter is essential for glucose transport activity. *Biochemica et Biophysica Acta* **1030**, 60-64.
- Fischbarg, J., Cheung, M., Czegledy, F., Li, J., Iserovich, P., Kuang, K., Hubbard, J., Garner, M., Rosen, O.M., Golde, D.W., Vera, J.C. (1993) Evidence that facilitative glucose transporters may fold as beta-barrels. *Proceedings of the National Academy of Science USA* **90**, 11658-11662.
- Foley, M. and Tilley, L. (1998) Protein trafficking in malaria-infected erythrocytes. *International Journal for Parasitology* **28**, 1671-1680.
- Fujioka, H. and Aikawa, M. (1993) Morphological changes of clefts in *Plasmodium*-infected erythrocytes under adverse conditions. *Experimental Parasitology* **76**, 302-307.
- Gamain, B., Smith, J.D., Miller, L.H., Baruch, D.I. (2001) Modifications in the CD36 binding domain of the *Plasmodium falciparum* variant antigen are responsible for the inability of chondroitin sulfate A adherent parasites to bind CD36. *Blood* **97**(10), 3268-3274.
- Garcia, J.C., Strube, M., Leingang, K., Keller, K., Mueckler, M.M. (1992) Amino acid substitution at tryptophan 388 and tryptophan 412 of the HepG2 (Glut1)

glucose transporter inhibit transport activity and targeting to the plasma membrane in *Xenopus* oocytes. *The Journal of Biological Chemistry* **267**(11), 7770-7776.

- Gero, A. M. and Kirk, K. (1994) Nutrient trafficking in *Plasmodium*-infected erythrocytes. *Parasitology Today* **10**(10), 393-401.
- Ginsburg, H. and Stein, W.D. (1987) Biophysical analysis of novel transport pathways induced in red blood cell membranes. *Journal of Membrane Biology* **96**, 1-10.
- Ginsburg, H., Kutner, S., Krugliak, M., Cabantchik, Z.I. (1985) Characterisation of permeation pathways appearing in the host membrane of *Plasmodium falciparum* infected red blood cells. *Molecular and Biochemical Parasitology* **14**, 313-322.
- Ginsburg, H., Kutner, S., Zangwil, M., Cabantchik, Z.I. (1986) Selectivity properties of pores induced in host erythrocyte membrane by *Plasmodium falciparum*. Effect of parasite maturation. *Biochimica et Biophysica Acta* **861**, 194-196.
- Goodyer, D., Hayes, D.J., Eisenthal, R. (1997) Efflux of 6-deoxy-D-glucose from *Plasmodium falciparum*-infected erythocytes via two saturable carriers. *Molecular and Biochemical Parasitology* **84**, 229-239.
- Gould, G.W. and Holman, G.D. (1993) The glucose transporter family: structure, function and tissue-specific expression. *Biochemical Journal* **295**, 329-341.
- Gowda, D.C. and Davidson, E.A. (1999) Protein glycosylation in the malaria parasite. *Parasitology Today* **15**(4), 147-152.
- Gritzmacher, C.A. and Reese, R.T. (1982) Translation *in vitro* of RNA from the human malaria parasite *Plasmodium falciparum*. *Bioscience Report* **2**(9), 667-673.
- Haldar, K., Uyetake, L., Ghori, N., Elmendorf, H.G., Li, W. (1991) The accumulation and metabolism of a fluorescent ceramide derivative in *Plasmodium falciparum*-infected erythrocytes. *Molecular and Biochemical Parasitology* **49**, 143-156.
- Hanahan, D., Jessee, J., Bloom, F.R. (1991) Plasmid transformation of *Escherichia coli* and other bacteria. *Methods in Enzymology* **204**, 63-114.
- Harper, P.A., Lisansky, E.T., Sasse, B.E. (1947) Malaria and other insect-borne diseases in the South Pacific campaign. *American Journal of Tropical medicine* **27**, 1-68.

- Hashiramoto, M., Kadowaki, T., Clark, A.E., Muraoka, A., Momomura, K., Sakura, H., Tobe, K., Akanuma, Y., Yazaki, Y., Holman, G.D., Kasuga, M. (1992) Site-directed mutagenesis of GLUT1 in helix 7 residue 282 results in pertubation of exofacial ligand binding. *The Journal of Biological Chemistry* **267**(25), 17502-17507.
- Hastings, I.M. and D'Alessandro, U. (2000) Modelling a predictable disaster: the rise and spread of drug-resistant malaria. *Parasitology Today* **16**(8), 340-347.
- Heal, K.G., Sheikh, N.A., Hollingdale, M.R., Morrow, W.J.W., Taylor-Robinson, A.W.T. (2001) Potentiation by a novel alkaloid glycoside adjuvant of a protective cytotoxic T cell immune response specific for a preerythrocytic malaria vaccine candidate antigen. *Vaccine* **19**, 4153-4161.
- Hediger, M.A., Coady, M.J., Ikeda, T.S., Wright, E.M. (1987) Expression cloning and cDNA sequencing of the Na+/glucose co-transporter. *Nature* **330**(6146), 379-381.
- Holder, A.A., Blackman, M.J., Borre, M., Burghaus, P.A., Chappel, J.A., Keen, J.K., Ling, I.T., Ogun, S.A., Owen, C.A., Sinha, K.A. (1994) Malaria parasites and erythrocyte invasion. *Biochemical Society Transactions* **22** (2), 291-295.
- Hommel, M. (1990) Cytoadherence of malaria-infected erythrocytes. *Blood Cells* **16**(2-3), 605-619.
- Howard, R.F. and Schmidt, C.M. (1995) The secretory pathway of *Plasmodium falciparum* regulates transport of p82/RAP-1 to the rhoptries. *Molecular and Biochemical Parasitology* **74**, 43-54.
- Howard, R.J. and Pasloske, B.L. (1993) Target antigens for asexual malaria vaccine development. *Parasitology Today* **9**(10), 369-372.
- Hresko, R.C., Kruse, M., Strube, M., Mueckler, M. (1994) Topology of the Glut 1 glucose transporter deduced from glycosylation scanning mutagenesis. *Journal of Biological Chemistry* **269**(32), 20482-20488.
- Hruz, P.W. and Mueckler, M.M. (1999) Cysteine-scanning mutagenesis of transmembrane segment 7 of the GLUT1 glucose transporter. *The Journal of Biological Chemistry* **279**(51), 36176-36180.
- Inukai, K., Katagiri, H., Takata, K., Asano, T., Anai, M., Ishihara, H., Nakazaki, M., Kikuchi, M., Yazaki, Y., Oka, Y. (1995) Characterization of rat GLUT5 and

functional analysis of chimeric proteins of GLUT1 glucose transporter and GLUT5 fructose transporter. *Endocrinology* **136**(11), 4850-4857.

- Jones, T.R. and Hoffman, S.L. (1994) Malaria vaccine development. *Clinical Microbiology Review* **7**, 303-310.
- Kassenbrock, C.R., Garcia, P.D., Wlater, P., Kelly, R.B. (1988) Heavy-chain binding protein recognises aberrant polypeptides translocated *in vivo*. *Nature* **333**, 90-93.
- Kayano, T., Burant, C.F., Fukumoto, H., Gould, G.W., Fan, Y., Eddy, R.L., Byers, M.G., Shows, T.B., Seino, S., Bell, G.I. (1990) Human facilitative glucose transporters. *The Journal of Biological Chemsitry* **265**(22), 13276-13282.
- Keough, D.T., Ng, A.L., Winzor, D.J., Emmerson, B.T., de Jersey, J. (1999) Purification and characterization of *Plasmodium falciparum* hypoxanthine–guanine–xanthine phosphoribosyltransferase and comparison with the human enzyme. *Molecular and Biochemical Parasitology* **98**, 29-41.
- Kirk, K. (2001) Membrane transport in the malaria-infected erythrocyte. *Physiological Reviews* **81**(2), 495-537.
- Kirk, K., Ashworth, K.J., Elford, B.C., Pinches, R.A., Ellory, J.C. (1991) Characteristics of $^{86}Rb^{+}$ transport in human erythrocytes infected with *Plasmodium falciparum*. *Biochemica et Biophysica Acta* **1061**, 305-308.
- Kirk, K., Horner, H.A., Kirk, J. (1996) Glucose uptake in *Plasmodium falciparum*-infected erythrocytes is an equilibrative not an active process. *Molecular and Biochemical Parasitology* **82**, 196-205.
- Kolakovich, K.A., Gluzman, I.Y., Duffin, K.L., Goldberg, D.E. (1997) Generation of heamoglobin peptides in the acidic digestive vacuole of *Plasmodium falciparum* implicates peptide transport in amino acid production. *Molecular and Biochemical Parasitology* **87**, 123-135.
- Krause, T., Luersen, K., Wrenger, C., Gilberger, T.W., Muller, S., Walter, R.D. (2000) The ornithine decarboxylase domain of the bifunctional ornithine decarboxylase/S-adenosylmethionine decarboxylase of *Plasmodium falciparum*: recombinant expression and catalytic properties of two different constructs. *Biochemical Journal* **352**(2), 287-297.
- Krieg PA, Melton DA. (1984) Functional messenger RNAs are produced by SP6 in vitro transcription of cloned cDNAs. *Nucleic Acids Res.* **1912**(18), 7057-70.

- Krishna, S., Woodrow, C., Webb, R., Penny, J., Takeyasu, K., Kimura, M., East, J.M. (2001) Expression and functional characterisation of a *Plasmodium falciparum* Ca2+-ATPase (PfATP4) belonging to a subclass unique to apicomplexan organisms. *Journal of Biological Chemistry* **276**(14), 10782-10787.
- Krishna, S., Woodrow, C.J., Burchmore, R.J.S., Saliba, K.J., Kirk, K. (2000) Hexose transport in asexual stages of *Plasmodium falciparum* and kinetoplastidae. *Parasitology Today* **16**(12), 516-521.
- Kumar, N. and Zheng, H. (1992) Nucleotide sequence of a *Plasmodium falciparum* stress protein with similarity to mammalian 78-kDa glucose-regulated protein. *Molecular and Biochemical Parasitology* **56**, 353-356.
- Kumar, N., Koski, G., Harada, M., Aikawa, M., Zheng, H. (1991) Induction and localisation of *Plasmodium falciparum* stress proteins related to the heat shock protein 70 family. *Molecular and Biochemical Parasitology* **48**, 47-58.
- Kumar, N., Syin, C., Carter, R., Quakyi, I., Miller, L.H. (1988) *Plasmodium falciparum* gene encodes a protein similar to the 78-kDa rat glucose-regulated stress protein. *Proceedings of the National Academy of Science of the United States of America* **85**, 6277-6281.
- Kwiatkowski, D. and Marsh, K. (1997) Development of a malaria vaccine. *Lancet* **350**, 1696-1701.
- Langreth, S.G.; Jensen, J.B.; Reese, R.T., Trager, W. (1978). Fine structure of human malaria *in vitro*. *Journal of Protozoology* **25**(4), 443-452.
- Lauer, S.A., Rathod, P.K., Ghori, N., Haldar, K. (1997) A membrane network for nutrient import in red cells infected with the malaria parasite. *Science* **276**, 1122-1125.
- Liem HH, Noy N, Muller-Eberhard U. (1994) Studies on the efflux of heme from biological membranes. *Biochim Biophys Acta.* **1194**(2), 264-70.
- Liman ER, Tytgat J, Hess P. (1992) Subunit stoichiometry of a mammalian K+ channel determined by construction of multimeric cDNAs. *Neuron.* **9**(5), 861-71.
- Lindsay, S.W. and Gibson, M.E. (1988) Bednets revisited – old idea new angle. *Parasitology Today* **4**.
- Lines, J.D. and Zaim, M. (2000) Insecticide products: treatment of mosquito nets at home. *Parasitology Today* **16**(3), 91-92.

- Lingelbach, K. (1997) Protein trafficking in the *Plasmodium falciparum*-infected erythrocyte – from models to mechanisms. *Annals of Tropical Medicine and Parasitology* **91**(5), 543-549.
- Lippincott-Schwartz, J., Yuan, L.C., Bonifacino, J.S., Klausner, R.D. (1989) Rapid redistribution of Golgi proteins into the ER in cells treated with Brefeldin A: evidence for the membrane cycling from Golgi to ER. *Cell* **56**, 801-813.
- Lodish, H., Baltimore, D., Berk, A., Zipursky, S.L., Matsudaira P., Darnell, J. (1995) Molecular Cell Biology. Third Edition. W. H. Freeman & Company.
- Malaria: an Online Resource (2001) http://www.rph.wa.gov.au/labs/haem/malaria.
- Matthews, G.M. (1999) Protein Expression: A Practical Approach. Expression in *Xenopus* oocytes and cell-free extracts. S. J. Higgins, B. D. Hames. USA, Oxford: 29-59.
- Misumi, Y., Misumi, Y., Miki, K., Takatsuki, A., Tamura, G., Ikehara, Y. (1986) Novel blockage by Brefeldin A of intracellular transport of secretory proteins in cultured rat hepatocytes. *The Journal of Biological Chemistry* **261**(24), 11398-11403
- Mueckler, M. (1994) Facilitative glucose transporters. *European Journal of Biochemistry* **219**, 713-725.
- Mueckler, M. and Makepeace, C. (1999) Transmembrane segment 5 of the Glut1 glucose transporter is an amphipathic helix that forms part of the sugar permeation pathway. *The Journal of Biological Chemistry* **274**(16), 10923-10926.
- Mueckler, M., Caruso, C., Baldwin, S.A., Panico, M., Blench, I., Morris, H.R., Allard, W.J., Lienhard, G.E., Lodish, H.F. (1985) Sequence and structure of a human glucose transporter. *Science* **229**, 941-945.
- Mueckler, M., Weng, W., Kruse, M. (1994) Glutamine 161 of Glut1 glucose transporter is crucial for transport activity and exofacial ligand binding. *The Journal of Biological Chemistry* **269**(32), 20533-20538.
- Munro, S. and Pelham, H.R.B. (1987) A C-terminal signal prevents secretion of luminal ER proteins. *Cell* **48**, 899-907.
- Mwenesi, H.A. (1999) Insecticide impregnated bednets for Africa – implimentation, prospects and challenges for malaria control. *Proceedings of the MIM African Malaria Conference,* 186-193.

- Noel, L.E. and Newgard, C.B. (1997) Structural domains that contribute to substrate specificity in facilitated glucose transporters are distinct from those involved in kinetic function: studies with GLUT-1/GLUT-2 chimeras. *Biochemistry* **36**(18), 5465-5475.
- Nussenzweig RS, Vanderberg J, Most H, Orton C. (1967) Protective immunity produced by the injection of x-irradiated sporozoites of plasmodium berghei. *Nature*. **216**,160-2.
- Oatey, P.B., Van Weering, D.H., Dobson, S.P., Gould, G.W., Tavare, J.M. (1997) GLUT4 vesicle dynamics in living 3T3 L1 adipocytes visualised with green-fluorescent protein. *Biochemical Journal* **327**(3), 637-642.
- Oka, Y., Asano, T., Shibasaki, Y., Lin, J-L., Tsuukda, K., Katagiri, H., Akanuma, Y., Takaku, F. (1990) C-terminal truncated glucose transporter is locked into an inward-facing form without transport activity. *Nature* **345**, 550-553.
- Oliveira-Ferreira, J. and Daniel-Ribeiro, C.T. (2001) Protective $CD8^+$ T cell responses against the pre-erythrocytic stages of malaria parasites: an overview. *Memoria Instituto Oswaldo Cruz* **96**(2), 221-227.
- Olliaro, P.L. and Yuthavong, Y. (1999) An overview of chemotherapeutic targets for antimalarial drug discovery. *Pharmacology and Therapy* **81**(2), 91-110.
- Olsowski, A., Monden, I., Keller, K. (1998) Cysteine-scanning mutagenesis of flanking regions at the boundary between external loop I or IV and transmembrane segment II or VII in the GLUT1 glucose transporter. *Biochemistry* **37**, 10738-10745.
- Olsowski, A., Monden, I., Krause, G., Keller, K. (2000) Cysteine scanning mutagenesis of helices 2 and 7 in GLUT1 identifies an exofacial cleft in both transmembrane segments. *Biochemistry* **39**, 2469-2474.
- Othoro, C., Lal, A.A. Nahlen, B., Koech, D., Orago, A.S.S., Udhayakumar, V. (1999) A low interleukin-10 tumor necrosis factor-α ratio is associated with malaria anemia in children residing in a holoendemic malaria region in Western Kenya. *The Journal of Infectious Diseases* **179**, 279-282.
- Pagano, R.E., Sepanski, M.A., Martin, O.C. (1989) Molecular trapping of a fluorescent ceramide analogue at the Golgi apparatus of fixed cells: interaction with endogenous lipids provides a *trans* Golgi marker for both light and electron microscopy. *Journal of Cell Biology* **109**, 2067-2079.

- Pao, S.S., Paulsen, I.T., Saier, M.H. (1998) Major facilitator superfamily. *Microbiology and Molecular Biology Reviews* **62**(1), 1-34.
- Parker, M.D., Hyde, R.J., Yao, S.Y.M., Robert, L.M., Cass, C.E., Young, J.D., Conkey, G.A.M., Baldwin, S.A. (2000) Identification of a nucleoside/nucleobase transporter from *Plasmodium falciparum*, a novel target for anti-malarial chemotherapy. *Biochemical Journal* **349**, 67-75.
- Penny, J.I., Hall, S.T., Woodrow, C.J., Cowan, G.M., Gero, A.M., Krishna, S. (1998) Expression of substrate-specific transporters encoded by *Plasmodium falciparum* in *Xenopus laevis* oocytes. *Molecular and Biochemical Parasitology* **93**(1), 81-89.
- Powell, K.A., Campbell, L.C., Tavare, J.M., Leader, D.P., Wakefield, J.A., Gould, G.W. (1999) Trafficking of Glut4-green fluorescent protein chimeras in 3T3-L1 adipocytes suggests distinct internalisation mechanisms regulating cell surface glut4 levels. *Biochemical Journal* **344**(2), 535-543.
- Preiser, P., Kaviratne, M., Khan, S., Bannister, L., Jarra, W. (2000) The apical organelles of malaria merozoites: host cell selection, invasion, host immunity and immune evasion. *Microbes and Infection* **2**, 1461-1477.
- Renia, L., Marussig, M.S., Grillot, D., Pied, S., Corradin, G., Miltgen, F., Del Giudice, G., Mazier, D. (1991) *In vitro* activity of $CD4^+$ and $CD8^+$ T lymphocytes from mice immunised with synthetic malaria peptides. *Proceedings of the National Academy of Science, USA* **88**, 7963-7967.
- Rohdich, F., Eisenreich, W., Wungsintawwekul, J., Hecht, S., Schuhr, C.A., Bacher, A. (2001) Biosynthesis of terpenoids 2C-Methyl-D-erythritol 2,4-cyclodiphosphate synthase (IspF) from *Plasmodium falciparum*. *European Journal of Biochemistry* **268**(11), 3190-3197.
- Rosenthal, P.J. and Meshnick, S.R (1996) Hemoglobin catabolism and iron utilization by malaria parasites. *Molecular and Biochemical Parasitology* **83**, 131-139.
- Rychlik, W., Spencer, W.J., Roads, R.E. (1990) Optimisation of the annealing temperature for DNA amplification *in vitro*. *Nucleic Acids Research* **18**, 6409-6412
- Sambrook, J., Fritsch, E.F., Maniatis, T. (1989) *Molecular cloning, a laboratory manual*.Cold Spring Harbor, Cold Spring Habor Laboratory Press.

- Saul, A., Lord R., Jones G.L., Spencer L. (1992) Protective immunization with invariant peptides of the *Plasmodium falciparum* antigen MSA2. *Journal of Immunology* **148**, 208-211.
- Schofield, L., Villaquiran, J., Ferreira, A., Schellekens, H., Nussenzweig, R.S., Nussenzweig, V. (1987) γ interferon $CD8^+$ cells and antibodies required for immunity to malaria sporozoites. *Nature* **330**, 664-666.
- Seatter, M.J., De La Rue, S.A., Porter, L.M., Gould, G.W. (1998) QLS motif in transmembrane helix VII of the glucose transporter family interacts with the C-1 position of D-glucose and is involved in substrate selection at the exofacial binding site. *Biochemistry* **37**, 1322-1326.
- Seguin, M.C., Klots, F.W., Scheneider, I., Weir, J.P., Goodbary, M., Slayter, M., Raney, J.J., Aniagolu, J.U., Green, S.J. (1994) Induction of nitrix oxide synthetase protects against malaria in mice exposed to irradiated *P. berghei* infected mosquitoes involvement of interferon-gamma and $CD8^+$ T cells. *Journal of Experimental Medicine* **180**, 353-358.
- Sharma, S. (2000) The Institute for Fundamental Research, Bombay, India, http://www.malaria.org/lifecycle.html
- Sherman, I.W. (1988) Mechanisms of molecular trafficking in malaria. *Parasitology* **96**, S57-S81.
- Sherman, I.W. and Tanigoshi, L. (1974) Glucose transport in the malarial (*Plasmodium lophurae*) infected erythrocyte. *Journal of Protozoology* **21**, 603-7.
- Singh, S., Puri, S.K., Singh, S.K., Srivastava, R., Gupta, R.C., Pandey, V.C. (1997) Characterisation of simian malaria parasite (*Plasmodium knowlesi*)-induced putrescine transport in rhesus monkey erythrocytes. A novel putrescine conjugate arrests *in vitro* growth of simian parasite (*Plasmodium knowlesi*) and cures multidrug resistant murine malaria (*Plasmodium yoelii*) infection *in vivo*. *Journal of Biological Chemistry* **272**, 13505-13511.
- Smart, T.G. and Krishek, B.J. (1995) *Xenopus* oocyte microinjection and ion-channel expression. *Neuromethods* **26**, 259-307.
- Tamori, Y., Hashiramoto, M., Clark, A.E, Mori, H., Muraoka, A., Kadowaki, T., Holman, G.D., Kasuga, M. (1994) Substitution at Pro^{385} of GLUT1 perturbs the glucose transport function by reducing conformational flexibility. *The Journal of Biological Chemistry* **269**(4), 2982-2986.

- Tanabe, K., (1990) Glucose transport in malaria infected erythrocytes. *Parasitology Today* **6**(7), 225-229.
- Tetaud, E., Barrett, M.P., Bringaud, F., Baltz, T. (1997) Kinetoplastid glucose transporters. *Biochemical Journal* **325**, 569-580.
- Toure', Y.T. (1999) Malaria vector population studies: potential contribution for selective control measures. *Proceedings of the MIM African Malaria Conference*, 179-185.
- Trager, W. and Jensen, J.B. (1976) Human malaria parasite in continuos cultures. *Science* **193**, 673-675.
- Tripatara, A. and Yuthavong, Y. (1986) Effect of inhibitors on glucose transport in malaria (*Plasmodium berghei*) infected erythrocytes. *International Journal for Parasitology* **16**, 441-446.
- Tsuji, M., Romero, P.J., Nussenzweig, R.S., Zavala, F. (1990) $CD4^+$ cytolitic T cell clone confers protection against murine malaria. *Journal of Experimental Medicine* **172**, 1353-1358.
- Upston, J.M. and Gero, A.M. (1995) Parasite-induced permeation of nucleosides in *Plasmodium falciparum* malaria. *Biochemica et Biophysica Acta* **1236**, 249-258.
- van Bemmelen, M.X., Beghdadi-Rais, C., Desponds, C., Vargas, E., Herrera, S., Reymond, C.D., Fasel, N. (2000) Expression and one-step purification of *Plasmodium* proteins in *Dictyostelium*. *Molecular and Biochemical Parasitology* **111**(2), 377-390.
- van Es, H.H., Karcz, S., Chu, F., Cowman, A.F., Vidal, S., Gros, P., Schurr, E. (1994) Expression of the *Plasmodium* PfMDR1 gene in mammalian cells is associated with increased susceptibility to chloroquine. *Molecular and Cellular Biology* **14**(4), 2419-2428.
- Van Hensbroek, M.B. (1996) A trial of artemether or quinine in children with cerebral malaria. *New England Journal of Medicine* **335**, 69-75.
- Van Wye, J., Ghori, N., Webster, P., Mitschel, R.R., Elmendorf, H.G., Haldar, K. (1996) Identification and localisation of rab6, separation of rab6 from ERD2 and implications for an 'unstacked' Golgi, in *Plasmodium falciparum*. *Molecular and Biochemical Parasitology* **83**, 107-120.

- Virtual Naval Hospital, Navy Medical Department Guide to Malaria Prevention and Control (1998) http://www.vnh.org/Malaria/Malaria.html
- Waddell, I.D., Zomerschoe, A.G., Voice, M.W., Burchell, A. (1992) Cloning and expression of a hepatic microsomal glucose transport protein. *Biochemical Journal* **286**, 173-177.
- Walmsley, A.R. (1988) The dynamics of the glucose transporter. *Trends in Biochemical Sciences* **13**, 226-231.
- Walmsley, A.R., Barrett, M.P., Bringaud, F., Gould, G.W. (1998) Sugar transporters from bacteria, parasites and mammals: structure activity relationships. *Trends in Biochemical Sciences* **23**, 476-481.
- Wang, J., Kim, S., Gallagher, S. (1995) Dealing with A/T content differences when using the H33258/TKO 100 DNA assay. *Hoefer news* **3**.
- Wang, L., Richie, T.L., Stowers, A., Nhan, D.H., Coppel, R.L. (2001) Naturally acquired antibody responses to *Plasmodium falciparum* merozoite surface protein 4 in a population living in an area of endemicity in Vietnam. *Infection and Immunology* **69**(7), 4390-4397.
- Weiss, W.R., Sedegah, M., Beaudoin, R.L., Miller, L.H., Good, M.F. (1988) $CD8^+$ T cells (cytotoxic/suppressor) are required for protection in mice immunised with malaria sporozoites. *Proceedings of the National Academy of Science, USA* **85**, 573-576.
- Wellner, M., Monden, I., Keller, K. (1994) The role of cysteine residues in glucose-transporter-GLUT1-mediated transport and transport inhibition. *Biochemical Journal* **299**, 813-817.
- Wellner, M., Monden, I., Mueckler, M.M., Keller, K. (1995) Functional consequences of proline mutations in the putative transmembrane segment 6 and 10 of the glucose transporter GLUT1. *European Journal of Biochemistry* **227**, 454-458.
- Winkler, S., Willheim, M., Baier, K., Schmid, D., Aichelburg, A., Graninger, W., Kremsner, P.G. (1999) Frequency of cytokine-producing T cells in patients of different age groups with *Plasmodium falciparum* malaria. *The Journal of Infectious Diseases* **179**, 209-216.
- Winstanley, P.A. (2000) Chemotherapy for *falciparum* malaria: the armoury, the problems and the prospects. *Parasitology Today* **16**(4), 146-153.

- Wiser, M.F., Lanners, H.N., Bafford, R.A., Favaloro, J.M. (1997) A novel alternative secretory pathway for the export of *Plasmodium* proteins into the host erythrocyte. *Proceedings of the National Academy of Science of the United States of America* **94**, 9108-9113.
- Withers-Martinez C, Carpenter EP, Hackett F, Ely B, Sajid M, Grainger M, Blackman MJ. (1999) PCR-based gene synthesis as an efficient approach for expression of the A+T-rich malaria genome. *Protein Eng.* **12**(12), 1113-20.
- Woodrow, C.J., Burchmore, B.J., Krishna, S. (2000) Hexose permeation pathways in *Plasmodium falciparum*-infected erythrocytes. *Proceedings of the National Academy of Science of USA* 97 (18), 9931-9936.
- Woodrow, C.J., Penny, J.L., Krishna, S. (1999) Intraerythrocytic *Plasmodium falciparum* expresses a high affinity facilitative hexose transporter. *The Journal of Biological Chemistry* **274**(11), 7272-7277.
- Wu, L., Fritz, J.D., Powers, A.C. (1998) Different functional domains of GLUT2 glucose transporter are required for glucose affinity and substrate specificity. *Endocrinology* **139**(10), 4250-4212.
- Yao, S.Y.M., Cass, C.E., Young, J.D. (2000) Membrane Transport, Chapter 3, The *Xenopus* oocyte expression system for the cDNA cloning and characterisation of plasma membrane transport proteins. S. A. Baldwin. USA, Oxford: 47-78.

APPENDIX I:

CLONING VECTORS

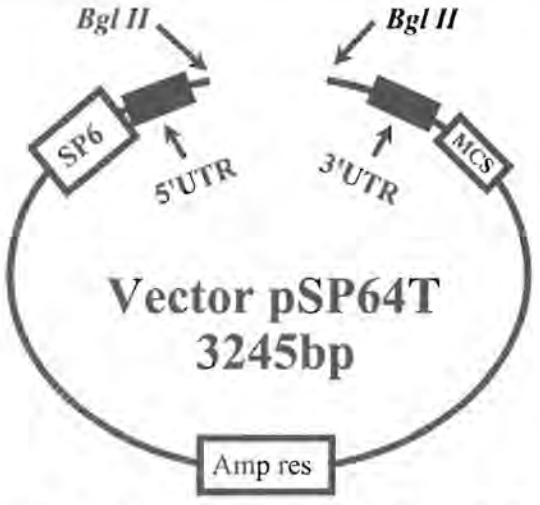

Figure Ia: Schematic representation of the *Xenopus* oocyte expression vector pSP64T. UTR = untranslated region of the β-globin gene of *Xenopus*, Amp^r = ampicillin resistant gene, SP6 = RNA promoter region used for cRNA transcription.

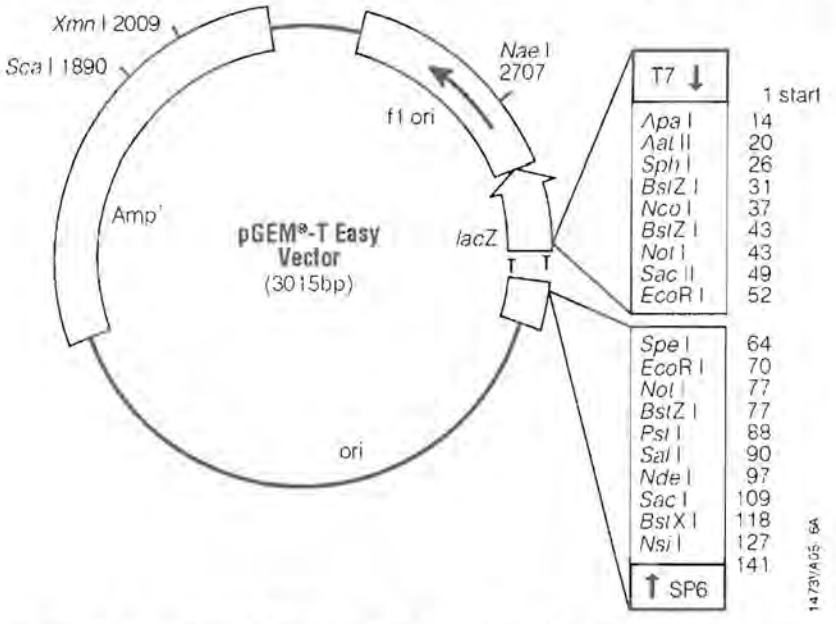

Figure Ib: pGEM®-T Easy Vector circle map. The vector is prepared by cutting Promega's pGEM-T Easy Vector with *Eco*R V and adding a 3' terminal thymidine to both ends. The vector contains a SP6 and T7 polymerase promoter flanking a multiple cloning site within the α-peptide coding region of the enzyme β-galactosidase. The vector also contains the origin of replication of the filamentous phage f1 (f1 ori) for the preparation of single-stranded DNA, as well as an ampicillin resistant gene.

APPENDIX II:

AMINO ACID STRUCTURES

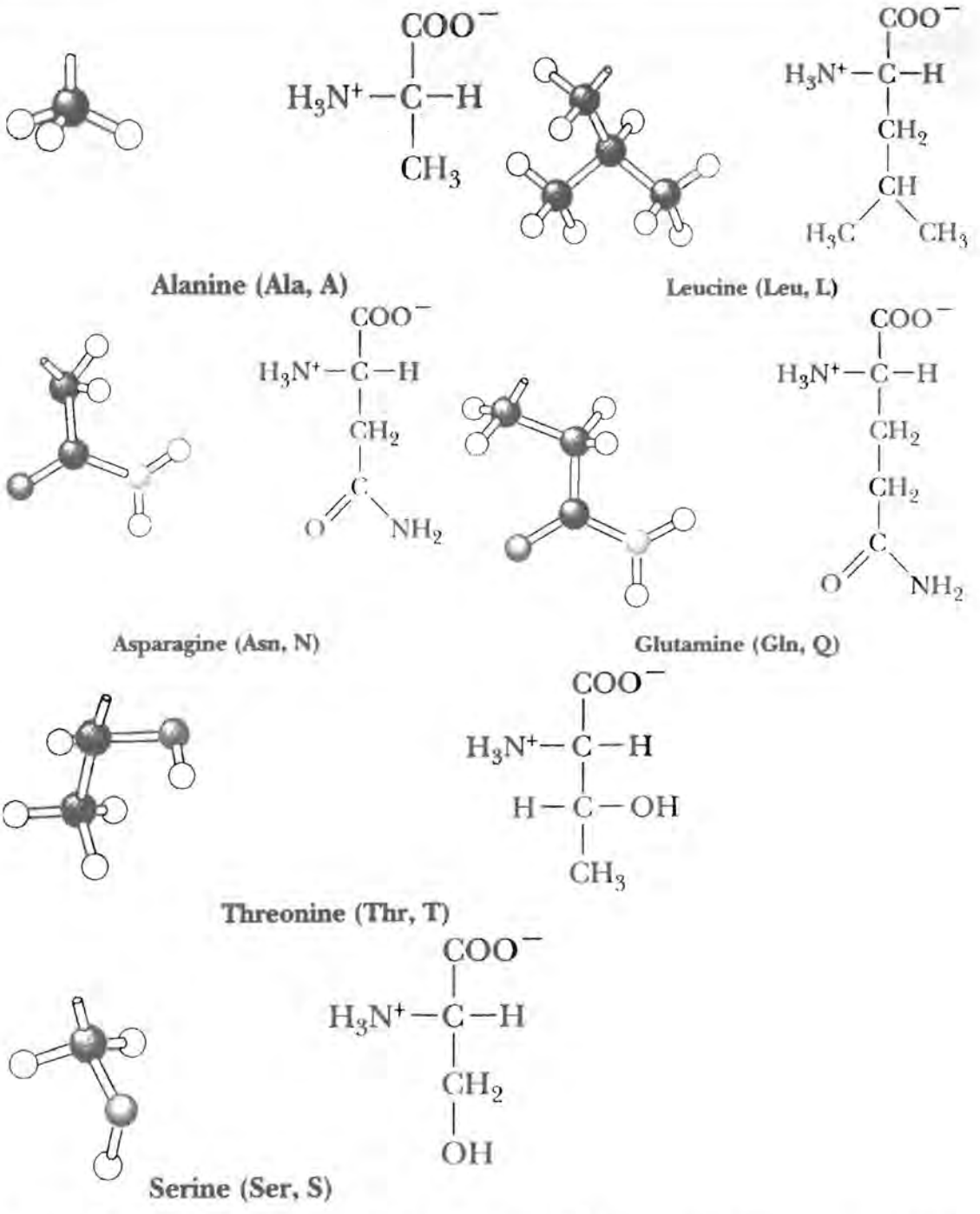

Figure IIa: Structures of amino acids used in the mutational experiments. Amino acids are shown in their predominant forms at pH 7. The R groups are shown as ball and stick models and can be seen as structures against a white background. Amino acids in green have polar, uncharged side chains. Amino acids in yellow have nonpolar side chains.

APPENDIX III:

OVERLAPPING ALIGNMENT OF FACILITATOR SUPERFAMILY HELICES

Figure IIIa: Amino acid sequence and helical mapping of the PfHT1 and GLUT1 glucose transporters and Chimeras 1 and 2. Transmembrane regions are in bold and underlined. The transmembrane region number is indicated above each region.

```
                                                                1
Chimaera 1 MTKSSKDICSENEGKKNGKSGFFSTSFKYVLSACIASFIFGYQVSV
Chimaera 2 MTKSSKDICSENEGKKNGKSGFFSTSFKYVLSACIASFIFGYQVSV
PfHT1      MTKSSKDICSENEGKKNGKSGFFSTSFKYVLSACIASFIFGYQVSV
Rat GLUT1  MEPSSKKLTGRLMLAVGGAVLGSLQFGYNTGVINAPQKVIEEFYNQ
                                                                2
Chimaera 1 LNTIKNFIVVEFEWCKGEKDRLNCSNNTIQSSFLLASVFIGAVLGC
Chimaera 2 LNTIKNFIVVEFEWCKGEKDRLNCSNNTIQSSFLLASVFIGAVLGC
PfHT1      LNTIKNFIVVEFEWCKGEKDRLNCSNNTIQSSFLLASVFIGAVLGC
Rat GLUT1  TWVHRYGESILPTTLTTLWSLSVAIFSVGGMIGSFSVGLFVNRFGR
                                3
Chimaera 1 GFSGYLVQFGRRLSLLIIYNFFFLVSILTSITHHFHTILFARLLSG
Chimaera 2 GFSGYLVQFGRRLSLLIIYNFFFLVSILTSITHHFHTILFARLLSG
PfHT1      GFSGYLVQFGRRLSLLIIYNFFFLVSILTSITHHFHTILFARLLSG
Rat GLUT1  RNSMLMMNLLAFVSAVLMGFSKLGKSFEMLILGRFIIGVYCGLTTG
                          4                     5
Chimaera 1 FGIGLVTVSVPMYISEMTHKDKKGAYGVMHQLFITFGIFVAVMLGL
Chimaera 2 FGIGLVTVSVPMYISEMTHKDKKGAYGVMHQLFITFGIFVAVMLGL
PfHT1      FGIGLVTVSVPMYISEMTHKDKKGAYGVMHQLFITFGIFVAVMLGL
Rat GLUT1  FVPMYVGEVSPTAFRGALGTLHQLGIVVGILIAQVFGLDSIMGNKD
                          6                           6
Chimaera 1 AMGEGPKADSTEPLTSFAKLWWRLMFLFPSVISLIGILALVVFFKE
Chimaera 2 AMGEGPKADSTEPLTSFAKLWWRLMFLFPSVISLIGILALVVFFKE
PfHT1      AMGEGPKADSTEPLTSFAKLWWRLMFLFPSVISLIGILALVVFFKE
Rat GLUT1  LWPLLLSIIFIPALLQCIVLPFCPESPRFLLINRNEENRAKSVLKK

Chimaera 1 ETPYFLFEKGRIEESKNILKKIYETDNVDEPQEMKEEGRQMMREKK
Chimaera 2 ETPYFLFEKGRIEESKNILKKIYETDNVDEPLNAIKEAVEQNESAK
PfHT1      ETPYFLFEKGRIEESKNILKKIYETDNVDEPLNAIKEAVEQNESAK
Rat GLUT1  LRGTADVTHDLQEMKEESRQMMREKKVTILELFRSPAYRQPILIAV
                                7                       8
Chimaera 1 VTILELFRSPAYRQPILIAVVLQLSQQLSGINAVFYYSTSIFEKAG
Chimaera 2 KNSLSLLSALKIPSYRYVIILGCLLSGLQQFTGINVLVSNSNELYK
PfHT1      KNSLSLLSALKIPSYRYVIILGCLLSGLQQFTGINVLVSNSNELYK
Rat GLUT1  VLQLSQQLSGINAVFYYSTSIFEKAGVQQPVYATIGSGIVNTAFTV
```

```
                                    8                                   9
Chimaera 1 VQQPVYATIGSGIVNTAFTVVSLFVVERAGRRTLHLIGLAGMAGCA
Chimaera 2 EFLDSHLITILSVVMTAVNFLMTFPAIYIVEKLGRKTLLLWGCVGV
PfHT1      EFLDSHLITILSVVMTAVNFLMTFPAIYIVEKLGRKTLLLWGCVGV
Rat GLUT1  VSLFVVERAGRRTLHLIGLAGMAGCAILMTIALALLEQLPWMSYLS
                                        10
Chimaera 1 VLMTIALALLEQLPWMSYLSIVAIFGFVAFFEVGPGPIPWFIVAEL
Chimaera 2 LVAYLPTAIANEINRNSNFVKILSIVATFVMIISFAVSYGPVLWIY
PfHT1      LVAYLPTAIANEINRNSNFVKILSIVATFVMIISFAVSYGPVLWIY
Rat GLUT1  IVAIFGFVAFFEVGPGPIPWFIVAELFSQGPRPAAIAVAGFSNWTS
                              11                        12
Chimaera 1 FSQGPRPAAVAVAGFSNWTSNFIVGMCFQYVEQLCGPYVFIIFTVL
Chimaera 2 LHEMFPSEIKDSAASLASLVNWVCAIIVVFPSDIIIKKSPSILFIV
PfHT1      LHEMFPSEIKDSAASLASLVNWVCAIIVVFPSDIIIKKSPSILFIV
Rat GLUT1  NFIVGMCFQYVEQLCGPYVFIIFTVLLVLFFIFTYFKVPETKGRTF
                12
Chimaera 1 LVLFFIFTYFKVPETKGRTFDEIASGFRQGGASQSDKTPEELFHPL
Chimaera 2 FSVMSILTFFFIFFFIKETKGRTFDEIASGFRQGGASQSDKTPEEL
PfHT1      FSVMSILTFFFIFFFIKETKGGEIGTSPYITMEERQKHMTKSVV
Rat GLUT1  DEIASGFRQGGASQSDKTPEELFHPLGADSQV

Chimaera 1 GADSQV
Chimaera 2 FHPLGADSQV
```